Title

An Approach to Nonlinear Oscillations Through Randomization

Author

Byun, Jaeseung

Publication Date

2024

Peer reviewed|Thesis/dissertation

An Approach to Nonlinear Oscillations Through Randomization

by

Jaeseung Byun

A dissertation submitted in partial satisfaction of the

requirements for the degree of

Doctor of Philosophy

in

Engineering - Mechanical Engineering

in the

Graduate Division

of the

University of California, Berkeley

Committee in charge:

Professor Fai Ma, Chair
Professor Simo Mäkiharju
Professor Per-Olof Persson

Spring 2024

An Approach to Nonlinear Oscillations Through Randomization

Abstract

An Approach to Nonlinear Oscillations Through Randomization

by

Jaeseung Byun

Doctor of Philosophy in Engineering - Mechanical Engineering

University of California, Berkeley

Professor Fai Ma, Chair

In this thesis, a novel investigation of deterministic nonlinear systems is presented. When autonomous dynamical systems are randomized by white-noise excitation, their behaviors are governed by diffusion equations. The core idea behind the method of randomization involves replacing a *nonlinear ordinary* differential equation of motion by a *linear partial* differential equation of diffusion.

Exact analytical solutions are feasible for only a limited number of nonlinear systems. However, some nonlinear systems, which are difficult to analyze using deterministic methods, possess stationary diffusion equations with exact solutions. These diffusion responses provide deeper insights into the qualitative behaviors of nonlinear systems, such as stability at multiple equilibria, limit cycles, and bifurcations.

To demonstrate the potential and feasibility of randomization, numerous nonlinear oscillators are considered. When both the deterministic systems and the associated randomized systems can be analyzed, there is complete agreement in their qualitative properties. Furthermore, some example systems inaccessible through deterministic approaches can be readily examined using randomization, suggesting that randomization could be an alternative tool for investigating nonlinear oscillations.

Keywords: Nonlinear dynamical system; Stochastic process; Stochastic differential equation; Random vibration; Randomization; Fokker-Planck equation; Forward diffusion equation

Contents

List of Figures

Acknowledgments

Firstly, I would like to extend my deepest gratitude to my parents, Changdae Byun and Sung Mee Seo, along with my sister Jungmyung Byun. Their unwavering trust and support have propelled me on this extraordinary journey towards earning my PhD. The very thought of studying in the US would have been inconceivable without their backing.

I am extraordinarily thankful to my advisor, Professor Fai Ma, whose guidance and support has been invaluable. My appreciation also extends to my committee members, Professor Simo Mäkiharju and Professor Per-Olof Persson. Their insightful comments and suggestions significantly enhanced my work.

A heartfelt thank you goes out to all of my colleagues and friends, whose assistance and moral support were pivotal to my journey. Without them, I would not be standing where I am today.

Finally, and most importantly, I would like to express my profound love for my wife Hyesik Kim. She is the miracle of my life and the sole inspiration for my endeavors. I dedicate my accomplishment today to her.

Chapter 1

Introduction

A proper understanding of nonlinear dynamical systems is central to advancements in physics, engineering, and biology. Highlighting nonlinearity in both damping and stiffness, the governing differential equation is expressed as follows:

$$\ddot{x} + \epsilon\alpha(x, \dot{x})\dot{x} + \beta(x, \dot{x}) = 0. \tag{1.1}$$

Here, $x(t)$ is the system response, $\alpha(x, \dot{x})$ is a nonlinear damping function with a damping constant ϵ, and $\beta(x, \dot{x})$ represents a nonlinear stiffness. Exact solutions to Eq. (1.1) are usually intractable, with few exceptions presented in complex mathematical forms such as incomplete elliptic integrals that obscure the system behavior.

Randomization introduces a novel approach by applying white-noise excitation to deterministic systems, thereby converting the deterministic response of motion into a stochastic process called Brownian motion. When the system is excited by white noise $W(t)$, the stochastic counterpart of Eq. (1.1) is given by

$$\ddot{X} + \epsilon\alpha\Big(X, \dot{X}\Big)\dot{X} + \beta\Big(X, \dot{X}\Big) = W(t), \tag{1.2}$$

with $X(t)$ indicating the stochastic response under white-noise excitation $W(t)$ characterized by zero mean and constant power spectral density S_0. The transition probability density for the response $X(t)$ is governed by the forward diffusion equation, also known as the Fokker-Planck equation:

$$\frac{\partial p}{\partial t} = -y\frac{\partial p}{\partial x} + \frac{\partial}{\partial y}\big((\epsilon\alpha y + \beta)p\big) + \pi S_0\frac{\partial^2 p}{\partial y^2}. \tag{1.3}$$

The function $p(x, y, t|x_0, y_0)$ here defines the transition probability density function of system states, where $y = \dot{x}$ and the initial condition is represented by (x_0, y_0). In essence, randomization replaces the nonlinear second-order ordinary differential equation of motion (1.1) by a linear second-order partial differential equation of diffusion.

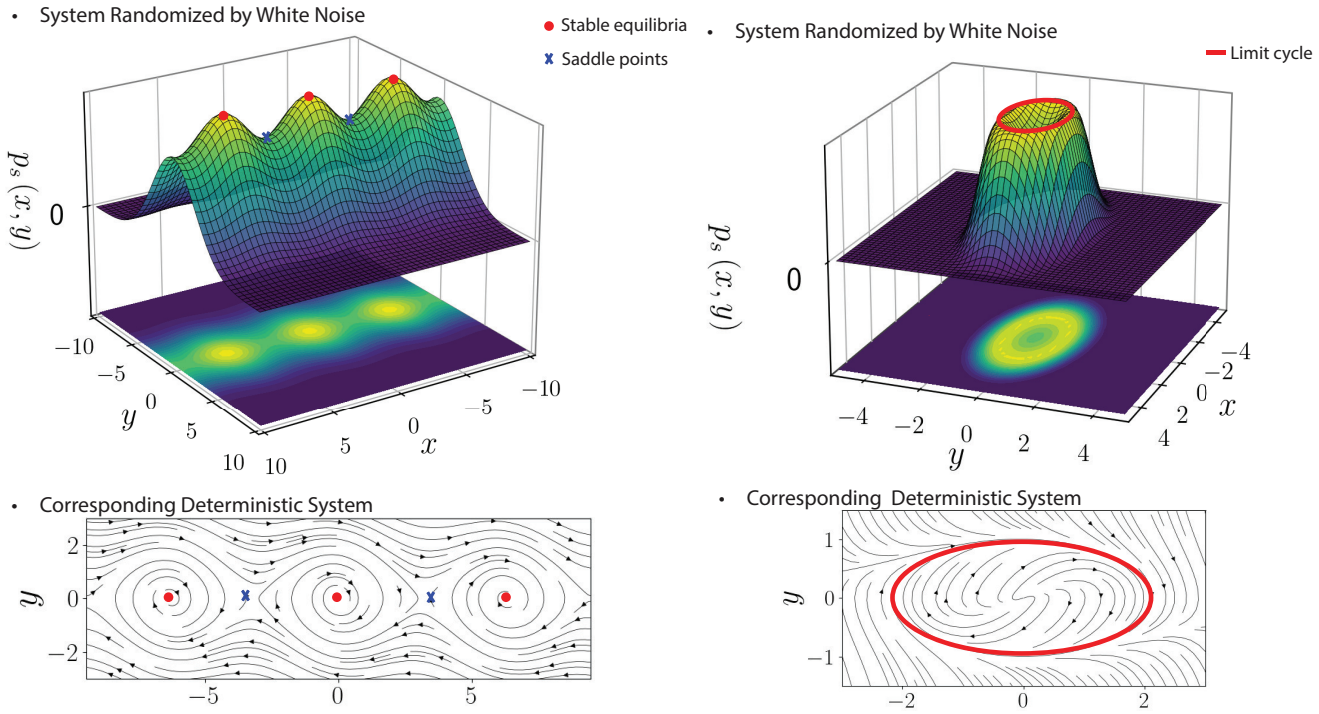

(a) Stable foci and saddle points

(b) Limit cycle

Figure 1.1: Identifying qualitative behaviors of nonlinear systems through randomization

As the system evolves, it may converge to a steady state. This state can be determined by solving the stationary diffusion equation, which is obtained from Eq. (1.3) by setting the time derivative to zero:

$$-y\frac{\partial p_s}{\partial x} + \frac{\partial}{\partial y}\big((\epsilon\alpha y + \beta)p_s\big) + \pi S_0 \frac{\partial^2 p_s}{\partial y^2} = 0, \tag{1.4}$$

where $p_s(x, y)$ is the stationary probability density function.

While few nonlinear systems allow for direct analytical solutions to Eq. (1.1), some associated stationary diffusion equations, as shown in Eq. (1.4), can be solved exactly. The reason being linear partial differential equations are sometimes more manageable than nonlinear ordinary differential equations. Such exact diffusion responses provide critical insight into the qualitative behaviors of nonlinear systems, identifying characteristics including nodes, foci, saddle points, limit cycles, and bifurcations. Notably:

- Stable equilibria, such as nodes and foci, manifest as peaks on a locally concave section of the stationary distribution $p_s(x, y)$—illustrated in Fig. 1.1a.

- Saddle points, with zero gradients in orthogonal directions, are distinctively positioned not to coincide with local extrema—depicted in Fig. 1.1a.
- Limit cycles may be inferred from crater curves on the surface of $p_s(x, y)$, where the density exhibits relative maxima—shown in Fig. 1.1b.

Nonetheless, exact solutions to the diffusion equations remain challenging due to increased dimensionality of the partial differential equation. This study introduces heuristic methodologies to address the stationary diffusion equations when traditional techniques fail.

The aim of this work is to thoroughly examine the qualitative behaviors of autonomous nonlinear systems using randomization, and to assess their steady-state dynamics through the exact solutions of the stationary diffusion equations.

The structure of the thesis proceeds as follows:

- Chapter 2 presents a comprehensive literature review on nonlinear systems and random vibrations, encompassing both historical background and recent progress.
- Chapter 3 provides a detailed exposition on the foundations of Brownian motion, nonlinear dynamics, and stochastic processes, including the derivation of the diffusion equation.
- Chapter 4 describes the method of randomization applied to nonlinear oscillators, analyses obtainable via the heuristic methods, and addresses the analytical nature of the solutions.
- Chapter 5 encapsulates significant findings and their relevance to understanding the complexities inherent in nonlinear dynamical systems.

Chapter 2

Literature Review

This chapter presents a comprehensive overview of the current literature on random vibration and nonlinear dynamical systems. It includes crucial insights from both historical works as well as recent developments in the areas of limit cycles and randomized nonlinear systems.

2.1 Random Vibration

Random vibration, which explores oscillatory motion under inherent uncertainties, has been shaped through the collective contributions of numerous researchers across generations. The theory integrates work in deterministic structural vibrations, probabilistic analysis of mechanical systems, and the study of stochastic processes.

The 17th-century investigations by Marin Mersenne and Galileo Galilei provided early momentum to the field with their independent studies on string vibrations [1]. Lord Rayleigh further elaborated on the deterministic theory of structural vibrations in *The Theory of Sound* (1877), focusing on the vibration and resonance of elastic solids and gases, as well as the propagation of acoustic waves in materials [2, 3]. A notable contribution from Rayleigh's work was identifying the fundamental frequency of vibration of a conservative system by applying the energy conservation principle.

A leap in understanding random vibrations followed the mathematical treatment of Brownian motion[1]. This phenomenon, observed by Robert Brown in 1827 and quantitatively explained by Albert Einstein in 1905, marked a significant advance in the mathematical analysis of random vibration [5, 6]. Wiener's subsequent introduction of spectral density as a key descriptor for stationary stochastic processes in 1930 has become foundational to the field [6].

In the early 20th century, the Langevin equation and the Fokker-Planck equation were developed to study Brownian motion [7]. Langevin introduced a random Markovian force to describe the random collisions between particles, leading to a stochastic differential equation

[1]Wiener process in physics and Brownian motion in mathematics are equivalent, as are Brownian motion in physics and the Ornstein-Uhlenbeck process in mathematics [4].

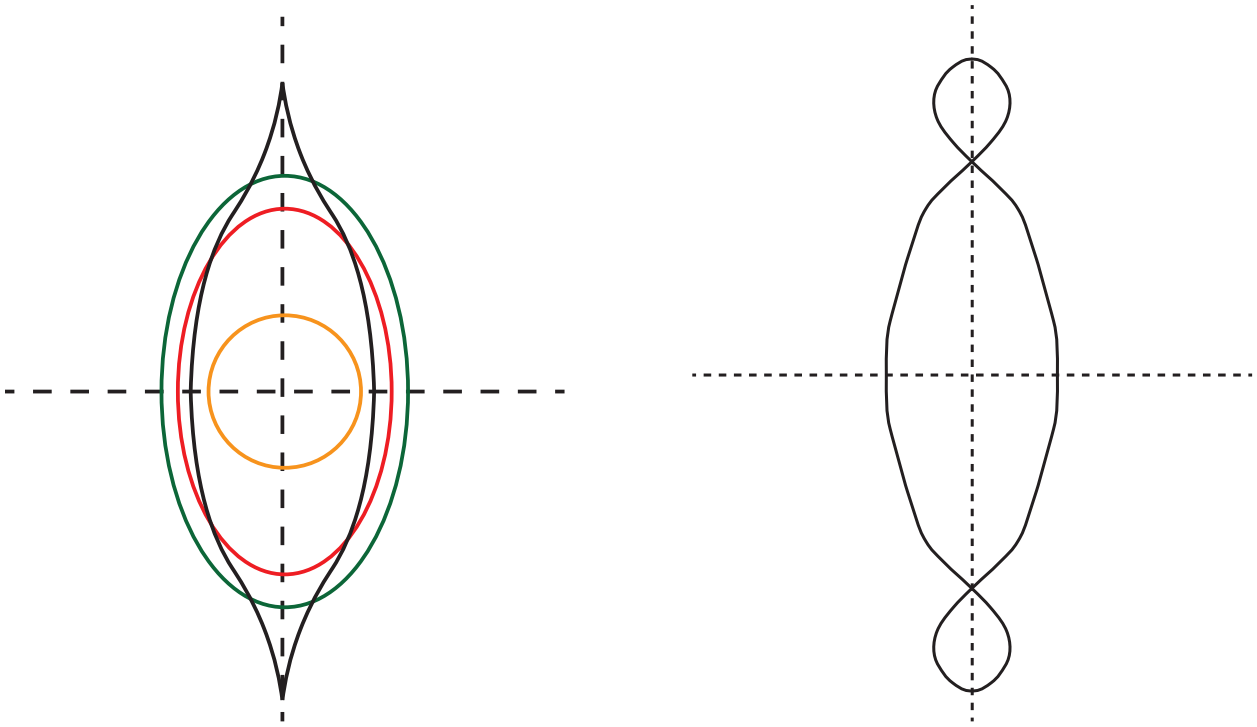

(a) The cusp-shaped orbits

(b) The loop-shaped orbit

Figure 2.1: Orbits of the Moon

for a Brownian particle [8]. Fokker introduced a partial differential equation that governs the probability density for the velocity of the Brownian particle under diffusion from interactions with the fluid [9]. This equation, now known as the Fokker-Planck equation or forward diffusion equation, also accounts for drift due to friction. The review by Uhlenbeck and Ornstein [10] introduced a Fokker-Planck equation associated with a constant diffusion coefficient and linear drift term, known as the Langevin equation. Wang and Uhlenbeck solved the diffusion equation for the Langevin equation using Fourier transform techniques [11][2].

2.2 Nonlinear Dynamical Systems

The contributions of Henri Poincaré in the domain of nonlinear dynamical systems substantially enhanced the understanding of motion related to celestial bodies. Among these enhancements is a refined understanding of the Moon's orbit, which demonstrates intricate interactions with both Earth and Sun. This refinement was achieved by Poincaré's sugges-

[2]Although it appears in a review paper, this example is considered original [12].

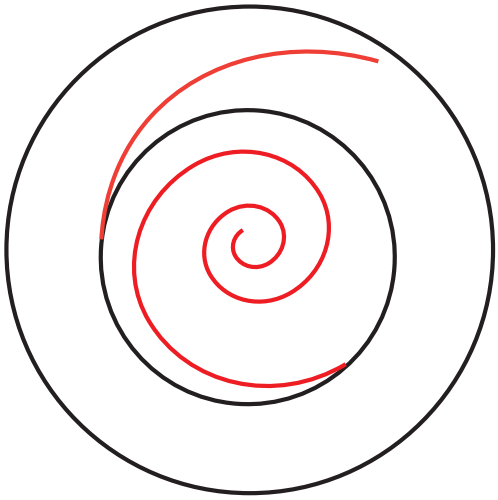

Figure 2.2: The limit cycle illustrated by Poincaré

tion of transitioning from a cusp-shaped orbit to a loop-shaped orbit, thereby providing a more precise periodic solution for moon's movements [13, 14] (see Fig. 2.1 [14]).

Moreover, the study conducted by Poincaré on limit cycles led to the creation of the first mathematical representations of a limit cycle, represented by a two-dimensional differential equation [15]:

$$\frac{dx}{x(x^2+y^2-1)-y(x^2+y^2+1)} = \frac{dy}{y(x^2+y^2-1)+x(x^2+y^2+1)}, \tag{2.1}$$

where the analytical form of the limit cycle is given by (Fig. 2.2 [15])

$$x^2+y^2=1. \tag{2.2}$$

George Duffing advanced to the field of mechanics, especially in the area of nonlinear dynamical systems, by examining mathematical and technical aspects of nonlinear adjustments to linear harmonic oscillators. Instances where a spring either stiffens or softens as it stretches were explored, which can be represented by incorporating a cubic term into the conventional linear Hooke's law [16]. The focus was on the following equation, encompassing both free oscillation and a harmonic forcing function [17]:

$$\frac{d^2x}{dt^2}+\chi\frac{dx}{dt}+\alpha x-\gamma x^3 = k\sin(\omega t). \tag{2.3}$$

The Duffing equation has been applied to understand various physical systems, including vibrating structures [18], electrical signal analysis of distribution lines [19], and modeling brain activity in biology [20].

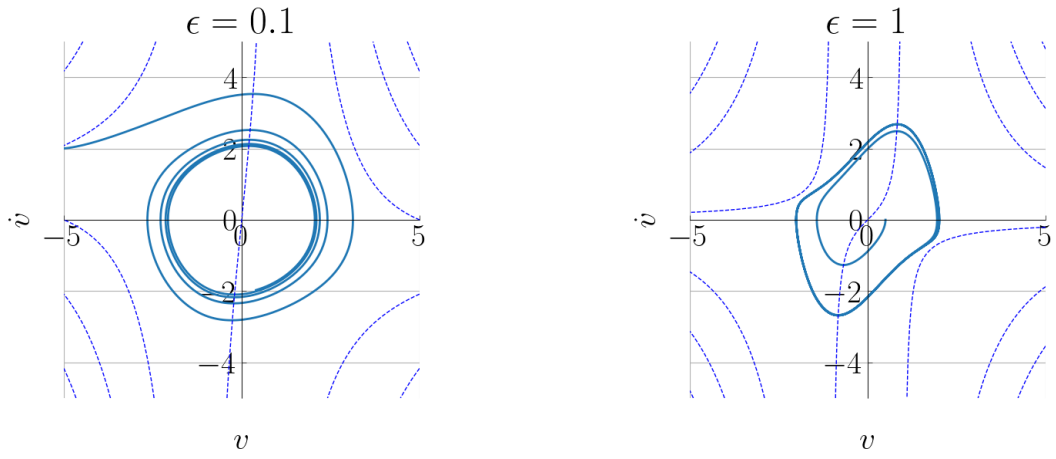

Figure 2.3: The Van der Pol limit cycle

Balthasar van der Pol's work in the 1920s marked the experimental study of nonlinear dynamical systems and chaos theory [21]. By working on the limit cycle of the Van der Pol oscillator [22], which is described by

$$\frac{d^2v}{dt^2} - \epsilon(1 - v^2)\dot{v} + v = 0, \tag{2.4}$$

the term *relaxation oscillation* emerged, indicating the deviation of the sinusoidal oscillation to diverging shapes of the oscillation, which form the limit cycle. This idea was further extended to other engineering applications, such as the modelling of heart-beat oscillation [23, 24]. The discovery of irregular noise, attributed to Van der Pol, is also considered as the first empirical observation of deterministic chaos [21].

Andronov and Pontryagin contributed to bifurcation theory. They introduced the concept of *structural stability*, which determines whether a system can maintain its behavior despite small alterations. This allowed them to identify points called structurally unstable points, where minor changes can lead to drastically different outcomes. Their work provided valuable insight into the behavior of dynamical systems near bifurcation points. [21, 25]

Edward Lorenz influenced the development of chaos theory by formulating the concept of the *strange attractor*, which is often used to demonstrate the behavior of chaotic systems. In a 1963 paper, it was revealed that a system exhibited varying outcomes when approximations were made for predicting weather and rounding off to different digits. The sensitivity to initial conditions was noted, suggesting that minimal variations in initial conditions might lead to significant disparities in the long-term system behavior [26].

2.3 Recent Developments

This section presents recent advancements in random vibrations and nonlinear dynamics, emphasizing the importance of multiple equilibria, limit cycles, and bifurcations in nonlinear systems.

Multiple equilibrium points play a crucial role in local stability analysis for nonlinear systems, which influences control system design in applications such as robotic motion tracking [27, 28] and neural network stability [29, 30]. However, identifying stability using Lyapunov methods can be challenging due to their inherent limitations, such as the difficulty of finding an appropriate Lyapunov function in the direct method and the inability to determine global stability in the indirect method.

Limit cycles are frequently observed in biological systems like heartbeat patterns [22, 31] and ecological interactions [32, 33], as well as engineering applications including robot locomotion [34–39] and power grid energy distribution [40]. Limit cycles assist in developing algorithms for robots to navigate safely around obstacles [41–44]. Although early research provided exact analytical forms of limit cycles [45, 46], later studies indicated that such descriptions are not always feasible [47–51], leading to the use of approximations and numerical models.

Comprehending equilibrium points and limit cycles is essential for analyzing bifurcations, as variations with system parameters can exhibit diverse qualitative behaviors [52]. Taking bifurcation into account in real-life scenarios proves to be practical, as it helps in prediction and control of system behavior under changing conditions. A notable example of the practical application of bifurcation analysis is in the design of stable rotordynamic systems, where avoiding bifurcation is crucial to ensure reliable performance and prevent failures [53, 54].

Randomization facilitates the qualitative analysis of nonlinear systems through stationary diffusion equations. Early research on solving these equations made significant progress [12, 55–61], but universal solutions remain elusive. Approximation strategies [62, 63] and machine learning techniques [64–67] offer potential improvements in solution accuracy. All the aforementioned studies have been limited to analyzing stochastic differential equations without considering the corresponding deterministic differential equations. This thesis introduces a framework that employs randomization to examine the qualitative behavior of deterministic nonlinear systems.

Chapter 3

Theoretical Background

This chapter presents the foundational theoretical concepts necessary for understanding the randomization of nonlinear dynamical systems.

3.1 Nonlinear Dynamical Systems

In the domain of classical mechanics, nonlinear dynamical systems are characterized as sets of second-order differential equations that do not adhere to the principle of linear superposition. The analysis within this thesis focuses on deterministic, autonomous systems described by the following equations:

$$\begin{aligned} \dot{x} &= a_1(x, y) \\ \dot{y} &= a_2(x, y), \end{aligned} \tag{3.1}$$

and in an alternative vector notation:

$$\dot{\mathbf{z}} = \boldsymbol{a}(\mathbf{z}), \tag{3.2}$$

where $\mathbf{z} = [x, y]^T$ symbolizes the state vector and $\boldsymbol{a}(\mathbf{z})$ denotes the system dynamics. Trajectories of the solution can be illustrated visually as curves in the phase plane, facilitating better understanding of the qualitative behavior of such systems. Further discussions will address Hamiltonian systems as employed in physics and will examine three distinct phenomena in nonlinear dynamical systems: multiple equilibrium points, limit cycles, and bifurcations.

3.2 Hamiltonian Systems

Hamiltonian systems, as a distinct category within nonlinear dynamical systems, feature prominently in classical mechanics. These systems are analyzed via the Lagrangian formalism in configuration space and the Hamiltonian formalism in phase space. Notably, phase space

trajectories of Hamiltonian systems constitute curves at constant values, absent temporal dependence within the Hamiltonian function.

The Hamiltonian function arises from the Legendre transformation of the Lagrangian $L(\boldsymbol{q}, \dot{\boldsymbol{q}}, t)$ [68]:

$$H(\boldsymbol{q}, \boldsymbol{p}) = \sum_{i=1}^{n} p_i \dot{q}_i - L(\boldsymbol{q}, \dot{\boldsymbol{q}}, t), \tag{3.3}$$

where $\boldsymbol{q}$ encapsulates the configuration variables and $\boldsymbol{p}$ the conjugate momenta. The momenta are defined as

$$p_i = \frac{\partial L}{\partial \dot{q}_i}, \quad i = 1, \ldots, n. \tag{3.4}$$

The Lagrangian function is most commonly expressed as the difference between kinetic and potential energy:

$$L(\boldsymbol{q}, \dot{\boldsymbol{q}}, \boldsymbol{t}) = T - V, \tag{3.5}$$

where T is the kinetic energy and V is the potential energy of the system. Canonical Hamiltonian equations offer a framework for describing the system dynamics:

$$\begin{aligned} \dot{q}_i &= \frac{\partial H}{\partial p_i}, \quad i = 1, \ldots, n, \\ \dot{p}_i &= -\frac{\partial H}{\partial q_i}, \quad i = 1, \ldots, n, \end{aligned} \tag{3.6}$$

which constitute phase space trajectories of Hamiltonian systems. The Hamiltonian is not always equal to the total energy of the system, but it is conserved if the Hamiltonian is not explicitly dependent on time. This can be shown by taking the time derivative of the Hamiltonian function (3.3):

$$\frac{dH}{dt} = \sum_{i=1}^{n} \frac{\partial H}{\partial q_i} \dot{q}_i + \sum_{i=1}^{n} \frac{\partial H}{\partial p_i} \dot{p}_i + \frac{\partial H}{\partial t}. \tag{3.7}$$

Within this framework, the first two terms negate each other under the canonical equations, and the final term vanishes if the Hamiltonian excludes dependency on time.

Recall that the nonlinear system of interest, defined in Eq. (1.1), is as follows:

$$\ddot{x} + \epsilon \alpha(x, \dot{x}) \dot{x} + \beta(x, \dot{x}) = 0.$$

Using the notations $\dot{x} = y$, $p = \dot{x}$, and $q = x$, and assuming an absence of damping ($\epsilon = 0$), the conservative Hamiltonian function is represented as

$$H(x, y) = y^2 - L(x, y). \tag{3.8}$$

This representation provides a description of the system dynamics through the Hamiltonian:

$$\begin{aligned} \dot{x} &= \frac{\partial H}{\partial y} = a_1(x, y), \\ \dot{y} &= -\frac{\partial H}{\partial x} = a_2(x, y). \end{aligned} \tag{3.9}$$

These expressions will be consistently applied throughout this thesis, except where otherwise specified.

Example 3.2.1. Consider a linear harmonic undamped oscillator of the form

$$\ddot{x} + x = 0.$$

The Hamiltonian function of this system is

$$H(x, y) = y^2 - \left(\frac{1}{2}y^2 - \frac{1}{2}x^2\right) = \frac{1}{2}x^2 + \frac{1}{2}y^2.$$

Therefore, the Hamiltonian is equal to the total energy of the system, and it is conserved.

Example 3.2.2. Consider an undamped nonlinear pendulum equation of the form:

$$\ddot{x} + \sin(x) = 0.$$

This can be written in the phase space as

$$\dot{x} = y = \frac{\partial H}{\partial y},$$
$$\dot{y} = -\sin(x) = -\frac{\partial H}{\partial x}.$$

Integration of the first equation gives

$$H(x, y) = \frac{1}{2}y^2 + c_1(x),$$

where $c_1(x)$ is an arbitrary function of x. Taking the derivative of $H(x, y)$ with respect to x and equating it to $-\sin(x)$ yields

$$\frac{\partial H}{\partial x} = \frac{\mathrm{d}c_1}{\mathrm{d}x} = \sin(x).$$

Therefore, the Hamiltonian function is

$$H(x, y) = \frac{1}{2}y^2 - \cos(x) + C,$$

where C is a constant.

3.3 Qualitative Behaviors of Nonlinear Systems

Investigating quantitative behaviors in nonlinear dynamical systems poses significant challenges due to the inherent difficulty of obtaining analytical solutions. However, it is possible to study the qualitative behaviors of these systems by examining equilibrium points, limit cycles, and bifurcations.

3.3.1 Multiple Equilibrium Points

Equilibrium points exist where the state of the system remains constant (i.e., $\dot{x} = 0$ and $\dot{y} = 0$). Techniques used to analyze equilibrium points of nonlinear dynamical systems align with approaches employed for linear dynamical systems.

Equilibrium points can be classified through the analysis of the Jacobian matrix of system dynamics, $\boldsymbol{a}(\mathbf{z})$, evaluated at the equilibrium points. The Jacobian matrix definition is as follows [69]:

$$\boldsymbol{J}(\mathbf{z}_{eq}) = \left.\frac{\partial \boldsymbol{a}}{\partial \mathbf{z}}\right|_{\mathbf{z}=\mathbf{z}_{eq}} = \begin{bmatrix} \frac{\partial a_1}{\partial x}(x_{eq}, y_{eq}) & \frac{\partial a_1}{\partial y}(x_{eq}, y_{eq}) \\ \frac{\partial a_2}{\partial x}(x_{eq}, y_{eq}) & \frac{\partial a_2}{\partial y}(x_{eq}, y_{eq}) \end{bmatrix}, \tag{3.10}$$

where $\mathbf{z}_{eq} = (x_{eq}, y_{eq})$ represents the equilibrium point. If the real part of eigenvalues of the Jacobian matrix is nonzero, then such an equilibrium point is called a hyperbolic equilibrium point. Hyperbolic equilibria can be classified into three types: node, focus (spiral point), and saddle point. Hyperbolic equilibrium points hold particular interest because local qualitative behavior can be determined by examining eigenvalues of the Jacobian matrix.

Eigenvalue analysis of the Jacobian matrix is analogous to the eigenvalue analysis of the system matrix in linear dynamical systems. For example, if all eigenvalues are real and negative, then the equilibrium point is a stable node. On the other hand, if eigenvalues are real and positive, it corresponds to an unstable node. Complex eigenvalues with non-zero real parts indicate a spiral point, and distinct real eigenvalues with different signs represent a saddle point.

Example 3.3.1. Consider a damped nonlinear pendulum of the form:

$$\ddot{x} + \epsilon\dot{x} + \sin(x) = 0, \tag{3.11}$$

where ϵ is a damping constant. This can be written in the phase space as

$$\begin{aligned} \dot{x} &= y, \\ \dot{y} &= -\epsilon y - \sin(x). \end{aligned} \tag{3.12}$$

Equilibrium points for this system are $(x_{eq}, y_{eq}) = (\pm n\pi, 0)$, and the Jacobian matrix of the system is

$$\boldsymbol{J}(x) = \begin{bmatrix} 0 & 1 \\ -\cos(x) & -\epsilon \end{bmatrix}.$$

Eigenvalues of the Jacobian matrix are

$$\lambda_{1,2} = -\frac{\epsilon}{2} \pm \sqrt{\frac{\epsilon^2}{4} - \cos(x)}.$$

For $0 < \epsilon < 2$, two equilibrium point types occur: saddle points with odd n having real eigenvalues of opposite signs, and stable spiral points with even n having complex conjugate

eigenvalues with negative real parts. For $\epsilon > 2$, stable nodes emerge when n is even, and saddle points when n is odd.

Although the eigenvalue analysis of the Jacobian matrix permits the discovery of a local qualitative behavior, this method is unsuitable for determining global qualitative behavior. Furthermore, the eigenvalues obtained from the Jacobian matrix do not provide an accurate representation of the behavior, as the eigenvalues are obtained from the linearized system.

To accurately analyze global qualitative behavior of the system, further investigation of nullclines and isoclines of the system is required [70]. Analyzing nullclines and isoclines for nonlinear dynamical systems is a challenging task, as nullclines/isoclines are not straight lines and only provide information on derivatives of state variables. In the following sections, an approach to study equilibria and assess the global qualitative behavior using randomization will be discussed, which serves as a significant contribution of this thesis.

3.3.2 Limit Cycles

A limit cycle is a closed, isolated trajectory unique to nonlinear dynamical systems. It arises from periodic solutions where the system state returns to its initial position after completing a period. In contrast, oscillatory linear systems generate closed, but non-isolated trajectories. Analysis of limit cycles generates valuable insights into the long-term behavior of system trajectories, which can be applied to diverse fields such as control systems design [35, 38, 71], trajectory planning [41, 42], and vibration analysis [72].

The Poincaré-Bendixson theorem [73] postulates that any bounded trajectory not converging toward an equilibrium point eventually approaches a closed orbit as $t \to \infty$. Moreover, the Bendixson-Dulac theorem [74] asserts that a two-dimensional system cannot contain a closed orbit if the dynamics vector $\boldsymbol{a}$ maintains zero divergence, i.e., $\nabla \cdot \boldsymbol{a} = 0$. Although these theorems hold theoretical significance, they frequently prove insufficient for confirming the existence of limit cycles. Section 4.5.2 explores an alternative qualitative method to verify the presence of limit cycles using a projected crater curve. In the subsequent sections, a brief discussion of the classification of limit cycles and their analytical forms in nonlinear dynamical systems is presented.

Classification of Limit Cycles

Limit cycles can be categorized into three distinct types based on stability: stable, unstable, and semi-stable.

Stable limit cycles cause system trajectories converging to a repeating pattern over time, as illustrated in Fig. 3.1a. Unstable limit cycles exhibit diverging system trajectories that do not settle into a repeating pattern, demonstrated in Fig. 3.1b. Semi-stable limit cycles show both converging and diverging behaviors, suggesting that the behavior of the system may settle into a repeating pattern from one direction but diverge from another, as presented in Fig. 3.1c.

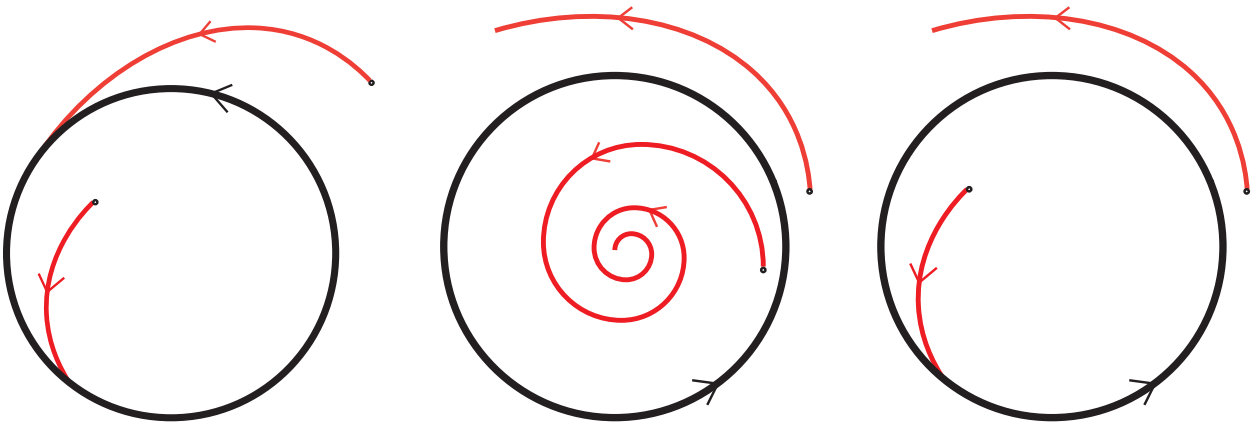

(a) Stable limit cycle: $\dot{r} = -r(r^2 - 1), \quad \dot{\theta} = 1$

(b) Unstable limit cycle: $\dot{r} = r(r^2 - 1), \quad \dot{\theta} = 1$

(c) Semi-stable limit cycle: $\dot{r} = r(r^2 - 1)^2, \quad \dot{\theta} = 1$

Figure 3.1: Classification of limit cycles

Analytical Form of Limit Cycles

The analytical form of limit cycles in nonlinear dynamical systems can be derived in a few cases. Three types of nonlinear dynamical systems of particular interest include (i) the Van der Pol-Rayleigh oscillator, (ii) a nonlinear oscillator with an elliptical limit cycle, and (iii) a Liénard-type oscillator.

Van der Pol-Rayleigh Oscillator

For a nonlinear oscillator of the form:

$$\ddot{x} - \epsilon\big(1 - x^2 - \dot{x}^2\big)\dot{x} + x = 0, \tag{3.13}$$

where ϵ is a damping constant, it is observed that the Van der Pol-Rayleigh equation admits an exact harmonic solution for any value of ϵ [46]:

$$x(t) = \cos(t + \phi). \tag{3.14}$$

Assuming $\phi = 0$ without loss of generality, a Hamiltonian can be derived from Eq. (3.9):

$$H = \frac{1}{2}x^2 + \frac{1}{2}\dot{x}^2, \tag{3.15}$$

where H is identical to the total energy of the undamped system. The time derivative of H can be computed as follows:

$$\frac{dH}{dt} = \frac{d}{dt}\left(\frac{1}{2}x^2 + \frac{1}{2}\dot{x}^2\right). \tag{3.16}$$

Using Eq. (3.13), it can be deduced that

$$\frac{dH}{dt} = \epsilon\big(1 - x^2 - \dot{x}^2\big)\dot{x}^2 = \epsilon(1 - 2H)\dot{x}^2 \tag{3.17}$$

Separating the equation and integrating both sides results in

$$\int \frac{dH}{1 - 2H} = -\frac{1}{2}\ln(1 - 2H) = \int \epsilon\dot{x}^2 dt. \tag{3.18}$$

As $t \to \infty$ in steady state, Eq. (3.18) becomes

$$1 - 2H = \lim_{t\to\infty}\left(C\exp\left(-2\epsilon\int_0^t \dot{x}^2 dt\right)\right) = 0. \tag{3.19}$$

Since H is constant, the energy of the system remains constant for motion on the limit cycle. Setting $H = 1/2$ results in the limit cycle trajectory:

$$x^2 + \dot{x}^2 = 1. \tag{3.20}$$

Elliptical Limit Cycle

A nonlinear oscillator of the form:

$$\ddot{x} - \epsilon\left(1 - \frac{x^2}{a^2} - \frac{\dot{x}^2}{b^2}\right)\dot{x} + \frac{b^2}{a^2}x = 0, \tag{3.21}$$

where ϵ is a constant, presents a limit cycle trajectory that is elliptical in nature:

$$x(t) = a\cos\left(\frac{bt}{a}\right) = a\cos(\omega t), \tag{3.22}$$

where $\omega = b/a$ can be interpreted as the angular frequency of the oscillator.

The trajectory of the oscillator forms an ellipse, demonstrated through the following derivation. By inserting (3.22) into (3.21), the result is

$$\ddot{x} + \frac{b^2}{a^2}x = -\left(\frac{b}{a}\right)^2 a\cos(\omega t) + \frac{b^2}{a}\cos(\omega t) = 0 \tag{3.23}$$

and

$$1 - \frac{x^2}{a^2} - \frac{\dot{x}^2}{b^2} = 1 - \cos^2(\omega t) - \frac{1}{b^2}\left(\frac{b}{a}\right)^2 a^2\sin^2(\omega t) = 0. \tag{3.24}$$

Thus, the trajectory of

$$\frac{x^2}{a^2} + \frac{\dot{x}^2}{b^2} = 1 \tag{3.25}$$

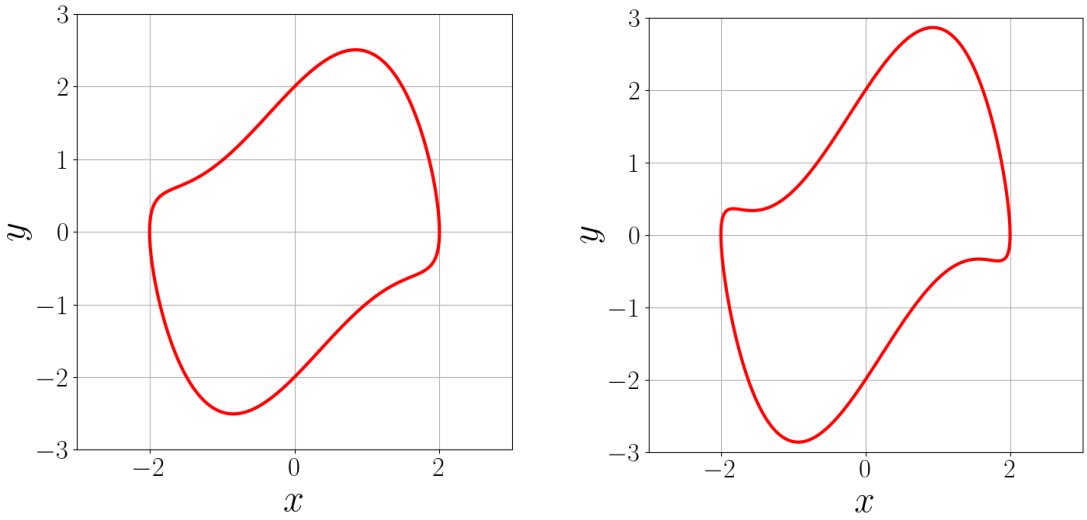

(a) $\epsilon = 1$ (b) $\epsilon = 1.5$

Figure 3.2: Analytical limit cycles of the Liénard-type oscillator

satisfies the equation of an ellipse. By scaling time with

$$\tau = \frac{b}{a}t, \tag{3.26}$$

Equation (3.21) can be rewritten as

$$\frac{\mathrm{d}^2x}{\mathrm{d}\tau^2} - \frac{\epsilon b}{a}\left(1 - \frac{x^2}{a^2} - \frac{1}{a^2}\left(\frac{\mathrm{d}x}{\mathrm{d}\tau}\right)^2\right)\frac{\mathrm{d}x}{\mathrm{d}\tau} + x = 0, \tag{3.27}$$

where the following relations are used:

$$\dot{x} = \frac{\mathrm{d}x}{\mathrm{d}t} = \frac{\mathrm{d}x}{\mathrm{d}\tau}\frac{\mathrm{d}\tau}{\mathrm{d}t} = \frac{\mathrm{d}x}{\mathrm{d}\tau}\frac{b}{a},$$
$$\ddot{x} = \frac{\mathrm{d}^2x}{\mathrm{d}t^2} = \frac{b}{a}\frac{\mathrm{d}^2x}{\mathrm{d}\tau^2}\frac{\mathrm{d}\tau}{\mathrm{d}t} = \left(\frac{b}{a}\right)^2\frac{\mathrm{d}^2x}{\mathrm{d}\tau^2}.$$

When the time is scaled, Eq. (3.21) evolves into Eq. (3.13), and the limit cycle is a circle of radius a for all $\epsilon > 0$.

Liénard-type Oscillator

The nonlinear oscillator of form [45, 48]:

$$\ddot{x} + \epsilon\big(x^2 - 1\big)\dot{x} + \frac{\epsilon^2}{16}x^3(x^2 - 4) + x = 0, \quad 0 < |\epsilon| < 2 \tag{3.28}$$

exhibits a limit cycle in algebraic form as follows (Fig. 3.2):

$$y^2 + \frac{\epsilon}{2}x\big(x^2-4\big)y + (x^2-4)\left(\frac{\epsilon^2}{16}x^2\big(x^2-4\big)+1\right) = 0, \quad y = \dot{x}. \tag{3.29}$$

Equation (3.29) can be verified as follows. First, the derivative of Eq. (3.29) with respect to t is

$$\left(2y + \frac{\epsilon}{2}x\big(x^2-4\big)\right)\dot{y} = -\frac{\epsilon}{2}\Big(\big(3x^2-4\big)y^2\Big) - \frac{\epsilon^2}{16}\Big(\big(x^2-4\big)\big(6x^3-8x\big)+2x\Big)y. \tag{3.30}$$

Inserting Eq. (3.30) into left side of Eq. (3.28) yields

$$\begin{aligned} -\frac{\epsilon}{2}\Big(\big(3x^2-4\big)y^2\Big) - \frac{\epsilon^2}{16}\Big(\big(x^2-4\big)\big(6x^3-8x\big)+2x\Big)y \\ + \left(2y + \frac{\epsilon}{2}x\big(x^2-4\big)\right)\left(\epsilon\big(x^2-1\big)y + \frac{\epsilon^2}{16}x^3(x^2-4) + x\right) = 0. \end{aligned} \tag{3.31}$$

Existence of Periodic Solutions

In this section, criteria for the existence of periodic solutions in a specific class of nonlinear systems will be introduced briefly. These criteria stem from the Poincaré-Bendixson theorem [75].

Consider a nonlinear system of the form:

$$\ddot{x} + f(x,\dot{x})\dot{x} + g(x) = 0, \tag{3.32}$$

where $f(x,\dot{x})$ and $g(x)$ are continuous functions. Unlike the previous Liénard-type oscillator, the damping coefficient functions depend on x and $\dot{x}$. Rewriting the equation in state space form yields

$$\begin{aligned} \dot{x} &= y, \\ \dot{y} &= -f(x,y)y - g(x). \end{aligned} \tag{3.33}$$

The following theorem provides a sufficient condition for the existence of periodic solutions in Eq. (3.32) [75]:

- There exists a positive constant r such that $f(x,y) > 0$ for all $x^2 + y^2 > r^2$.
- $f(0,0) < 0$.
- $g(0) = 0$, and $g(x) > 0$ for all $x > 0$, and $g(x) < 0$ for all $x < 0$.
- $\int_0^x g(\xi)d\xi$ goes to infinity as x goes to infinity.

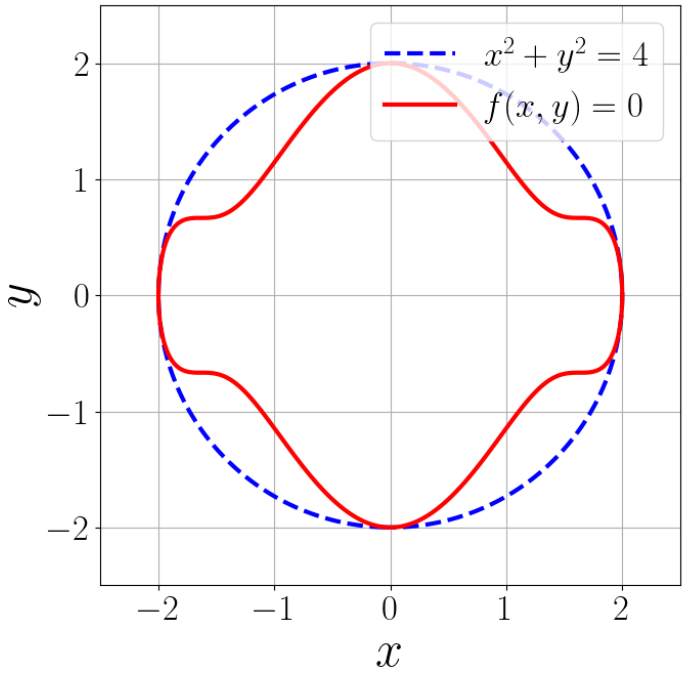

Figure 3.3: First condition of the existence theorem in Example 3.3.2 with $\epsilon = \sqrt{3}$

Example 3.3.2. Consider a nonlinear system of form:

$$\ddot{x} + \epsilon \left(4y^2 + \frac{\left(x^2 - 4\right)\left(\epsilon^2 x^2 \left(x^2 - 4\right) + 16\right)}{4} \right) y + x \left(\frac{3\epsilon^2 x^4}{16} - \epsilon^2 x^2 + \epsilon^2 + 1 \right) = 0 \tag{3.34}$$

where $y = \dot{x}$ and ϵ is a positive constant. By applying the existence theorem, it can be deduced that the system exhibits a periodic solution. The first condition is satisfied since, for any $r > 2$, $f(x, y) > 0$ always holds true (Fig. 3.3). Additionally,

$$f(0, 0) = -16\epsilon < 0, \tag{3.35}$$

which satisfies the second condition. The fourth condition is met as the polynomial function goes to infinity as x goes to infinity.

The third condition is fulfilled if

$$\frac{3\epsilon^2 x^4}{16} - \epsilon^2 x^2 + \epsilon^2 + 1 > 0, \tag{3.36}$$

since x consistently meets the third condition. Analyzing the minima of the right-hand side of Eq. (3.36) reveals

$$x_{\min} = \pm\sqrt{\frac{8}{3}} \tag{3.37}$$

and the value of the function at the minima is

$$y_{\min} = -\frac{\epsilon^2}{3} + 1. \tag{3.38}$$

Therefore, Eq. (3.36) is satisfied if

$$0 < \epsilon < \sqrt{3}, \tag{3.39}$$

where $\epsilon = \sqrt{3}$ is a bifurcation point. Consequently, the system possesses a periodic solution for $\epsilon < \sqrt{3}$.

Although the existence criteria do not confirm the presence of a periodic solution for $\epsilon \geq \sqrt{3}$, the system maintains a periodic solution for $\epsilon \geq \sqrt{3}$, as displayed in Fig. 3.4. This limitation can be resolved by employing randomization, which will be discussed in the subsequent chapter.

3.3.3 Bifurcation

Bifurcation represents a change in the behavior of a dynamical system due to parameter variations. Bifurcation can be classified into two major categories: local bifurcation and global bifurcation. Local bifurcation occurs when an equilibrium point of the system experiences a qualitative change locally, such as in a saddle-node bifurcation or a Hopf bifurcation. A saddle-node bifurcation takes place if the equilibrium point corresponds to a zero eigenvalue, while a Hopf bifurcation occurs when the equilibrium point is associated with a pair of purely imaginary complex conjugate eigenvalues. Global bifurcation arises when periodic trajectories align with equilibrium points, such as in a homoclinic bifurcation.

In this section, an example involving bifurcation is introduced. The subsequent chapter includes the utilization of randomization for analyzing such bifurcations.

Example 3.3.3. Recalling the extended Liénard equation in Eq. (3.32):

$$\ddot{x} + f(x, \dot{x})\dot{x} + g(x) = 0,$$

where

$$f(x, \dot{x}) = \epsilon\left(4\dot{x}^2 + \frac{\big(x^2-4\big)\Big(\epsilon^2x^2\big(x^2-4\big)+16\Big)}{4}\right), \quad g(x) = x\left(\frac{3\epsilon^2x^4}{16} - \epsilon^2x^2 + \epsilon^2 + 1\right). \tag{3.40}$$

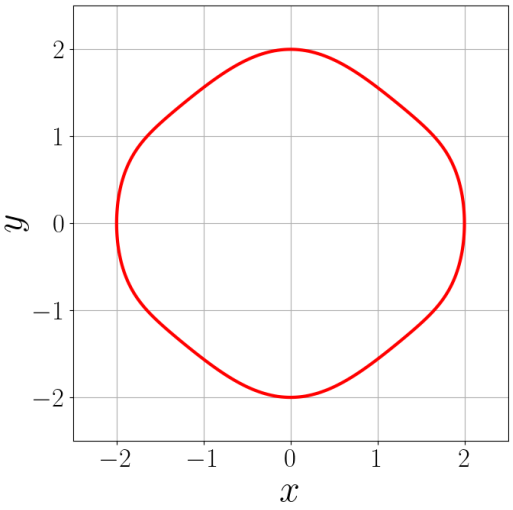

(a) $\epsilon = 1$

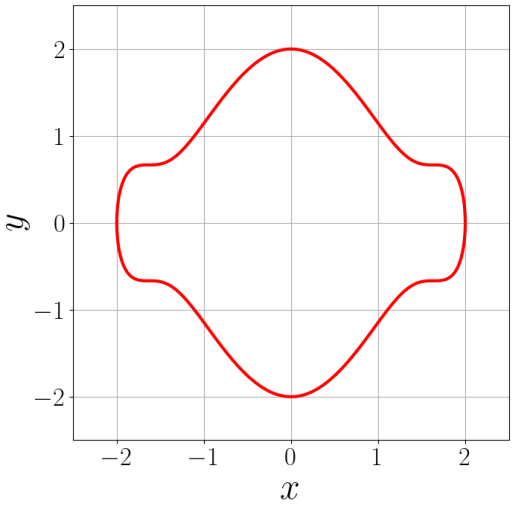

(b) $\epsilon = \sqrt{3}$, non-hyperbolic equilibria

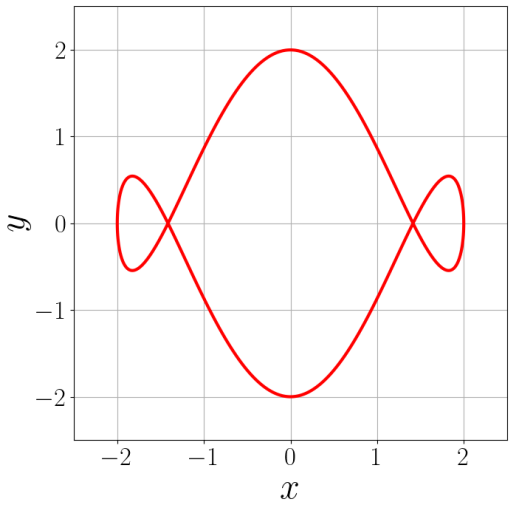

(c) $\epsilon = 2$, homoclinic bifurcation

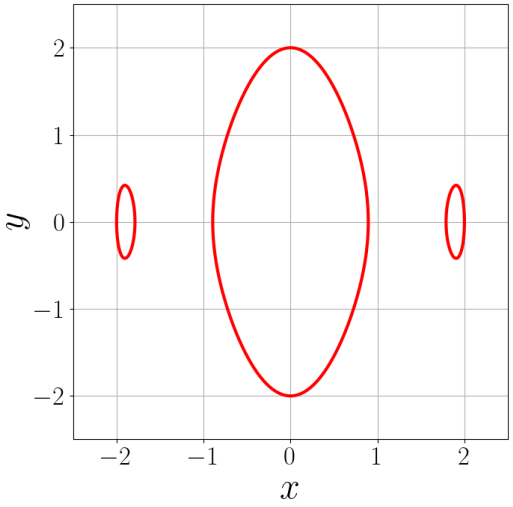

(d) $\epsilon = 2.5$

Figure 3.4: Bifurcation of the extended Liénard-type oscillators

The equilibrium points of the system and their associated eigenvalues of the Jacobian matrix are

$$
\begin{aligned}
&x_{eq,0} = 0, \quad y_{eq,0} = 0, \quad \lambda_{1,2}(x_{eq,0}, y_{eq,0}) = 8\epsilon \pm \sqrt{63\epsilon^2 - 1},\\
&x_{eq,1} = \frac{-\sqrt{3}\sqrt{8 - \frac{4\sqrt{\mu^2-3}}{\mu}}}{3}, \quad y_{eq,1} = 0,\\
&\lambda_{1,2}(x_{eq,1}, y_{eq,1}) = \frac{-16\mu^3}{27} - \frac{16\mu^2\sqrt{\mu^2-3}}{27} + \frac{8\mu}{3} + \frac{16\sqrt{\mu^2-3}}{9}\\
&\pm \frac{2\sqrt{-243\mu^2 + 486\mu\sqrt{\mu^2-3} + 16\left(2\mu^3 + 2\mu^2\sqrt{\mu^2-3} - 9\mu - 6\sqrt{\mu^2-3}\right)^2 + 729}}{27},\\
&x_{eq,2} = \frac{\sqrt{3}\sqrt{8 - \frac{4\sqrt{\mu^2-3}}{\mu}}}{3}, \quad y_{eq,2} = 0,\\
&\lambda_{1,2}(x_{eq,2}, y_{eq,2}) = \frac{-16\mu^3}{27} - \frac{16\mu^2\sqrt{\mu^2-3}}{27} + \frac{8\mu}{3} + \frac{16\sqrt{\mu^2-3}}{9}\\
&\pm \frac{2\sqrt{-243\mu^2 + 486\mu\sqrt{\mu^2-3} + 16\left(2\mu^3 + 2\mu^2\sqrt{\mu^2-3} - 9\mu - 6\sqrt{\mu^2-3}\right)^2 + 729}}{27},\\
&x_{eq,3} = \frac{-\sqrt{3}\sqrt{8 + \frac{4\sqrt{\mu^2-3}}{\mu}}}{3}, \quad y_{eq,3} = 0,\\
&\lambda_{1,2}(x_{eq,3}, y_{eq,3}) = \frac{-16\mu^3}{27} - \frac{16\mu^2\sqrt{\mu^2-3}}{27} + \frac{8\mu}{3} - \frac{16\sqrt{\mu^2-3}}{9}\\
&\pm \frac{2\sqrt{-243\mu^2 + 486\mu\sqrt{\mu^2-3} + 16\left(2\mu^3 + 2\mu^2\sqrt{\mu^2-3} - 9\mu - 6\sqrt{\mu^2-3}\right)^2 + 729}}{27},\\
&x_{eq,4} = \frac{\sqrt{3}\sqrt{8 + \frac{4\sqrt{\mu^2-3}}{\mu}}}{3}, \quad y_{eq,4} = 0,\\
&\lambda_{1,2}(x_{eq,4}, y_{eq,4}) = \frac{-16\mu^3}{27} - \frac{16\mu^2\sqrt{\mu^2-3}}{27} + \frac{8\mu}{3} - \frac{16\sqrt{\mu^2-3}}{9}\\
&\pm \frac{2\sqrt{-243\mu^2 + 486\mu\sqrt{\mu^2-3} + 16\left(2\mu^3 + 2\mu^2\sqrt{\mu^2-3} - 9\mu - 6\sqrt{\mu^2-3}\right)^2 + 729}}{27}.
\end{aligned}
\tag{3.41}
$$

Figure 3.4 showcases the limit cycle of the extended Liénard-type oscillator for various values of ϵ. Two non-hyperbolic equilibrium points with a zero eigenvalue at $\epsilon = \sqrt{3}$ can be

observed, and each equilibrium point diverges to one saddle point and one unstable focus when $\epsilon > \sqrt{3}$. The zero eigenvalue can be confirmed from Eq. (3.41):

$$\lambda_1 = \frac{-16\mu^3}{27} + \frac{8\mu}{3} + \frac{-729 + 2\sqrt{16(2\mu^3 - 9\mu)^2} + 729}{27} = 0. \tag{3.42}$$

A homoclinic bifurcation takes place at $\epsilon = 2$, where the limit cycle of the system coincides with the equilibrium points $(\pm\sqrt{2}, 0)$. Once the system surpasses the homoclinic bifurcation, two additional limit cycles emerge with $\epsilon > 2$, as displayed in Fig. 3.4.

In the next chapter, a novel approach to assess the qualitative behavior of nonlinear dynamical systems through randomization will be introduced. This delves into the fundamental principles of Brownian motion, provided in the subsequent section.

3.4 Theory of Brownian Motion

The theory of Brownian motion is a key concept within the field of stochastic processes. The derivation of the diffusion equation holds particular importance as it establishes the foundation for the framework of randomization.

In order to derive the diffusion equation, weakly stationary stochastic processes are assumed. In these processes, the mean remains constant, and the correlation between two random variables is based solely on their time difference. Moreover, the randomized dynamical system relies on a Markov process—a concept that will be elaborated upon in the following section.

3.4.1 Markov Processes

A Markov process $X(t)$ represents a stochastic process in which the probability of the future depends solely on the present state, not on the sequence of events that preceded it. This means that

$$P(X(t_n) \leq x_n | x_1, \ldots, x_{n-1}) = P(X(t_n) \leq x_n | x_{n-1}), \tag{3.43}$$

where $t_n > t_{n-1} > \cdots > t_1$. If $X(t)$ is a Markov process, any two increments of different time interval are independent. The time intervals must be non-overlapping, for instance, $X(t_n) - X(t_{n-1})$ and $X(t_2) - X(t_1)$ are independent given that $t_n > t_{n-1} \geq t_2 > t_1$.

The Markov property is an important characteristic for simplifying the analysis of the process. For example, the Markov property is used to derive the solution of the diffusion equation, also known as the Fokker-Planck equation. It is also worth noting that a nonlinear system excited by white noise is a Markov process, which is a pivotal statement when applying randomization. White noise $W(t)$ itself is not a Markov process because it is incoherent in the sense that $W(t_1)$ and $W(t_2)$ are uncorrelated for any two points $t_1 \neq t_2$. In the case of white noise, neither past nor present events influence future events.

Markov processes can be fully characterized with the concept of transition probability. The transition probability distribution, with continuous t and $X(t)$, takes the form of a conditional probability:

$$P(X(t) \leq x | X(t_0) = x_0), \tag{3.44}$$

where x_0 denotes an initial time. If Eq. (3.44) is differentiable, transition probability density is

$$p(x, t|x_0, t_0) = \frac{\partial}{\partial x} P(X(t) \leq x | X(t_0) = x_0). \tag{3.45}$$

Recalling the joint probability density (B.1) and assuming initial probability density $p(x_1)$, the joint probability density can be written as

$$p(x_1, t_1; x_2, t_2; \ldots; x_n, t_n) = p(x_1, t_1) p(x_n, t_n | x_{n-1}, t_{n-1}) \ldots p(x_2, t_2 | x_1, t_1). \tag{3.46}$$

One can demonstrate that a Markov process is also Markovian in reverse, i.e., for arbitrary instants $t_1 < t_2 < \cdots < t_n$, the transition probability satisfies

$$p(x_1, t_1 | x_2, t_2; x_3, t_3; \ldots; x_n, t_n) = p(x_1, t_1 | x_2, t_2). \tag{3.47}$$

3.4.2 Chapman-Kolmogorov Equation

Given a Markov process $X(t)$ with transition probability density $p(x, t|y, s)$, where $s < t$, and considering an intermediate state between the starting state x_1 at time t_1 and the end state x_2 at time t_2, the probability density can be written as

$$p(x_2, t_2; x_1, t_1) = \int_{-\infty}^{\infty} p(x_2, t_2; x, t; x_1, t_1) dx = \int_{-\infty}^{\infty} p(x_2, t_2 | x, t) p(x, t | x_1, t_1) p(x_1, t_1) dx \tag{3.48}$$

Since the x_1 and t_1 do not depend on x, dividing both sides by $p(x_1, t_1)$ results in

$$p(x_2, t_2 | x_1, t_1) = \frac{p(x_2, t_2; x_1, t_1)}{p(x_1, t_1)} = \int_{-\infty}^{\infty} p(x_2, t_2 | x, t) p(x, t | x_1, t_1) dx. \tag{3.49}$$

The obtained equation is known as the Chapman-Kolmogorov equation or Smoluchowski equation, which acts as a conservation law for probability. It should be noted that the presence of a Markov process is a sufficient condition for the Chapman-Kolmogorov equation, although the reverse does not always hold true. If the underlying Markov process is a diffusion process, the Chapman-Kolmogorov equation can be formulated as a parabolic partial differential equation, called a diffusion equation. The solution of the diffusion equation provides the transition probability density $p(x, t|y, s)$, which fully determines the response of the given system.

An *irreducible* Markov process has all its states reachable from any other state and is *ergodic* if it returns to every state it previously visited with a probability of one as time progresses. When both conditions are satisfied, the process entails an equilibrium distribution

independent of the initial distribution, which implies that

$$\lim_{t\to\infty} p(x,t|y,s) = p_s(x), \qquad \int_{-\infty}^{\infty} p_s(x)dx = 1. \tag{3.50}$$

This stationary probability density function $p_s(x)$ is independent of the initial position x_0 and t; determining it can assist in the analysis of deterministic nonlinear oscillators with the framework of randomization.

3.4.3 Diffusion Processes

The diffusion equation is important to understand and successfully utilize the method of randomization, where the drift and diffusion coefficients are directly related to the coefficients of a randomized dynamical system.

A physical system modeled by a Markov process can be classified as a diffusion process when it satisfies the diffusion assumptions, illustrated in Eq. (3.52). Considering a Markov process $X(t)$ with a transition probability function $p(x,t|y,s)$, where $s < t$, and taking a time increment Δt, the moments of change in the spatial coordinate are given by

$$m_n(x,t) = \int_{-\infty}^{\infty} (z-x)^n p(z,t+\Delta t|x,t)dz = \mathbb{E}\big[(\Delta X)^n | X(t) = x\big]. \tag{3.51}$$

In order for the Markov process to be classified as a diffusion process, the following diffusion assumptions must hold:

$$\begin{aligned}
\lim_{\Delta t\to 0} \frac{1}{\Delta t} m_1(x,t) &= \lim_{\Delta t\to 0} \frac{1}{\Delta t}\mathbb{E}\big[\Delta X|X(t)=x\big] = m(x,t),\\
\lim_{\Delta t\to 0} \frac{1}{\Delta t} m_2(x,t) &= \lim_{\Delta t\to 0} \frac{1}{\Delta t}\mathbb{E}\Big[(\Delta X)^2|X(t)=x\Big] = \sigma(x,t),\\
\lim_{\Delta t\to 0} \frac{1}{\Delta t} m_n(x,t) &= \lim_{\Delta t\to 0} \frac{1}{\Delta t}\mathbb{E}\big[(\Delta X)^n|X(t)=x\big] = 0, \qquad n>2.
\end{aligned} \tag{3.52}$$

Equation (3.52) asserts that, in small-time intervals, the spatial coordinate undergoes only minor changes. The first and second moments are proportional to Δt, whereas higher moments display an order higher than Δt.

If these assumptions hold true, a Markov process is classified as a diffusion process. This can be verified for specific physical systems such as the Langevin equation. The functions $m(x,t)$ and $\sigma(x,t)$ are respectively referred to as drift and diffusion coefficients. Analogous definitions also apply to vector stochastic processes. A system excited by white noise always satisfies the diffusion assumptions under the assumption of Markovian behavior.

The Markov process $X(t)$, characterized by a transition probability function $p(x,t|y,s)$, where $s < t$, can be examined through the arbitrary function $R(x)$ which diminishes sufficiently fast when $x \to \pm\infty$:

$$\int_{-\infty}^{\infty} \frac{\partial}{\partial t} p(x,t|y,s)R(x)dx = \int_{-\infty}^{\infty} \lim_{\Delta t\to 0} \frac{p(x,t+\Delta t|y,s) - p(x,t|y,s)}{\Delta t} R(x). \tag{3.53}$$

The right-hand side of the above equation can be rewritten as

$$\begin{aligned}\int_{-\infty}^{\infty} &\lim_{\Delta t\to 0}\frac{p(x,t+\Delta t|y,s)-p(x,t|y,s)}{\Delta t}R(x)\\ &=\lim_{\Delta t\to 0}\frac{1}{\Delta t}\left(\int_{-\infty}^{\infty}R(x)p(x,t+\Delta t|y,s)dx-\int_{-\infty}^{\infty}R(z)p(z,t|y,s)dz\right).\end{aligned}\tag{3.54}$$

Using the Chapman-Kolmogorov equation yields

$$\begin{aligned}\lim_{\Delta t\to 0}\frac{1}{\Delta t}&\left(\int_{-\infty}^{\infty}R(x)\int_{-\infty}^{\infty}p(x,t+\Delta t|z,t)p(z,t|y,s)dzdx-\int_{-\infty}^{\infty}R(z)p(z,t|y,s)dz\right)\\ &=\lim_{\Delta t\to 0}\frac{1}{\Delta t}\int_{-\infty}^{\infty}p(z,t|y,s)\left(\int_{-\infty}^{\infty}R(x)p(x,t+\Delta t|z,t)dx-R(z)\right)dz.\end{aligned}\tag{3.55}$$

Expanding $R(x)$ about the intermediate state z results in

$$R(x)=R(z)+R'(z)(x-z)+\frac{1}{2}R''(z)(x-z)^2+O(x-z)^3.\tag{3.56}$$

By applying the diffusion assumptions, the following expression is obtained:

$$\begin{aligned}&\int_{-\infty}^{\infty}R(x)p(x,t+\Delta t|z,t)dx-R(z)=\int_{-\infty}^{\infty}R'(z)(x-z)p(x,t+\Delta t|z,t)dx\\ &+\int_{-\infty}^{\infty}\frac{1}{2}R''(z)(x-z)p(x,t+\Delta t|z,t)dx+\int_{-\infty}^{\infty}O(x-z)^3p(x,t+\Delta t|z,t)dx\\ &=R'(z)m(z,t)\Delta t+\frac{1}{2}R''(z)\sigma(z,t)\Delta t+o(\Delta t).\end{aligned}\tag{3.57}$$

Inserting this result into Eq. (3.55) yields

$$\int_{-\infty}^{\infty}\frac{\partial}{\partial t}p(x,t|y,s)R(x)dx=\int_{-\infty}^{\infty}p(z,t|y,s)\left(R'(z)m(z,t)+\frac{1}{2}R''(z)\sigma(z,t)\right)dz\tag{3.58}$$

Integration by parts of the first term on the right-hand side gives

$$\begin{aligned}\int_{-\infty}^{\infty}pR'(z)m(z,t)dz&=pR(z)m\big|_{-\infty}^{\infty}-\int_{-\infty}^{\infty}R(z)\frac{\partial}{\partial z}\Big(p\big(z,t|y,s\big)m(z,t)\Big)dz\\ &=-\int_{-\infty}^{\infty}R(z)\frac{\partial}{\partial z}\Big(p\big(z,t|y,s\big)m(z,t)\Big)dz.\end{aligned}\tag{3.59}$$

Similarly, the second term on the right-hand side can be written as

$$\begin{aligned}\int_{-\infty}^{\infty}pR''(z)\sigma dz&=pR'(z)\sigma\big|_{-\infty}^{\infty}-\int_{-\infty}^{\infty}R'(z)\frac{\partial}{\partial z}\Big(p\big(z,t|y,s\big)\sigma(z,t)\Big)dz\\ &=-\int_{-\infty}^{\infty}R'(z)\frac{\partial}{\partial z}\Big(p\big(z,t|y,s\big)\sigma(z,t)\Big)dz.\end{aligned}\tag{3.60}$$

Integration by parts again yields

$$\begin{aligned}\int_{-\infty}^{\infty} pR''(z)\sigma dz &= -pR(z)\sigma\big|_{-\infty}^{\infty} + \int_{-\infty}^{\infty} R(z)\frac{\partial^2}{\partial z^2}\Big(p\big(z,t|y,s\big)\sigma(z,t)\Big)dz \\ &= \int_{-\infty}^{\infty} R(z)\frac{\partial^2}{\partial z^2}\Big(p\big(z,t|y,s\big)\sigma(z,t)\Big)dz.\end{aligned} \tag{3.61}$$

Equation (3.58) then becomes

$$\begin{aligned}\int_{-\infty}^{\infty} pR'(z)mdz &= pR(z)m\big|_{-\infty}^{\infty} - \int_{-\infty}^{\infty} R(z)\frac{\partial}{\partial z}\Big(p\big(z,t|y,s\big)m(z,t)\Big)dz \\ &= \int_{-\infty}^{\infty} R(z)\left(-\frac{\partial}{\partial z}\Big(p\big(z,t|y,s\big)m(z,t)\Big) + \frac{1}{2}\frac{\partial^2}{\partial z^2}\Big(p\big(z,t|y,s\big)\sigma(z,t)\Big)\right)dz.\end{aligned} \tag{3.62}$$

As a consequence, by replacing z by x on the right-hand side,

$$\int_{-\infty}^{\infty} \frac{\partial p}{\partial t}R(x)dx = \int_{-\infty}^{\infty} R(x)\left(-\frac{\partial}{\partial x}(pm) + \frac{1}{2}\frac{\partial^2}{\partial x^2}(p\sigma)\right)dx. \tag{3.63}$$

Factoring out $R(x)$ yields

$$\int_{-\infty}^{\infty} R(x)\left(\frac{\partial p}{\partial t} + \frac{\partial}{\partial x}(pm) - \frac{1}{2}\frac{\partial^2}{\partial x^2}(p\sigma)\right) = 0. \tag{3.64}$$

Given that $R(x)$ is arbitrary it results in a partial differential equation for $p(x,t|y,s)$:

$$\frac{\partial p}{\partial t} = -\frac{\partial}{\partial x}(pm) + \frac{1}{2}\frac{\partial^2}{\partial x^2}(p\sigma). \tag{3.65}$$

Equation (3.65), known as the forward diffusion or Fokker-Planck equation, is a parabolic linear partial differential equation. It was first proposed by Einstein and Smoluchowski, although its name was given later by Adrian Fokker who worked with Max Planck [9]. The forward diffusion equation is more general than the earlier work on diffusion equations; it contains a convection term in addition to the diffusion term. Similarly, it can be shown that the transition probability $p(x,t|y,s)$ satisfies the backward diffusion equation, also known as the Kolmogorov equation:

$$-\frac{\partial p}{\partial s} = m\frac{\partial p}{\partial y} + \frac{1}{2}\sigma\frac{\partial^2 p}{\partial x^2}. \tag{3.66}$$

The forward and backward diffusion equations are adjoint differential equations; the solution of one is equivalent to the solution of the other. The term *diffusion equation* will be used throughout this thesis to indicate the forward diffusion equation, unless specified otherwise.

Chapter 4

Qualitative Analysis by Randomization

This chapter expounds on the importance of randomization in uncovering qualitative behaviors of nonlinear systems. To randomize deterministic systems, white-noise excitation is added to the equations of motion. An extensive analysis of qualitative behaviors of deterministic systems is conducted by finding the exact solution for the stationary diffusion equation associated with randomized systems.

4.1 Framework of Randomization

Consider a deterministic nonlinear dynamical system, governed by Eq. (3.2):

$$\dot{\mathbf{z}} = \boldsymbol{a}(\mathbf{z}).$$

In certain circumstances, it is advantageous to introduce white noise $W(t)$ to randomize the system. This yields

$$\dot{\mathbf{Z}} = \boldsymbol{a}(\mathbf{Z}) + \boldsymbol{b}W(t), \tag{4.1}$$

where $\mathbf{Z} = [X, Y]^T$ represents a two-dimensional vector of diffusion processes, and $\boldsymbol{b} = [b_1, b_2]^T$ is a constant vector. This approach can be extended to an n-dimensional system, as shown in Eq. (4.2):

$$\begin{bmatrix} \dot{X}_1(t) \\ \dot{X}_2(t) \\ \vdots \\ \dot{X}_n(t) \end{bmatrix} = \begin{bmatrix} a_1(\mathbf{Z}) \\ a_2(\mathbf{Z}) \\ \vdots \\ a_n(\mathbf{Z}) \end{bmatrix} + \begin{bmatrix} b_1 \\ b_2 \\ \vdots \\ b_n \end{bmatrix} W(t). \tag{4.2}$$

In this generalization, $\boldsymbol{b}$ is a constant vector and $W(t)$ denotes zero-mean white noise characterized by power spectral density S_0. Defining $\boldsymbol{\sigma}$ as

$$\boldsymbol{\sigma} = [\sigma_{ij}(\mathbf{z}, t)] = 2\pi S_0 \boldsymbol{b}\boldsymbol{b}^T, \tag{4.3}$$

the system response $\mathbf{Z}(t)$ constitutes a diffusion process, defined by its transition probability $p(\mathbf{z}, t|\mathbf{z}_0)$. This probability satisfies the diffusion equation given by

$$\frac{\partial p}{\partial t} = -\sum_{i=1}^{n} \frac{\partial}{\partial x_i}\big(a_i(\mathbf{z})p\big) + \frac{1}{2}\sum_{i=1}^{n}\sum_{j=1}^{n} \frac{\partial^2}{\partial x_i \partial x_j}\big(\sigma_{ij}(\mathbf{z}, t)p\big), \tag{4.4}$$

where the following relations hold:

$$\begin{aligned} a_i(\mathbf{z}) &= \lim_{\Delta t \to 0} \frac{1}{\Delta t}\mathbb{E}\big[\Delta X_i | \mathbf{z}\big], \\ \sigma_{ij}(\mathbf{z}, t) &= \lim_{\Delta t \to 0} \frac{1}{\Delta t}\mathbb{E}\big[\Delta X_i \Delta X_j | \mathbf{z}\big]. \end{aligned} \tag{4.5}$$

This formulation applies to any autonomous dynamical system, regardless of its nonlinearity, and solving the diffusion equations achieves a complete specification of the system response.

Recalling the deterministic system of interest introduced in Eq. (1.1):

$$\ddot{x} + \epsilon\alpha(x, \dot{x}) + \beta(x, \dot{x}) = 0,$$

it can be represented in state-space form as described in Eq. (4.6):

$$\dot{\mathbf{z}} = \begin{bmatrix} \dot{x} \\ \dot{y} \end{bmatrix} = \begin{bmatrix} y \\ -\epsilon\alpha(x, y) - \beta(x, y) \end{bmatrix}. \tag{4.6}$$

Randomizing this system using white noise $W(t)$ results in

$$\ddot{X} + \epsilon\alpha\Big(X, \dot{X}\Big) + \beta\Big(X, \dot{X}\Big) = W(t),$$

which can alternatively be represented by

$$\dot{\mathbf{Z}} = \begin{bmatrix} \dot{X} \\ \dot{Y} \end{bmatrix} = \begin{bmatrix} Y \\ -\epsilon\alpha(X, Y) - \beta(X, Y) \end{bmatrix} + \begin{bmatrix} 0 \\ 1 \end{bmatrix} W(t). \tag{4.7}$$

In this case, the following expressions are applicable:

$$\begin{bmatrix} a_1(\mathbf{Z}) \\ a_2(\mathbf{Z}) \end{bmatrix} = \begin{bmatrix} Y \\ -\epsilon\alpha(X, Y) - \beta(X, Y) \end{bmatrix}, \qquad [\sigma_{ij}(\mathbf{z}, t)] = 2\pi S_0 \boldsymbol{b}\boldsymbol{b}^T = 2\pi S_0 \begin{bmatrix} 0 & 0 \\ 0 & 1 \end{bmatrix}. \tag{4.8}$$

Assuming $p(\mathbf{z}, t|\mathbf{z}_0)$ represents the transition probability density of the system, the associated diffusion equation takes the following form:

$$\frac{\partial p}{\partial t} = -y\frac{\partial p}{\partial x} + \frac{\partial}{\partial y}\big((\epsilon\alpha + \beta)p\big) + \pi S_0 \frac{\partial^2 p}{\partial y^2}.$$

Determining the transition probability $p(\mathbf{z}, t|\mathbf{z}_0)$ for a system typically involves solving either a nonlinear stochastic ordinary differential equation or a linear second-order partial differential equation of diffusion.

Notably, when the transition probability $p(\mathbf{z}, t|\mathbf{z}_0)$ attains a relative maximum value, it lies along the trajectory passing through $\mathbf{z}_0 = [x_0, \dot{x}_0]^T$ in the phase plane. In steady-state conditions, the diffusion equation can be further simplified to

$$0 = -y\frac{\partial p_s}{\partial x} + \frac{\partial}{\partial y}\big((\epsilon\alpha + \beta)p_s\big) + \pi S_0 \frac{\partial^2 p_s}{\partial y^2}.$$

Here, $p_s(\mathbf{z})$ denotes the stationary probability density function, which is sufficient for identifying key qualitative behaviors of the deterministic system.

Randomization considerably simplifies and enhances the understanding of deterministic systems when studying their qualitative behaviors, even though this might seem counterintuitive. One could think that the linear partial differential equation of diffusion for randomized systems would be harder to solve than the nonlinear ordinary differential equation governing deterministic systems due to increased dimensionality.

However, the linear nature of the partial differential equation allows for the application of various mathematical techniques usually not applicable to nonlinear ordinary differential equations of deterministic systems.

Moreover, the probability density of randomized systems streamlines the comprehension of the behavior and structure of deterministic systems. Analyzing the stationary probability density function becomes easier in identifying the stability of equilibrium points, limit cycles, or bifurcations—information that is more challenging to extract from the deterministic nonlinear ordinary differential equation alone.

4.2 Linear Systems

This section presents two examples to illustrate the application of randomization to linear systems: Linear systems with damping and damped harmonic oscillators. The solutions of the related diffusion equations are obtained using the Fourier transform method.

Linear Damping

Consider a deterministic linear dynamical system represented by the following differential equation:

$$m\ddot{x} + c\dot{x} = 0. \tag{4.9}$$

By denoting $\dot{x} = v$, the system can be rewritten as

$$m\dot{v} + cv = 0, \tag{4.10}$$

where m denotes the mass of the particle, and c signifies the damping constant. The solution to this system takes the form:

$$v(t) = v_0 \exp\left(-\frac{c}{m}t\right). \tag{4.11}$$

To introduce randomization in the aforementioned linear system, consider adding white noise $W(t)$, which results in the Langevin equation [11, 76]:

$$m\frac{dV}{dt} + cV = W(t), \qquad t > 0. \tag{4.12}$$

In this case, $V(0) = v_0$ and $W(t)$ represents white noise with zero mean and constant power spectral density. Consequently, the deterministic velocity $v(t)$ transforms into a diffusion process $V(t)$.

The excitation $W(t)$ accounts for the force of random collisions between the heavy Brownian particle and lighter fluid particles. The mean effect of these collisions causes the Brownian particle to slow down. It is expected that under random disturbance, the mean path of $X(t)$ aligns with the deterministic solution. When $W(t)$ is applied over the interval $-\infty < t < \infty$, the response $X(t)$ becomes weakly stationary, implying that $\mathbb{E}\big[X(t)\big]$ is constant and independent of any initial conditions. The mean-square response can be determined by

$$\mathbb{E}\big[X^2(t)\big] = \int_{-\infty}^{\infty} S_X(\omega)d\omega = S_0 \int_{-\infty}^{\infty} \big|H(i\omega)\big|^2 d\omega = S_0 \int_{-\infty}^{\infty} \left|\frac{1}{i\omega + \beta}\right|^2 d\omega, \tag{4.13}$$

where $S_X(\omega)$ represents the power spectral density of $X(t)$, and $H(i\omega)$ is the transfer function of the system. Assuming that $H(i\omega)$ is a rational function, it can be expressed as

$$H(i\omega) = \frac{i\omega B_1 + B_0}{-\omega^2 A_2 + i\omega A_1 + A_0}. \tag{4.14}$$

Integrating the transfer function over the entire frequency range yields

$$\int_{-\infty}^{\infty} \big|H(i\omega)\big|^2 d\omega = \pi\left(\frac{B_0^2 A_2 + B_1^2 A_0}{A_0 A_1 A_2}\right). \tag{4.15}$$

Since $A_0 = \beta$, $A_1 = 1$, $A_2 = 0$, $B_1 = 0$, and $B_0 = 1$, the following result is obtained:

$$\mathbb{E}\big[X^2(t)\big] = S_0 \int_{-\infty}^{\infty} \left|\frac{1}{i\omega + \beta}\right|^2 d\omega = \frac{\pi S_0}{\beta}. \tag{4.16}$$

Consider a first-order system with drift and diffusion coefficients $a(X)$ and $b(X)$, represented by

$$\dot{X} = a(X) + b(X)W(t).$$

By defining

$$m(x,t) = -\beta x, \qquad \sigma(x,t) = 2\pi S_0 b^2(x,t) = 2\pi S_0, \tag{4.17}$$

where $\beta = {}^{c}\!/_{m}$, similar results can be obtained using the procedure outlined in Section 3.4.3. Integrating the governing equation over a time increment Δt provides

$$X(t+\Delta t) - X(t) + \beta \int_t^{t+\Delta t} X(u)du = \int_t^{t+\Delta t} W(u)du. \tag{4.18}$$

Application of the mean-value theorem leads to

$$\Delta X = -\beta X(\tau)\Delta t + \int_t^{t+\Delta t} W(u)du, \tag{4.19}$$

where $t < \tau < t + \Delta t$ denotes the time when the mean value of $X(t)$ is taken. Averaging this equation results in

$$\mathbb{E}[\Delta X] = -\beta \mathbb{E}\big[X(\tau)\big]\Delta t + \int_t^{t+\Delta t} \mathbb{E}\big[W(u)\big]du = -\beta \mathbb{E}\big[X(\tau)\big]\Delta t. \tag{4.20}$$

Therefore,

$$m(x,t) = \lim_{\Delta t \to 0} \frac{1}{\Delta t} \mathbb{E}\big[\Delta X | X(t) = x\big] = -\lim_{\Delta t \to 0} \beta \mathbb{E}\big[X(\tau)\big] = -\beta x. \tag{4.21}$$

Additionally,

$$\mathbb{E}\Big[(\Delta X)^2 | X(t)\Big] = \beta^2 X^2 (\Delta t)^2 + \int_t^{t+\Delta t} \int_t^{t+\Delta t} \mathbb{E}\big[W(u)W(v)\big]dudv. \tag{4.22}$$

Given that $\mathbb{E}\big[W(u)W(v)\big] = 2\pi S_0 \delta(u-v)$, where $\delta(u-v)$ represents the Dirac delta function, Eq. (4.22) can be modified as

$$\mathbb{E}\Big[(\Delta t)^2 | X(t)\Big] = \beta^2 X^2 (\Delta t)^2 + 2\pi S_0 \Delta t. \tag{4.23}$$

Consequently,

$$\sigma(x,t) = \lim_{\Delta t \to 0} \frac{1}{\Delta t} \mathbb{E}\Big[(\Delta t)^2 | X(t) = x\Big] = 2\pi S_0. \tag{4.24}$$

Verification for higher moments of Δx demonstrates that

$$\lim_{\Delta t \to 0} \frac{1}{\Delta t} \mathbb{E}\big[(\Delta t)^n | X(t) = x\big] = 0, \qquad n > 2. \tag{4.25}$$

This finding indicates that diffusion assumptions are satisfied, and the associated diffusion equation is

$$\frac{\partial p(x,t)}{\partial t} = -\frac{\partial}{\partial x}\big(m(x,t)p(x,t)\big) + \frac{1}{2}\frac{\partial^2}{\partial x^2}\big(\sigma(x,t)^2 p(x,t)\big). \tag{4.26}$$

Substituting (4.17) into the diffusion equation yields

$$\frac{\partial p(x,t)}{\partial t} = \beta \frac{\partial}{\partial x}\big(x p(x,t)\big) + \pi S_0 \frac{\partial^2}{\partial x^2} p(x,t), \tag{4.27}$$

which constitutes a parabolic partial differential equation. Solving the diffusion equation provides the transition probability $p(x,t|x_0)$. The initial condition for this equation can be expressed as

$$p(x,0|x_0) = \delta(x - x_0). \tag{4.28}$$

The diffusion equation cannot be solved using separation of variables; however, it can be reduced to a first-order partial differential equation through the application of the Fourier transform. Define the Fourier transform of $p(x,t|x_0)$ and the inverse Fourier transform of $\phi(\omega,t)$ as follows:

$$\begin{aligned} \mathcal{F}[p] &= \int_{-\infty}^{\infty} p(x,t|x_0) e^{i\omega x} dx = \phi(\omega,t), \\ \mathcal{F}^{-1}[\phi] &= \frac{1}{2\pi}\int_{-\infty}^{\infty} \phi(\omega,t) e^{-i\omega x} d\omega = p(x,t|x_0). \end{aligned} \tag{4.29}$$

Since differentiation with respect to the spatial coordinate x corresponds to multiplication by $-i\omega$ in the frequency domain, as observed from

$$\frac{\partial}{\partial x} p(x,t|x_0) = \frac{1}{2\pi}\int_{-\infty}^{\infty} -i\omega\phi(\omega,t) e^{-i\omega x} d\omega = \mathcal{F}^{-1}[-i\omega\phi], \tag{4.30}$$

the equation can be written as

$$\mathcal{F}\left[\frac{\partial p}{\partial x}\right] = -i\omega\phi, \qquad \mathcal{F}\left[\frac{\partial^2 p}{\partial x^2}\right] = -\omega^2\phi. \tag{4.31}$$

Likewise, differentiation of $\mathcal{F}[p]$ with respect to ω is equivalent to multiplication by ix, exemplified by

$$\frac{\partial}{\partial \omega}\phi(\omega,t) = \frac{\partial}{\partial \omega}\mathcal{F}[p] = \int_{-\infty}^{\infty} ixp(x,t|x_0) e^{i\omega x} dx = \mathcal{F}[ixp], \tag{4.32}$$

resulting in

$$\mathcal{F}\left[\frac{\partial}{\partial x}(xp)\right] = -i\omega\mathcal{F}[xp] = -\omega\mathcal{F}[ixp] = -\omega\frac{\partial\phi}{\partial\omega}. \tag{4.33}$$

Taking the Fourier transform of the diffusion equation produces

$$\frac{\partial\phi}{\partial t} = -\beta\omega\frac{\partial\phi}{\partial\omega} - \omega^2\pi S_0\phi. \tag{4.34}$$

The initial condition can then be expressed as

$$\phi(\omega, 0) = \int_{-\infty}^{\infty} p(x, 0|x_0)e^{i\omega x}dx = \mathcal{F}\big[\delta(x - x_0)\big] = e^{i\omega x_0}. \tag{4.35}$$

Equation (4.34) represents a first-order linear partial differential equation solvable through the method of characteristics. Rewriting the equation as

$$\frac{\partial\phi}{\partial t} + \beta\omega\frac{\partial\phi}{\partial\omega} = -\omega^2\pi S_0\phi, \tag{4.36}$$

with initial condition given by $\phi(\omega, 0) = e^{i\omega x_0}$, results in auxiliary equations:

$$\frac{dt}{1} = \frac{d\omega}{\beta\omega} = \frac{d\phi}{-\omega^2\pi S_0\phi}. \tag{4.37}$$

From the first part of these auxiliary equations, a separable differential equation emerges:

$$\frac{dt}{1} = \frac{d\omega}{\beta\omega}, \tag{4.38}$$

leading to the solution

$$\omega e^{-\beta t} = c_1. \tag{4.39}$$

Similarly, the second part of the auxiliary equations provides

$$\phi\exp\left(\frac{\pi S_0}{2\beta}\omega^2\right) = c_2. \tag{4.40}$$

The general solution can be expressed as

$$\phi\exp\left(\frac{\pi S_0}{2\beta}\omega^2\right) = f(\omega e^{-\beta t}), \tag{4.41}$$

or equivalently,

$$\phi(\omega, t) = f(\omega e^{-\beta t})\exp\left(-\frac{\pi S_0}{2\beta}\omega^2\right), \tag{4.42}$$

where f represents an arbitrary function. Applying the given initial condition leads to

$$\phi(\omega, 0) = f(\omega) \exp\left(-\frac{\pi S_0}{2\beta}\omega^2\right) = e^{i\omega x_0}, \tag{4.43}$$

resulting in

$$f(\omega) = \exp\left(i\omega x_0 + \frac{\pi S_0}{2\beta}\omega^2\right). \tag{4.44}$$

Hence, the following expression is obtained:

$$\phi(\omega, t) = \exp\left(i\omega x_0 e^{-\beta t} - \frac{\pi S_0}{2\beta}\omega^2\Big(1 - e^{-2\beta t}\Big)\right). \tag{4.45}$$

Note that a normal random variable with probability density defined by

$$p(x) = \frac{1}{\sqrt{2\pi}\sigma} \exp\left(-\frac{(x-\mu)^2}{2\sigma^2}\right) \tag{4.46}$$

has the characteristic function

$$\phi(\omega) = \exp\left(i\mu\omega - \frac{\sigma^2\omega^2}{2}\right). \tag{4.47}$$

Therefore, the transition probability follows as

$$p(x, t|x_0) = \frac{1}{\sqrt{2\pi}\sigma(t)} \exp\left(-\frac{\big(x - \mu(t)\big)^2}{2\sigma^2(t)}\right), \tag{4.48}$$

where

$$\mu(t) = x_0 \exp(-\beta t), \qquad \sigma(t) = \sqrt{\frac{\pi S_0}{\beta}\big(1 - \exp(-2\beta t)\big)}. \tag{4.49}$$

The diffusion equation associated with the Langevin equation cannot be solved by separation of variables; that is $p(x, t|x_0) \neq f(x)g(t)$. The response process $X(t)$ follows a normal distribution with mean μ and variance σ for all t, which is consistent with the results obtained from Eq. (4.10). As time $t \to \infty$, the mean $\mu(t)$ converges to zero due to damping, while the limiting value of $\sigma^2(t)$ becomes ${}^{\pi S_0}/_{\beta}$, as illustrated in Fig. 4.1. Consequently, the random collisions represented by white noise $W(t)$ contribute to slowing down the Brownian particle, but the uncertainty in the response remains bounded. These characteristics can be taken into consideration when designing systems. Furthermore, the stationary probability density of the Langevin equation in the steady state is given by

$$p_s(x) = \lim_{t\to\infty} p(x, t|x_0) = \frac{1}{\sqrt{2\pi}\sigma} \exp\left(-\frac{x^2}{2\sigma^2}\right), \tag{4.50}$$

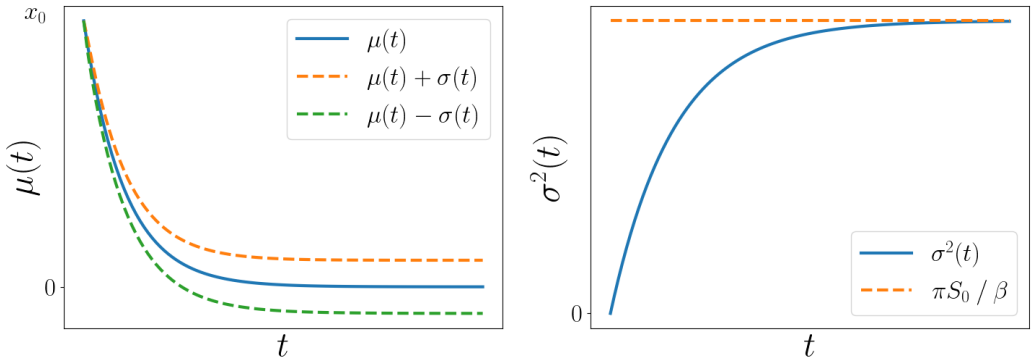

Figure 4.1: Mean and variance of the Langevin equation

where

$$\sigma^2 = \frac{\pi S_0}{\beta}. \tag{4.51}$$

Additionally, the stationary probability density can be determined as the solution to the following equation:

$$\beta \frac{d}{dx}\big(x p_s(x)\big) + \pi S_0 \frac{d^2 p_s}{dx^2} = 0. \tag{4.52}$$

Notably, the stationary probability density is identical the solution acquired by considering a stationary excitation $W(t)$ for $-\infty < t < \infty$. When β equals zero (no damping), the diffusion equation simplifies to the heat conduction equation:

$$\frac{\partial p}{\partial t} = \pi S_0 \frac{\partial^2 p}{\partial x^2}, \tag{4.53}$$

which implies that there is no stationary probability density for the velocity of the Brownian particle in the absence of damping.

Linear Damping with Linear Stiffness

Consider a deterministic linear single-degree-of-freedom mechanical system represented by the following form:

$$\ddot{x} + c\dot{x} + kx = 0, \tag{4.54}$$

where c is damping constant and k is stiffness. The system can be randomized by introducing a white-noise excitation $W(t)$ on the right-hand side of the equation, resulting in the stochastic differential equation below:

$$\ddot{X} + c\dot{X} + kX = W(t), \qquad \dot{X}(0) = \dot{x}_0, \qquad X(0) = x_0. \tag{4.55}$$

Here, $W(t)$ represents a white noise process with zero mean and a constant power spectral density S_0. To construct a state-space representation of the system, a two-dimensional state vector $\mathbf{Z}$ is defined as

$$\mathbf{Z} = \begin{bmatrix} X \\ Y = \dot{X} \end{bmatrix}.$$

The corresponding state-space representation of the system is given by

$$\dot{\mathbf{Z}} = \begin{bmatrix} 0 & 1 \\ -k & -c \end{bmatrix} \mathbf{Z} + \begin{bmatrix} 0 \\ 1 \end{bmatrix} W(t), \qquad \mathbf{Z}(0) = \mathbf{z}_0 = \begin{bmatrix} x_0 \\ \dot{x}_0 \end{bmatrix}. \tag{4.56}$$

Define $p(\mathbf{z}, t|\mathbf{z}_0)$ as the transition probability density of the state vector $\mathbf{z}$ at time t, given the initial state $\mathbf{z}_0$. The diffusion equation for the system is expressed as

$$\frac{\partial p}{\partial t} = -y\frac{\partial p}{\partial x} + \frac{\partial}{\partial y}\big((cy + kx)p\big) + \pi S_0 \frac{\partial^2 p}{\partial y^2} \tag{4.57}$$

with a corresponding initial condition

$$p(\mathbf{z}, 0|\mathbf{z}_0) = \delta(x - x_0)\delta(y - \dot{x}_0). \tag{4.58}$$

Since the state vector is two-dimensional, a two-fold Fourier transform of $p(\mathbf{z}, t|\mathbf{z}_0)$ is proposed in order to solve the diffusion equation, which can be expressed as

$$\mathcal{F}[p] = \int_{-\infty}^{\infty}\int_{-\infty}^{\infty} p(\mathbf{z}, t|\mathbf{z}_0) e^{-i\boldsymbol{\omega}\cdot\mathbf{z}} dxdy = \phi(\boldsymbol{\omega}, t), \tag{4.59}$$

where $\boldsymbol{\omega} = \Big[\omega_x, \omega_y\Big]^T$ is the two-dimensional frequency vector. The inverse Fourier transform of ϕ can also be used to obtain the expression of p:

$$\mathcal{F}[\phi]^{-1} = \frac{1}{4\pi^2}\int_{-\infty}^{\infty}\int_{-\infty}^{\infty} \phi(\boldsymbol{\omega}, t) e^{i\boldsymbol{\omega}\cdot\mathbf{z}} d\omega_x d\omega_y = p(\mathbf{z}, t|\mathbf{z}_0). \tag{4.60}$$

The Fourier transform of the partial derivative terms can be obtained by taking the partial derivative of ϕ. For example, the partial derivative of ϕ with respect to ω_x is

$$\frac{\partial \phi}{\partial \omega_y} = \mathcal{F}[iyp].$$

Taking the inverse Fourier transform of both sides of the equation results in

$$iyp = \mathcal{F}^{-1}\left[\frac{\partial \phi}{\partial \omega_y}\right].$$

By virtue of the Eq. (4.30), the x derivative of yp can be expressed as

$$i\frac{\partial(yp)}{\partial x} = \mathcal{F}^{-1}\left[-i\omega_x\frac{\partial\phi}{\partial\omega_y}\right].$$

Finally, the Fourier transform of the above equation is

$$\mathcal{F}\left[\frac{\partial(yp)}{\partial x}\right] = -i\omega_x\frac{\partial\phi}{\partial\omega_y}. \tag{4.61}$$

The following results can be derived when a similar approach is employed:

$$\mathcal{F}\left[\frac{\partial}{\partial y}(yp)\right] = -\omega_y\frac{\partial\phi}{\partial\omega_y}, \qquad \mathcal{F}\left[\frac{\partial}{\partial y}(xp)\right] = -\omega_y\frac{\partial\phi}{\partial\omega_x}, \qquad \mathcal{F}\left[\frac{\partial^2 p}{\partial y^2}\right] = \omega_y^2\phi. \tag{4.62}$$

Taking the Fourier transform of (4.57) and using the above results, the following partial differential equation can be obtained:

$$\frac{\partial\phi}{\partial t} = \omega_x\frac{\partial\phi}{\partial\omega_y} - c\omega_y\frac{\partial\phi}{\partial\omega_y} - k\omega_y\frac{\partial\phi}{\partial\omega_x} - \pi S_0\omega_y^2\phi \tag{4.63}$$

with the initial condition being

$$\phi(\boldsymbol{\omega}, 0) = \exp(-i\boldsymbol{\omega}\cdot\mathbf{z}_0). \tag{4.64}$$

Considering the first-order partial differential equation:

$$\frac{\partial\phi}{\partial t} + k\omega_y\frac{\partial\phi}{\partial\omega_x} + (c\omega_y - \omega_x)\frac{\partial\phi}{\partial\omega_y} = -\pi S_0\omega_y^2\phi. \tag{4.65}$$

By employing the method of characteristics, the auxiliary equations become

$$\frac{dt}{1} = \frac{d\omega_x}{k\omega_y} = \frac{d\omega_y}{c\omega_y - \omega_x} = \frac{d\phi}{-\pi S_0\omega_y^2\phi}. \tag{4.66}$$

Unfortunately, these equations cannot be integrated since the equations are not separable. However, the stationary probability density function p_s can be determined through a heuristic approach. The stationary probability density is governed by Eq. (4.57) with $t \to \infty$,

$$-y\frac{\partial p_s}{\partial x} + \frac{\partial}{\partial y}\big((cy + kx)p_s\big) + \pi S_0\frac{\partial^2 p_s}{\partial y^2} = 0. \tag{4.67}$$

This equation is precisely satisfied if

$$\begin{aligned} -y\frac{\partial p_s}{\partial x} + \frac{\partial}{\partial y}(kxp_s) &= 0, \\ \frac{\partial}{\partial y}(cyp_s) + \pi S_0\frac{\partial^2 p_s}{\partial y^2} &= 0. \end{aligned} \tag{4.68}$$

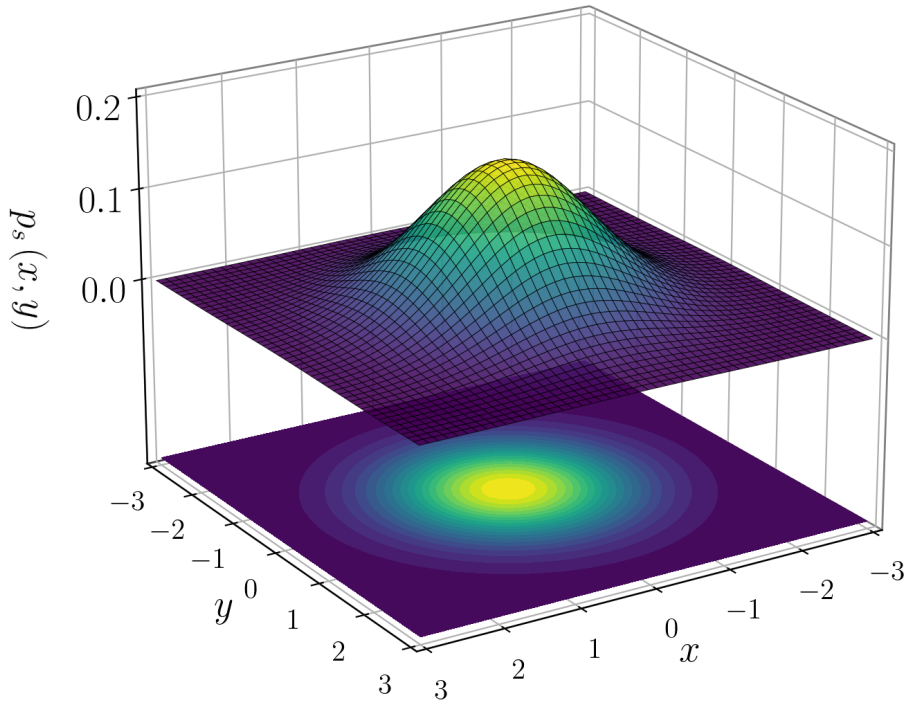

Figure 4.2: The stationary probability density function of the randomized linear mechanical system

The first-order partial differential equation can be solved by the method of characteristics highlighted in Section A.2.2. The general solution can then be represented as

$$p_s = h\left(\frac{1}{2}kx^2 + \frac{1}{2}y^2\right) = h(H), \tag{4.69}$$

where h is an arbitrary function. Furthermore, the first part of Eq. (4.68) can be written as

$$\frac{\partial}{\partial y}\left(cyp_s + \pi S_0 \frac{\partial p_s}{\partial y}\right) = 0, \tag{4.70}$$

which leads to

$$cyp_s + \pi S_0 \frac{\partial p_s}{\partial y} = e(x). \tag{4.71}$$

Since p_s and its first-order derivatives vanish as $|x| + |y| \to \infty$, it follows that $e(x) = 0$. Substituting $p_s = e(H)$ in the above equation shows

$$cyh + \pi S_0 \frac{dh}{dH} y = 0. \tag{4.72}$$

Canceling y and integrating gives

$$h = A \exp\left(\frac{-cH}{\pi S_0}\right), \tag{4.73}$$

where A is a normalization constant. Consequently, the stationary probability density is

$$p_s(x, y) = \frac{\exp\left(\frac{-c}{\pi S_0}\left(\frac{1}{2}kx^2 + \frac{1}{2}y^2\right)\right)}{\int_{-\infty}^{\infty}\int_{-\infty}^{\infty} \exp\left(\frac{-c}{\pi S_0}\left(\frac{1}{2}kx^2 + \frac{1}{2}y^2\right)\right) dxdy}. \tag{4.74}$$

It is verified that the expression above is a solution by utilizing

$$\frac{\partial}{\partial x} p_s(x, y) = p_s(x, y)\left(-\frac{ck}{\pi S_0} x\right), \qquad \frac{\partial}{\partial y} p_s(x, y) = p_s(x, y)\left(-\frac{c}{\pi S_0} y\right). \tag{4.75}$$

As a result of the uniqueness of the solution, this is the only possible solution. In the steady state, x, y are independent and jointly normal. Since the damping constant c is non-zero,

$$\mathbb{E}[x] = \mathbb{E}[y] = 0. \tag{4.76}$$

In the steady state,

$$\sigma_x^2 = \frac{\pi S_0}{ck}, \qquad \sigma_y^2 = \frac{\pi S_0}{c}. \tag{4.77}$$

A contour of the stationary probability density is included in Fig. 4.2, which indicates a stable focus at the origin. When $c = 0$, the stationary probability density does not exist since the origin is a center.

4.3 Nonlinear Damping

In the presence of nonlinearity in dynamical systems, solution techniques employing Fourier transform, as introduced in Section 4.2, are no longer applicable due to the existence of nonlinear drift/diffusion coefficients in the diffusion equation. Therefore, alternative approaches, primarily heuristic methods, can be employed to solve the diffusion equation. The randomization of nonlinear systems and corresponding solution methods are presented until the end of this chapter. Consider a nonlinear system of the form:

$$\ddot{x} + g(\dot{x}) = 0, \qquad t > 0. \tag{4.78}$$

Rewriting the equation with velocity yields

$$\dot{v} + g(v) = 0, \tag{4.79}$$

where $g(v)$ is a nonlinear function. Without loss of generality, let $v = x$, then

$$\dot{x} + g(x) = 0. \tag{4.80}$$

Introducing a white-noise excitation $W(t)$ on the right-hand side of the equation results in the randomized system:

$$\dot{X} + g(X) = W(t). \tag{4.81}$$

The diffusion equation and the stationary probability density function associated with the response $X(t)$ can now be determined. Denote $p(x, t|x_0)$ as the transition probability, with the diffusion equation given by

$$\frac{\partial p}{\partial t} = \frac{\partial}{\partial x}\big(g(x)p\big) + \pi S_0 \frac{\partial^2 p}{\partial x^2}, \tag{4.82}$$

where $p(x, 0|x_0) = \delta(x - x_0)$. As $t \to \infty$, $p(x, t|x_0) \to p_s(x)$ and the stationary probability density satisfies

$$\frac{d}{dx}\big(g(x)p_s(x)\big) + \pi S_0 \frac{d^2 p_s}{dx^2} = \frac{d}{dx}\left(g(x)p_s + \pi S_0 \frac{dp_s}{dx}\right) = 0. \tag{4.83}$$

Since both $p_s(x)$ and dp_s/dx vanish as $|x| \to \infty$,

$$g(x)p_s + \pi S_0 \frac{dp_s}{dx} = 0. \tag{4.84}$$

Integrating the above equation yields

$$p_s(x) = A \exp\left(-\frac{1}{\pi S_0}\int_0^x g(z)dz\right), \tag{4.85}$$

with A being a normalization constant:

$$A = \left(\int_{-\infty}^{\infty} \exp\left(-\frac{1}{\pi S_0}\int_0^x g(z)dz\right)dx\right)^{-1}. \tag{4.86}$$

For $g(x) = 0$, the diffusion equation reduces to the heat conduction equation

$$\frac{\partial p}{\partial t} = \pi S_0 \frac{\partial^2 p}{\partial x^2}. \tag{4.87}$$

In this case, stationary probability density does not exist because damping is absent.

Example 4.3.1. Consider a nonlinear oscillator described by the following equation:

$$\dot{x} + ax + bx^3 = 0, \qquad t > 0, \tag{4.88}$$

where a, b are positive constants. Applying the procedure outlined above, the system can be randomized by introducing a white-noise excitation $W(t)$ with zero mean and constant power spectral density S_0:

$$\dot{X} + aX + bX^3 = W(t). \tag{4.89}$$

Let $p(x, t|x_0)$ be the transition probability. The diffusion equation is

$$\frac{\partial p}{\partial t} = \frac{\partial}{\partial x}\big((ax + bx^3)p\big) + \pi S_0 \frac{\partial^2 p}{\partial x^2}, \tag{4.90}$$

where $p(x, 0|x_0) = \delta(x - x_0)$. As $\lim_{t\to\infty} p(x, t|x_0) = p_s(x)$, the stationary probability density satisfies

$$\frac{d}{dx}\left((ax + bx^3)p_s(x) + \pi S_0 \frac{dp_s}{dx}\right) = 0. \tag{4.91}$$

Given that both $p_s(x)$ and dp_s/dx vanish as $|x| \to \infty$,

$$(ax + bx^3)p_s + \pi S_0 \frac{dp_s}{dx} = 0. \tag{4.92}$$

Integrating the above equation results in

$$p_s(x) = A \exp\left(-\frac{1}{\pi S_0}\left(\frac{ax^2}{2} + \frac{bx^4}{4}\right)\right), \tag{4.93}$$

with A being a normalization constant:

$$A = \left(\int_{-\infty}^{\infty} \exp\left(-\frac{1}{\pi S_0}\left(\frac{ax^2}{2} + \frac{bx^4}{4}\right)\right) dx\right)^{-1}. \tag{4.94}$$

If $a < 0$ and $b < 0$, then A approaches infinity and stationary probability density does not exist because the system is unstable.

Example 4.3.2. The function $g(x)$ in Eq. (4.81) need not be differentiable. Consider the following deterministic nonlinear oscillator

$$\dot{x} + k\,\mathrm{sgn}(x) = 0, \qquad t > 0. \tag{4.95}$$

The randomized system is described by

$$\dot{X} + k\,\mathrm{sgn}(X) = W(t), \tag{4.96}$$

where k is a positive constant, $X(0) = x_0$, and $W(t)$ is white noise with zero mean and constant power spectral density S_0. The signum function $\mathrm{sgn}(X)$ is defined as

$$\mathrm{sgn}(X) = \begin{cases} 1 & X > 0 \\ 0 & X = 0\,. \\ -1 & X < 0 \end{cases} \tag{4.97}$$

The diffusion equation and stationary probability density associated with the response $X(t)$ can be constructed in a manner similar to the previous example. An unconstrained Brownian particle subjected to Coulomb friction is governed by

$$\ddot{Y} + k\,\mathrm{sgn}\Big(\dot{Y}\Big) = W(t). \tag{4.98}$$

In terms of velocity, the equation assumes the form

$$\dot{V} + k\,\mathrm{sgn}(V) = W(t), \tag{4.99}$$

which is identical to Eq. (4.96) with $X = V$. Let $p(x,t|x_0)$ be the transition probability. The forward diffusion equation for the transition probability $p(x,t|x_0)$ can be expressed as

$$\frac{\partial p}{\partial t} = \frac{\partial}{\partial x}\big(k\,\mathrm{sgn}(x)p\big) + \pi S_0 \frac{\partial^2 p}{\partial x^2}, \tag{4.100}$$

where $p(x,0|x_0) = \delta(x - x_0)$. As the limit of $p(x,t|x_0)$ approaches infinity, the stationary probability density satisfies

$$\frac{d}{dx}\left(k\,\mathrm{sgn}(x)p_s(x) + \pi S_0 \frac{dp_s}{dx}\right) = 0. \tag{4.101}$$

Integrating the above equation yields

$$\frac{dp_s}{dx} + \frac{k}{\pi S_0}\,\mathrm{sgn}(x)p_s = C. \tag{4.102}$$

Since both $p_s(x)$ and dp_s/dx vanish as $|x| \to \infty$, the constant $C = 0$. Consequently, the stationary probability density is given by

$$p_s(x) = \frac{k}{2\pi S_0}\exp\left(-\frac{k}{\pi S_0}|x|\right). \tag{4.103}$$

As expected, $p_s(x)$ reaches a maximum when the velocity $x = 0$. Nevertheless, due to continual large collision forces acting on the Brownian particle, there is a small chance that the velocity $x \neq 0$ in the steady state. The discontinuity of the magnitude of the Coulomb friction $d|x|/dx = \mathrm{sgn}(x)$ can also be confirmed.

4.4 Linear Damping with Nonlinear Stiffness

This section considers a nonlinear dynamical system of the following form:

$$\ddot{x} + c\dot{x} + g(x) = 0, \tag{4.104}$$

where c is a positive constant, $g(x)$ is a nonlinear function. The randomization of the system results in

$$\ddot{X} + c\dot{X} + g(X) = W(t). \tag{4.105}$$

Here, $X(0) = x_0$ and $\dot{X}(0) = \dot{x}_0$ are initial conditions, and $W(t)$ is stationary Gaussian white noise with zero mean and constant power spectral density S_0. In the state-space form, the system is given by

$$\begin{aligned} \dot{\mathbf{Z}} &= \begin{bmatrix} \dot{X} \\ \ddot{X} \end{bmatrix} = \begin{bmatrix} \dot{X} \\ \dot{X} \end{bmatrix} = \boldsymbol{a}(\mathbf{Z}) + \boldsymbol{b}W(t), \\ \boldsymbol{a}(\mathbf{Z}) &= \begin{bmatrix} Y \\ -cY - g(X) \end{bmatrix}, \qquad \boldsymbol{b} = \begin{bmatrix} 0 \\ 1 \end{bmatrix}. \end{aligned} \tag{4.106}$$

Let $p(\mathbf{z}, t|\mathbf{z}_0)$ denote the transition probability of the system, for which the associated diffusion equation is given by

$$\frac{\partial p}{\partial t} = -y\frac{\partial p}{\partial x} + \frac{\partial}{\partial y}\Big(\big(cy + g(x)\big)p\Big) + \pi S_0 \frac{\partial^2 p}{\partial y^2}. \tag{4.107}$$

The initial condition is

$$p(\mathbf{z}, 0|\mathbf{z}_0) = \delta(\mathbf{z} - \mathbf{z}_0) = \delta(x - x_0)\delta(y - \dot{x}_0). \tag{4.108}$$

The governing equation for stationary probability density can be deduced as follows:

$$-y\frac{\partial p_s}{\partial x} + \frac{\partial}{\partial y}\Big(\big(cy + g(x)\big)p_s\Big) + \pi S_0 \frac{\partial^2 p_s}{\partial y^2} = 0. \tag{4.109}$$

If a candidate solution p_s satisfies the equations

$$-y\frac{\partial p_s}{\partial x} + \frac{\partial}{\partial y}\big(g(x)p_s\big) = 0, \qquad \frac{\partial}{\partial y}(cyp_s) + \pi S_0 \frac{\partial^2 p_s}{\partial y^2} = 0, \tag{4.110}$$

then p_s will be accepted as the solution of Eq. (4.109). To determine p_s, the method of characteristics is employed in Eq. (4.110), resulting in the following general solution[1]:

$$p_s(x, y) = h\bigg(\int g(x)dx + \frac{1}{2}y^2\bigg) = h(H). \tag{4.111}$$

[1]The detailed procedure is presented in Example A.2.3.

The arbitrary function h is defined, with Eq. (4.110), leading to

$$\frac{\partial}{\partial y}\left(cyp_s + \pi S_0 \frac{\partial p_s}{\partial y}\right) = 0. \tag{4.112}$$

Integrating the above equation over y yields

$$cyp_s + \pi S_0 \frac{\partial p_s}{\partial y} = e(x). \tag{4.113}$$

Since p_s and its first-order derivatives vanish as $|x| + |y| \to \infty$, $e(x)$ becomes zero:

$$cyp_s + \pi S_0 \frac{\partial p_s}{\partial y} = 0. \tag{4.114}$$

Substituting $p_s = h(H)$ into this equation leads to

$$cyh + \pi S_0 \frac{dh}{dH} y = 0. \tag{4.115}$$

Canceling y and integrating, the solution becomes

$$h = A \exp\left(-\frac{cH}{\pi S_0}\right), \tag{4.116}$$

where A is a normalization constant. The stationary probability density can be expressed as

$$p_s(x, y) = \frac{\exp\left(\frac{-c}{\pi S_0}\left(\int g(x)dx + \frac{1}{2}y^2\right)\right)}{\int_{-\infty}^{\infty}\int_{-\infty}^{\infty} \exp\left(\frac{-c}{\pi S_0}\left(\int g(x)dx + \frac{1}{2}y^2\right)\right)dxdy}. \tag{4.117}$$

Given that there is only one solution for the problem, the result is unique. Additionally, it is worth noting that although x and y are independent, they are not jointly normally distributed. Furthermore, the governing partial differential equation cannot be solved via separation of variables due to its incompatibility with such a technique as one side depends on x while the other side depends on y. To illustrate this, let

$$p_s(x, y) = X(x)Y(y). \tag{4.118}$$

Upon substitution,

$$-yY\frac{dX}{dx} + cyX\frac{dY}{dy} + CXY + g(x)X\frac{dY}{dy} + \pi S_0 X\frac{d^2Y}{dy^2} = 0. \tag{4.119}$$

Dividing both sides by yXY results in

$$-\frac{1}{X}\frac{dX}{dx} + \frac{C}{Y}\frac{dY}{dy} + \frac{C}{y} + \frac{g(x)}{yY}\frac{dY}{dy} + \frac{\pi S_0}{yY}\frac{d^2Y}{dy^2} = 0. \tag{4.120}$$

This equation cannot be rewritten so that one side depends only on x while the other side depends on y. Thus, the solution $p_s(x, y)$ cannot be found by separation of variables.

4.5 Nonlinear Damping with Nonlinear Stiffness

This section focuses on randomization of a nonlinear dynamical system with nonlinear stiffness and damping. Heuristic methods for solving the diffusion equation related to such systems are examined in detail.

4.5.1 Heuristic Framework of Solving the Diffusion Equation

The analysis now broadens to encompass a nonlinear damping term of the form $f(H)$, where $H = \int g(x)dx + \dot{x}^2/2$. The nonlinear dynamical system, described by a nonlinear stiffness term $g(x)$ and a nonlinear damping term $f(H)$, can be represented as

$$\ddot{x} + \epsilon f(H)\dot{x} + g(x) = 0, \qquad t > 0. \tag{4.121}$$

Upon introducing white noise, the stochastic equation becomes

$$\ddot{X} + \epsilon f(H)\dot{X} + g(X) = W(t), \tag{4.122}$$

where $W(t)$ is a white noise process with zero mean and a constant power spectral density of S_0, and $H\Big(X, \dot{X}\Big)$. When $H = H(x)$, Eq. (4.121) is referred to as the Liénard equation. Should $g(x)$ function as a restoring force, then

$$G(x) = \int g(x)dx \tag{4.123}$$

corresponds to the work done by the restoring force and, consequently, denotes the potential energy. As a result, $G(x)$ is positive and strictly increasing. By formulating a Hamiltonian function,

$$H\Big(X, \dot{X}\Big) = H(X, Y) = G(X) + \frac{1}{2}Y^2. \tag{4.124}$$

In state space form, Eq. (4.122) can be expressed as

$$\dot{\mathbf{Z}} = \boldsymbol{a}(\mathbf{Z}) + \boldsymbol{b}W(t), \tag{4.125}$$

where $\mathbf{Z} = [X, Y]^T$, $\boldsymbol{a}(\mathbf{Z}) = \Big[Y, -\epsilon f\big(H(\mathbf{Z})\big) - g(X)\Big]^T$ and $\boldsymbol{b} = [0, 1]^T$. The diffusion equation associated with the transition probability $p(x, y, t|x_0, y_0)$ is as follows:

$$\frac{\partial p}{\partial t} = -y\frac{\partial p}{\partial x} + \frac{\partial}{\partial y}\Big(\big(\epsilon f(H)y + g(x)\big)p\Big) + \pi S_0\frac{\partial^2 p}{\partial y^2}. \tag{4.126}$$

The stationary probability density $p_s(x, y)$ serves as the solution of the stationary diffusion equation, denoted by

$$-y\frac{\partial p_s}{\partial x} + \frac{\partial}{\partial y}\Big(\big(\epsilon f(H)y + g(x)\big)p_s\Big) + \pi S_0\frac{\partial^2 p_s}{\partial y^2} = 0. \tag{4.127}$$

If

$$-y\frac{\partial p_s}{\partial x}+\frac{\partial}{\partial y}\big(g(x)p_s\big)=0 \tag{4.128}$$

and

$$\frac{\partial}{\partial y}\big(\epsilon f(H)yp_s\big)+\pi S_0\frac{\partial^2 p_s}{\partial y^2}=0 \tag{4.129}$$

are satisfied, then p_s is the solution to Eq. (4.127). Utilizing the method of characteristics, the general solution of Eq. (4.128) can be obtained as follows:

$$p_s=h\bigg(G(x)+\frac{1}{2}y^2\bigg)=h(H), \tag{4.130}$$

In this case, h is an arbitrary function. Additionally, Eq. (4.129) can be expressed as

$$\frac{\partial}{\partial y}\bigg(\epsilon f(H)yp_s+\pi S_0\frac{\partial p_s}{\partial y}\bigg)=0, \tag{4.131}$$

and upon integrating the equation over y, it results in

$$\epsilon f(H)yp_s+\pi S_0\frac{\partial p_s}{\partial y}=e(x), \tag{4.132}$$

where $e(x)$ is an arbitrary function. Since $\epsilon f(H)yp_s+\pi S_0{}^{\partial p_s}/_{\partial y}$ vanishes as $|x|+|y|\to\infty$, $e(x)$ becomes zero:

$$g(x)p_s+\pi S_0\frac{\partial p_s}{\partial y}=0. \tag{4.133}$$

By substituting $p_s=h(H)$ into the equation, the following equation emerges:

$$\epsilon f(H)yh+\pi S_0 y\frac{dh}{dH}=0. \tag{4.134}$$

Cancelling y and integrating the above equation over H yields

$$h=A\exp\bigg(-\frac{\epsilon}{\pi S_0}\int f(H)dH\bigg), \tag{4.135}$$

where A denotes a normalization constant. Consequently, the stationary probability density can be obtained:

$$\begin{aligned} p_s(x,y)&=A\exp\bigg(-\frac{\epsilon}{\pi S_0}\int f(H)dH\bigg),\\ A&=\frac{1}{\int_{-\infty}^{\infty}\int_{-\infty}^{\infty}\exp\Big(-\frac{\epsilon}{\pi S_0}\int f(H)dH\Big)dxdy}. \end{aligned} \tag{4.136}$$

Given the uniqueness of the stationary solution, Eq. (4.136) is the only solution.

Level-Curve Analysis

A level curve of $p_s(x, y)$ is a continuous set of points along which the stationary probability density $p_s(x, y)$ is constant. If $p_s(x, y) = p_s(H)$, the level curves can be described by

$$H = C. \tag{4.137}$$

It can be demonstrated that

$$\frac{d}{dH}p_s(H) = -\frac{A\epsilon}{\pi S_0}f(H)\exp\left(-\frac{\epsilon}{\pi S_0}\int f(H)dH\right) = -\frac{\epsilon}{\pi S_0}p_s f(H). \tag{4.138}$$

This implies that

$$\frac{\partial p_s}{\partial x} = \frac{d}{dH}p_s(H) = -\frac{\epsilon}{\pi S_0}p_s f(H)g(x), \qquad \frac{\partial p_s}{\partial y} = \frac{d}{dH}p_s(H) = -\frac{\epsilon}{\pi S_0}p_s f(H)y. \tag{4.139}$$

The level curve C exhibiting the highest probability corresponds to

$$\frac{d}{dH}p_s(H) = 0, \tag{4.140}$$

which is equivalent to

$$f(H) = 0. \tag{4.141}$$

Additionally, the projection of $p_s(x, y)$ onto a vertical plane achieves a relative maximum at C, conditioned by

$$\frac{\partial p_s}{\partial x} = \frac{\partial p_s}{\partial y} = 0. \tag{4.142}$$

When the corresponding deterministic equation exhibits a limit cycle, the stationary probability density $p_s(x, y)$ displays a substantial value on said limit cycle. Although a limit cycle might not strictly be a level curve, its similarity to the projected crater curve—where $p_s(x, y)$ demonstrates a relative maximum in a direction normal to the limit cycle projected onto the phase plane—remains evident.

In cases where the deterministic equation possesses a limit cycle, it is useful to conduct an analysis of the level curves of the stationary probability density. By examining these level curves, one can enhance their understanding of the system's behavior and its relation to the limit cycle. While the limit cycle itself might not be a level curve, it plays a significant role in characterizing the dominant features of the system.

Validity of Heuristic Formulation

The solution is constructed by separating the stationary diffusion equation into two component equations, as shown in Eq. (4.110), and solving each equation separately. This approach proves successful since $p_s(x, y) = p_s(H)$ remains constant on the level curves specified by $H = C$. This leads to a directional derivative of $p_s(x, y)$ along a level curve that is proportional to $\boldsymbol{\nabla} p_s \cdot \boldsymbol{T}$, where $\boldsymbol{T}$ represents the vector tangent to the aforementioned level curve. Consequently, the first component equation is valid, while the solution of the second component equation is facilitated by the dependence of H on y^2. It is worth noting that typically, the stationary diffusion equation cannot be solved through the method of separation of variables.

The gradient of $p_s(x, y)$ can be expressed as

$$\boldsymbol{\nabla} p_s = \begin{bmatrix} \frac{\partial p_s}{\partial x} \\ \frac{\partial p_s}{\partial y} \end{bmatrix} = -\frac{\epsilon}{\pi S_0} p_s f(H) \begin{bmatrix} g(x) \\ y \end{bmatrix}. \tag{4.143}$$

Additionally, normal lines to the level curve $H = C$ and vectors tangent to them, respectively, are given by

$$\boldsymbol{\nabla} H = \begin{bmatrix} \frac{\partial H}{\partial x} \\ \frac{\partial H}{\partial y} \end{bmatrix} = \begin{bmatrix} g(x) \\ y \end{bmatrix}, \qquad \boldsymbol{T} = \begin{bmatrix} -y \\ g(x) \end{bmatrix}. \tag{4.144}$$

Thus, the directional derivative of $p_s(x, y)$ along a level curve appears proportional to $\boldsymbol{\nabla} p_s \cdot \boldsymbol{T}$, which can be seen in

$$\boldsymbol{\nabla} p_s \cdot \boldsymbol{T} = -y \frac{\partial p_s}{\partial x} + \frac{\partial}{\partial y}\big(g(x) p_s\big) = -\frac{\epsilon}{\pi S_0} p_s f(H)\big(-y g(x) + g(x) y\big) = 0. \tag{4.145}$$

Similarly, the directional derivative of $p_s(x, y)$ normal to a level curve yields $\boldsymbol{\nabla} p_s \cdot \boldsymbol{\nabla} H$, as indicated in

$$\boldsymbol{\nabla} p_s \cdot \boldsymbol{\nabla} H = \frac{\partial p_s}{\partial x} g(x) + \frac{\partial p_s}{\partial y} y = -\frac{\epsilon}{\pi S_0} p_s f(H)\Big(\big(g(x)\big)^2 + y^2\Big). \tag{4.146}$$

This directional derivative vanishes on the limit cycle $f(H) = 0$. For positive damping, $f(H) > 0$ causing $p_s(x, y)$ to decrease; for negative damping, $f(H) < 0$ resulting in an increase of $p_s(x, y)$. The stationary probability density will be determined for certain special cases. Let us recall Eq. (4.104). The Hamiltonian function and level curve can be defined as follows:

$$H(x, y) = \int g(x) dx + \frac{1}{2} y^2, \qquad \epsilon f(H) = C. \tag{4.147}$$

It can be concluded that the limit cycle does not exist if $C > 0$. The stationary probability density is expressed as

$$p_s(x, y) = A \exp\left(-\frac{\epsilon}{\pi S_0} \int f(H) dH\right) = A \exp\left(-\frac{C}{\pi S_0}\left(\int g(x) dx + \frac{1}{2} y^2\right)\right). \tag{4.148}$$

It should be noted that this cannot be solved by the separation of variables, as demonstrated in Eq. (4.120).

Extended Heuristic Formulation

To further extend the heuristic formulation, a nonlinear deterministic equation of the following form is considered[2]:

$$\ddot{x} + \epsilon\left(H_u f(H) - \frac{\pi S_0}{\epsilon}\frac{H_{uu}}{H_u}\right)\dot{x} + \frac{H_x}{H_u} = 0. \tag{4.149}$$

In this equation, ϵ represents a damping constant, $y = \dot{x}$, $u = y^2/2$, $H(x,u)$ denotes the Hamiltonian function, $f(H)$ is a function of H, and S_0 is a constant power spectral density satisfying $\mathbb{E}\big[W(t)W(t+\tau)\big] = 2\pi S_0\delta(\tau)$. Randomization of Eq. (4.149) yields

$$\ddot{X} + \epsilon\left(H_U f(H) - \frac{\pi S_0}{\epsilon}\frac{H_{UU}}{H_U}\right)\dot{X} + \frac{H_X}{H_U} = W(t). \tag{4.150}$$

It can be shown that if H is Eq. (4.124), $H_U = 1, \quad H_{UU} = 0, \quad H_X = g(X)$ and

$$\epsilon\left(H_U f(H) - \frac{\pi S_0}{\epsilon}\frac{H_{UU}}{H_U}\right) = f(H), \quad \frac{H_X}{H_U} = g(X). \tag{4.151}$$

The stationary probability density of Eq. (4.150) becomes

$$p_s(x,y) = A\exp\left(-\frac{\epsilon}{\pi S_0}\int f(H)dH\right)H_u. \tag{4.152}$$

This result is deduced by solving the stationary diffusion equation of Eq. (4.150):

$$-y\frac{\partial p_s}{\partial x} + \frac{\partial}{\partial y}\left(\left(\epsilon y\left(H_u f(H) - \frac{\pi S_0}{\epsilon}\frac{H_{uu}}{H_u}\right) + \frac{H_x}{H_u}\right)p_s\right) + \pi S_0\frac{\partial^2 p_s}{\partial y^2} = 0. \tag{4.153}$$

The solution can be constructed by separating the stationary diffusion equation into two component equations

$$\begin{aligned} &-y\frac{\partial p_s}{\partial x} + \frac{\partial}{\partial y}\left(\frac{H_x}{H_u}p_s\right) = 0, \\ &\frac{\partial}{\partial y}\left(\epsilon y\left(H_u f(H) - \frac{\pi S_0}{\epsilon}\frac{H_{uu}}{H_u}\right)p_s\right) + \pi S_0\frac{\partial^2 p_s}{\partial y^2} = 0. \end{aligned} \tag{4.154}$$

[2]This section has been modified and extended from the work of Caughey and Ma (1982) [77].

By letting $p_s(x,y) = \phi(x,y)H_u$ and recognizing that $u = y^2/2$,

$$-y\frac{\partial p_s}{\partial x} + \frac{\partial}{\partial y}\left(\frac{H_x}{H_u}p_s\right) = -y\frac{\partial}{\partial x}(\phi H_u) + y\frac{\partial}{\partial u}(H_x\phi) = -yH_u\frac{\partial \phi}{\partial x} + yH_x\frac{\partial \phi}{\partial u} \tag{4.155}$$

This leads to the expression

$$-H_u\frac{\partial \phi}{\partial x} + H_x\frac{\partial \phi}{\partial u} = 0. \tag{4.156}$$

Using the method of characteristics, the general solution can then be written as[3]

$$\phi(x,y) = h(H). \tag{4.157}$$

where h is an arbitrary function. Furthermore,

$$\frac{\partial}{\partial y}\left(\epsilon y\left(H_u f(H) - \frac{\pi S_0}{\epsilon}\frac{H_{uu}}{H_u}\right)p_s + \pi S_0\frac{\partial p_s}{\partial y}\right) = 0 \tag{4.158}$$

implies that

$$\epsilon y\left(H_u f(H) - \frac{\pi S_0}{\epsilon}\frac{H_{uu}}{H_u}\right)p_s + \pi S_0\frac{\partial p_s}{\partial y} = 0. \tag{4.159}$$

By substituting $p_s = h(H)H_u$, the expression becomes

$$\epsilon y\left(\frac{H_u f(H)}{\pi S_0} - \frac{1}{\epsilon}\frac{H_{uu}}{H_u}\right)hH_u + h\frac{\partial H_u}{\partial y} + H_u\frac{\partial h}{\partial y} = 0. \tag{4.160}$$

As

$$\frac{\partial H_u}{\partial y} = yH_{uu}, \quad \frac{\partial h}{\partial y} = \frac{\mathrm{d}h}{\mathrm{d}H}\frac{\partial H}{\partial y} = \frac{\mathrm{d}h}{\mathrm{d}H}yH_u, \tag{4.161}$$

Eq. (4.160) can be further expressed as

$$yH_u^2\left(\frac{\epsilon}{\pi S_0}f(H)h + \frac{\mathrm{d}h}{\mathrm{d}H}\right) = 0. \tag{4.162}$$

Integrating both sides with respect to H results in

$$h = A\exp\left(-\frac{\epsilon}{\pi S_0}\int f(H)dH\right). \tag{4.163}$$

Thus, $p_s(x,y)$ is given by

$$p_s(x,y) = h(H)H_u = A\exp\left(-\frac{\epsilon}{\pi S_0}\int f(H)dH\right)H_u. \tag{4.164}$$

[3]The detailed derivation is provided in Example A.2.4

Due to the uniqueness of the solution, this is the only possible solution. The level curves of $p_s(x, y)$ are expressed by

$$-\frac{\epsilon}{\pi S_0}\int f(H)dH + \ln H_u = C. \tag{4.165}$$

The separation of the stationary diffusion equation is valid as $p_s(x, y)$ remains constant along its level curves. The gradient of $p_s(x, y)$, as given by Eq. (4.166), is

$$\boldsymbol{\nabla} p_s = \begin{bmatrix} \frac{\partial p_s}{\partial x} \\ \frac{\partial p_s}{\partial y} \end{bmatrix} = p_s \begin{bmatrix} -\frac{\epsilon}{\pi S_0} f(H) H_x + \frac{H_{ux}}{H_u} \\ -\frac{\epsilon}{\pi S_0} y f(H) H_u + \frac{y H_{uu}}{H_u} \end{bmatrix}. \tag{4.166}$$

This gradient is perpendicular to the level curves of $p_s(x, y)$. The vector tangent to the level curves is given by

$$\boldsymbol{T} = \begin{bmatrix} \frac{\epsilon}{\pi S_0} y f(H) H_u - \frac{y H_{uu}}{H_u} \\ -\frac{\epsilon}{\pi S_0} f(H) H_x + \frac{H_{ux}}{H_u} \end{bmatrix}. \tag{4.167}$$

The directional derivative of $p_s(x, y)$ along a level curve is proportional to

$$\boldsymbol{T} \cdot \boldsymbol{\nabla} p_s = \frac{\partial p_s}{\partial x}\left(\frac{\epsilon}{\pi S_0} y f(H) H_u - \frac{y H_{uu}}{H_u}\right) + \frac{\partial p_s}{\partial y}\left(-\frac{\epsilon}{\pi S_0} f(H) H_x + \frac{H_{ux}}{H_u}\right) = 0. \tag{4.168}$$

Rearranging Eq. (4.168),

$$-\frac{y H_{uu}}{H_u}\frac{\partial p_s}{\partial x} + \frac{H_{ux}}{H_u}\frac{\partial p_s}{\partial y} = -f(H)\frac{\epsilon}{\pi S_0}\left(y H_u \frac{\partial p_s}{\partial x} - H_x \frac{\partial p_s}{\partial y}\right), \tag{4.169}$$

which, using Eq. (4.166), can be further expressed as

$$-\frac{y H_{uu}}{H_u}\frac{\partial p_s}{\partial x} + \frac{H_{ux}}{H_u}\frac{\partial p_s}{\partial y} = f(H) p_s \frac{\epsilon}{\pi S_0}\left(\frac{y H_x H_{uu} - y H_u H_{ux}}{H_u}\right). \tag{4.170}$$

Thus, the equation becomes

$$-f(H)\frac{\epsilon}{\pi S_0}\left(y H_u \frac{\partial p_s}{\partial x} - H_x \frac{\partial p_s}{\partial y}\right) = f(H)\frac{\epsilon}{\pi S_0} p_s \left(\frac{y H_x H_{uu} - y H_u H_{ux}}{H_u}\right). \tag{4.171}$$

By canceling the common terms and calculating the derivatives, the following expression is obtained:

$$-y\frac{\partial p_s}{\partial x} + \frac{\partial}{\partial y}\left(\frac{H_x}{H_u} p_s\right) = -y\frac{\partial p_s}{\partial x} + \frac{H_x}{H_u}\frac{\partial p_s}{\partial y} + H_u\left(y H_u \frac{\partial p_s}{\partial x} - H_x \frac{\partial p_s}{\partial y}\right) = 0. \tag{4.172}$$

Example 4.5.1. Consider a nonlinear oscillator with a Hamiltonian function described by

$$H(x, y) = \frac{1}{2} a(x) y^2 + b(x), \tag{4.173}$$

where $a(x)$ and $b(x)$ represent arbitrary nonlinear coefficient functions of x. Since

$$H_x = a'(x)y^2 + b'(x), \quad H_u = a(x), \quad H_{uu} = 0, \tag{4.174}$$

The resulting nonlinear equation of motion Eq. (4.150) is

$$\ddot{x} + \epsilon a(x) f(H)\dot{x} + \frac{\frac{1}{2}a'(x)\dot{x}^2 + b'(x)}{a(x)} = 0. \tag{4.175}$$

Randomizing this equation yields

$$\ddot{X} + \epsilon a(X) f(H)\dot{X} + \frac{\frac{1}{2}a'(X)\dot{X}^2 + b'(X)}{a(X)} = W(t). \tag{4.176}$$

The probability density for this system is given by

$$p_s(x,y) = A\exp\left(-\frac{\epsilon}{\pi S_0}\int f(H)dH\right)H_u = A\exp\left(-\frac{\epsilon}{\pi S_0}\int f(H)dH\right)a(x). \tag{4.177}$$

It can also be confirmed that Eq. (4.174) is an extended form of the Van der Pol-Rayleigh equation. With $a(x) = 1$, $b(x) = x^2/2$, $H(x,y) = y^2/2 + x^2/2$, and $H_u = 1$, Eq. (4.174) aligns with Eq. (4.235) when $f = -(1-2H)$.

Example 4.5.2. Consider a nonlinear oscillator with discontinuities, where the Hamiltonian function is expressed as

$$H(x,y) = B|y| - \ln\big(1 + B|y|\big) + B^2\int g(x)dx, \tag{4.178}$$

with $B = \gamma/\epsilon$ and $g(x)$ an arbitrary function of x. The relevant partial derivatives from the formulation of Eq. (4.150) are derived as follows:

$$\begin{aligned}
H(x,u) &= B\sqrt{2u} - \ln\Big(1 + B\sqrt{2u}\Big) + B^2\int g(x)dx, \quad H_x = B^2 g(x), \quad f(H) = 1\\
H_u &= \frac{B}{\sqrt{2u}} - \frac{1}{1 + B\sqrt{2u}\frac{B}{\sqrt{2u}}} = \frac{B^2}{1 + B\sqrt{2u}}, \quad H_{uu} = \frac{-B^3}{(1 + B\sqrt{2u})^2\sqrt{2u}},\\
H_u &- \frac{H_{uu}}{H_u} = \frac{B^2}{1 + B\sqrt{2u}} + \frac{1 + B\sqrt{2u}}{B^2}\frac{B^3}{(1 + B\sqrt{2u})^2\sqrt{2u}} = \frac{By}{|y|} = B\,\mathrm{sgn}(y),\\
&\frac{H_x}{H_u} = g(x)(1 + B|y|).
\end{aligned} \tag{4.179}$$

These results lead to the following nonlinear equation of motion

$$\ddot{x} + \epsilon B\,\mathrm{sgn}(\dot{x}) + \big(1 + B|y|\big)g(x) = 0. \tag{4.180}$$

The corresponding randomized system is

$$\ddot{X} + \gamma \operatorname{sgn}\left(\dot{X}\right) + \left(1 + \frac{\gamma}{\epsilon}\left|\dot{X}\right|\right) g(X) = W(t). \tag{4.181}$$

The stationary probability density is given by

$$p_s(x, y) = A \exp\left(-\frac{\gamma}{\pi S_0}\left(|y| + \frac{\gamma}{\epsilon}\int g(x)dx\right)\right). \tag{4.182}$$

4.5.2 Projected Crater Curve Analysis

In this section, the *projected crater curve* is introduced, which is a closed curve representing the edge of a crater-shaped stationary probability density projected onto the $x - y$ plane. It consists of points (x, y) where the density attains relative maxima. A projected crater curve is essential for analyzing the limit cycle of a deterministic nonlinear system, as there are instances where the level curve of the maximum probability does not coincide with the limit cycle. For example, a limit cycle is a level curve if there exists a closed level curve with maximum value of p_s as depicted in Fig. 4.3b. In some cases, however, the level curve with the highest probability does not align with the limit cycle. Consider a nonlinear oscillator with a stationary probability density given by

$$p_s(x, y) = A \exp\left(\frac{\epsilon}{\pi S_0}\left(-x^4 - y^4 - xy\right)\right)\left(x^2 + 2y^2\right). \tag{4.183}$$

As illustrated in Fig. 4.3a, the level curve with the highest probability comprises two points, which neither form a closed curve nor a limit cycle. Nonetheless, the existence of a crater curve implies a high likelihood of a limit cycle occurring in the corresponding deterministic system.

The concepts of the crater curve and projected crater curve are further elaborated in Fig. 4.4. The analytical expression for a crater curve can be derived by collecting the maxima $z - r$ slices of the probability density. Let $p_s(x, y)$ denote the stationary probability density of the randomized nonlinear system, and $p_s(r, \theta)$ represent its equivalent in polar coordinates. The projected crater curve $C(x, y)$ can be defined as

$$C(x, y) = \boldsymbol{\nabla} p_s(x, y) \cdot \boldsymbol{\nabla} l(x, y) = 0, \text{ where } l(x, y) = x^2 + y^2. \tag{4.184}$$

In a manner comparable to Eq. (4.184), the projected crater curve can be represented in polar coordinates as

$$C(r, \theta) = \frac{\partial p_s(r, \theta)}{\partial r} = 0. \tag{4.185}$$

The interpretation of Eq. (4.185) is demonstrated in Fig. 4.5. When an $r - \theta$ slice is created, the local maximum resides at the point where the radial derivative of the sliced probability density equals zero. By repeatedly expanding the slice from 0 to 2π, the projected crater curve corresponding to the condition $\partial p_s(r, \theta)/\partial r = 0$ can be determined.

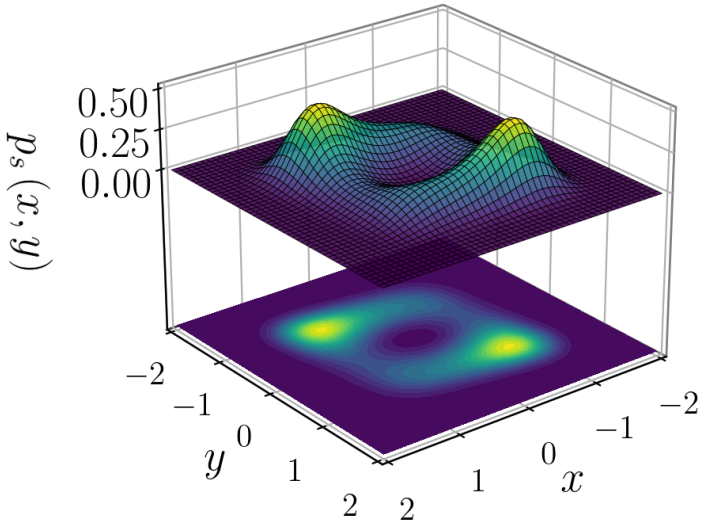

(a) Crater curve aligned with a level curve

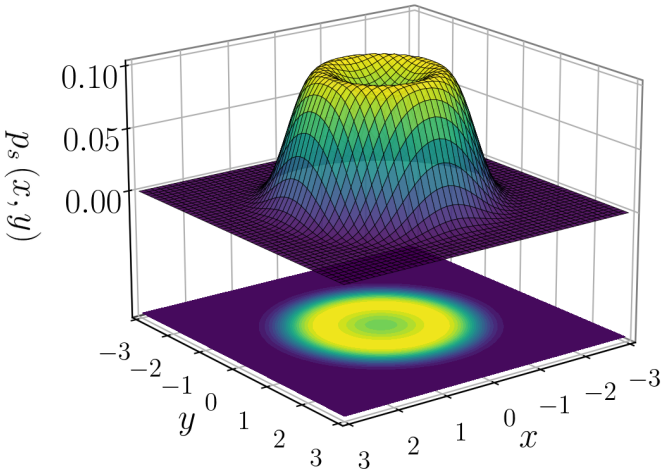

(b) Crater curve not aligned with a level curve

Figure 4.3: Crater-shaped stationary probability density functions with $\epsilon = \pi S_0$

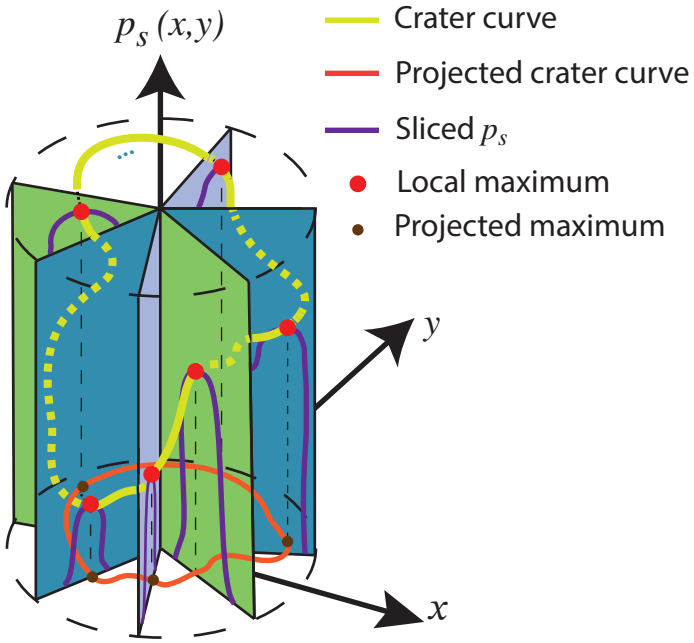

Figure 4.4: Illustration of the crater curve and the projected crater curve

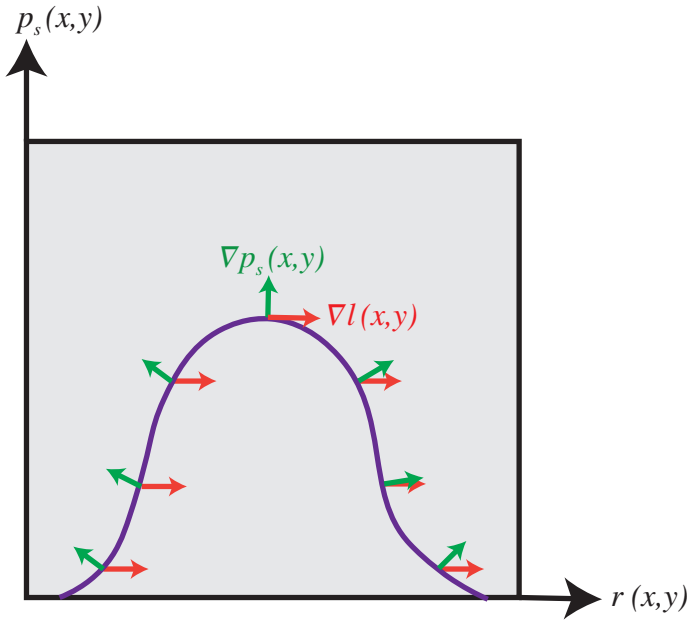

Figure 4.5: Derivation of the projected crater curve

Example 4.5.3. Consider the stationary probability density of the form

$$p_s(x,y) = A\exp\left(\frac{\epsilon}{\pi S_0}\left(\frac{x^2}{2a^2}+\frac{y^2}{2b^2}\right)\left(1-\frac{x^2}{2a^2}-\frac{y^2}{2b^2}\right)\right).$$

The projected crater curve can be obtained as

$$\boldsymbol{\nabla} p_s(x,y)\cdot\boldsymbol{\nabla} l(x,y) = \boldsymbol{\nabla}\left(\frac{\epsilon}{\pi S_0}\left(\frac{x^2}{2a^2}+\frac{y^2}{2b^2}\right)\left(1-\frac{x^2}{2a^2}-\frac{y^2}{2b^2}\right)\right)\cdot\boldsymbol{\nabla}\big(x^2+y^2\big) = 0. \tag{4.186}$$

By processing the derivatives and simplifying the equation, the projected crater curve becomes

$$\frac{x^2}{2a^2}+\frac{y^2}{2b^2} = 1. \tag{4.187}$$

This result concurs with the findings in Section 3.3.2, where the crater curve is identical to a level curve.

Example 4.5.4. Revisit Eq. (4.183). The projected crater curve can be acquired using a procedure analogous to Eq. (4.186),

$$\boldsymbol{\nabla} p_s(x,y)\cdot\boldsymbol{\nabla} l(x,y) = \boldsymbol{\nabla}\left(\frac{\epsilon}{\pi S_0}\big(x^2+2y^2\big)\exp\big(-4x^3-4y^3-2xy\big)\right)\cdot\boldsymbol{\nabla}\big(x^2+y^2\big) = 0. \tag{4.188}$$

Equivalently,

$$\left[2x+\frac{\epsilon}{\pi S_0}(x^2+2y^2)(-4x^3-y), 4y+\frac{\epsilon}{\pi S_0}(-x-4y^3)(x^2+2y^2)\right]\cdot[2x,2y] = 0. \tag{4.189}$$

Computing the dot product yields the projected crater curve:

$$\frac{\epsilon}{\pi S_0}\big(-2x^6-4x^4y^2-x^3y-2x^2y^4-2xy^3-4y^6\big)+x^2+2y^2 = 0. \tag{4.190}$$

The same result can be obtained using polar coordinates. The stationary probability density in polar coordinates is as follows:

$$p_s(r,\theta) = \big(2r^2\sin\theta+r^2\cos^2\theta\big)\exp\left(\frac{\epsilon}{\pi S_0}\big(-r^4\sin^4\theta-r^4\cos^4\theta-r^2\sin\theta\cos\theta\big)\right). \tag{4.191}$$

Taking a derivative with respect to r, the projected crater curve is obtained by Eq. (4.192), which is equivalent to Eq. (4.188) when substituting $x = r\cos\theta$ and $y = r\sin\theta$:

$$\frac{\partial p_s}{\partial r} = 4r^2\left(\frac{\epsilon}{\pi S_0}\big(-4r^4\sin^6\theta+2r^4\sin^2\theta-2r^4-r^2\sin^3\theta\cos\theta-r^2\sin\theta\cos\theta\big)+\sin^2\theta+1\right)$$
$$\times\exp\left(\frac{\epsilon}{\pi S_0}\big(-r^4\sin^4\theta-r^4\cos^4\theta-r^2\sin\theta\cos\theta\big)\right) = 0 \tag{4.192}$$

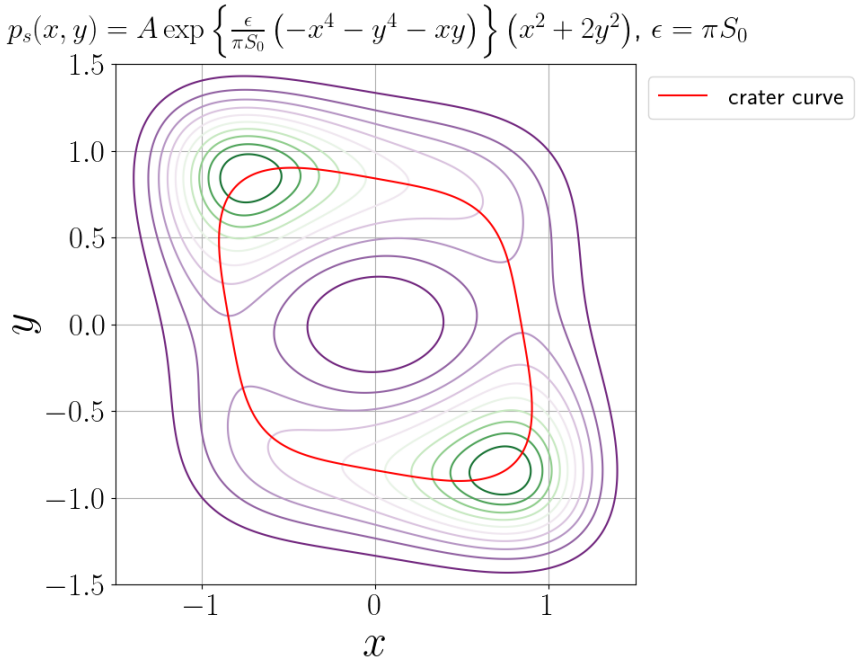

Figure 4.6: The crater curve of Eq. (4.183)

Since the exponential term is always positive, Eq. (4.192) can be reduced to

$$\frac{\epsilon}{\pi S_0}\left(-4r^4\sin^6\theta + 2r^4\sin^2\theta - 2r^4 - r^2\sin^3\theta\cos\theta - r^2\sin\theta\cos\theta\right) + \sin^2\theta + 1 = 0. \quad (4.193)$$

It can be demonstrated that Eq. (4.188) and (4.192) are equivalent by replacing $x = r\cos\theta$ and $y = r\sin\theta$ in Eq. (4.188). The plotted projected crater curve based on these solutions is illustrated in Fig. 4.6.

With the formulation of the projected crater curve, it becomes possible to further emphasize certain analytical properties from the stationary probability density, such as critical points. Consider the generalized stationary probability density of the form:

$$p_s(x,y) = A\exp\left(-D(x^{m_1} + C_1x^{m_2}y^{m_3} + C_2y^{m_4})\right)(x^{n_1} + C_3x^{n_2}y^{n_3} + C_4y^{n_4}), \quad (4.194)$$

where $\{m_i, n_i, C_i\}$ and $x^{n_1} + C_3x^{n_2}y^{n_3} + C_4y^{n_4}$ are nonnegative. Critical points can be obtained by taking the partial derivative of the projected crater curve with respect to x and y, then setting them equal to zero, which results in

$$(x_c, y_c) = \left(0, \pm\left(\frac{n_1}{Dm_1}\right)^{\frac{1}{m_1}}\right), \quad \left(\pm\left(\frac{n_1}{Dm_1}\right)^{\frac{1}{m_1}}, 0\right). \quad (4.195)$$

This outcome indicates that critical points do not depend on the proportional coefficients C_i of the stationary probability density but are solely affected by the constant D. In Section 4.6, these properties will be further explored.

4.5.3 Heuristic Framework Using Variation of Parameters

In the aforementioned section, it has been illustrated that stationary diffusion equations for randomized nonlinear dynamical systems can be solved using heuristic methods. Nevertheless, this formulation does not encompass all nonlinear systems. For instance, the heuristic method presented in Section 4.5.1 fails to address the nonlinear oscillator with a stationary probability density represented by

$$p_s(x,y) = A\exp\bigg(\frac{\epsilon}{\pi S_0}\big(-x^2-y^2-x^2y^2\big)\bigg)\big(x^2+2y^2\big). \tag{4.196}$$

Hence, an alternative heuristic formulation is proposed which uncovers a new set of analytical solutions to stationary diffusion equations. This formulation is considered to be the most generalized, as it not only includes previous formulations but also encompasses a new set of nonlinear oscillators whose stationary probability density can be solved by the proposed method.

Taking into account the nonlinear dynamical system introduced in Eq. (1.1),

$$\ddot{x} + \epsilon\alpha(x,\dot{x})\dot{x} + \beta(x,\dot{x}) = 0,$$

the corresponding randomized system given by Eq. (1.2) is

$$\ddot{X} + \epsilon\alpha\Big(X,\dot{X}\Big)\dot{X} + \beta\Big(X,\dot{X}\Big) = W(t),$$

which can be expressed as

$$\ddot{X} + \epsilon\alpha(X,Y)\dot{X} + \beta(X,Y) = W(t), \tag{4.197}$$

where $Y = \dot{X}$, ϵ is a constant, and $\alpha(X,Y)$, $\beta(X,Y)$ are arbitrary functions of X and Y. Additionally, $W(t)$ is a white noise process with a zero mean and a constant power spectral density of S_0. Eq. (4.197) is governed by the stationary diffusion equation

$$-y\frac{\partial p_s}{\partial x} + \frac{\partial}{\partial y}\big((\epsilon y\alpha+\beta)p_s\big) + \pi S_0\frac{\partial^2 p_s}{\partial y^2} = 0. \tag{4.198}$$

Assuming that the stationary probability density for Eq. (4.197) is expressed as

$$p_s(x,y) = A\exp\bigg(-\frac{\epsilon}{\pi S_0}\phi(x,y)\bigg)g(x,y), \tag{4.199}$$

two component equations can be constructed:

$$-y\frac{\partial p_s}{\partial x} + \frac{\partial}{\partial y}(\beta p_s) = 0, \tag{4.200}$$

and

$$\frac{\partial}{\partial y}(\epsilon y \alpha p_s) + \pi S_0 \frac{\partial^2 p_s}{\partial y^2} = \frac{\partial}{\partial y}\left(\epsilon y \alpha p_s + \pi S_0 \frac{\partial p_s}{\partial y}\right) = 0, \tag{4.201}$$

which leads to

$$\epsilon y \alpha p_s + \pi S_0 \frac{\partial p_s}{\partial y} = 0 \tag{4.202}$$

Suppose that $p_s(x, y) = \exp\big(-D\phi(x, y)\big)g(x, y)$, where $D = \epsilon/\pi S_0$. Applying this expression to p_s in the first equation of Eq. (4.200) yields

$$-y\frac{\partial p_s}{\partial x} + \frac{\partial}{\partial y}(\beta p_s) = yD\frac{\partial \phi}{\partial x} g \exp(-D\phi) - y\frac{\partial g}{\partial x}\exp(-D\phi) + \frac{\partial}{\partial y}(\beta p_s) = 0. \tag{4.203}$$

After working out the derivatives,

$$\begin{aligned} yD\frac{\partial \phi}{\partial x} g \exp(-D\phi) - y\frac{\partial g}{\partial x}\exp(-D\phi) + \frac{\partial \beta}{\partial y} g \exp(-D\phi) \\ - D\beta\frac{\partial \phi}{\partial y} g \exp(-D\phi) + \beta\frac{\partial g}{\partial y}\exp(-D\phi) = 0. \end{aligned} \tag{4.204}$$

By rearranging the terms, the following equation is obtained:

$$\frac{\partial \beta}{\partial y} + \left(\frac{1}{g}\frac{\partial g}{\partial y} - D\frac{\partial \phi}{\partial y}\right)\beta = y\left(\frac{1}{g}\frac{\partial g}{\partial x} - D\frac{\partial \phi}{\partial x}\right). \tag{4.205}$$

This equation is a first-order ordinary differential equation that can be solved using the variation of parameters [78]. The solution is given by

$$\beta(x, y) = \int \left(I(x, y) y\left(\frac{1}{g}\frac{\partial g}{\partial x} - D\frac{\partial \phi}{\partial x}\right)\right) dy \Big/ I(x, y), \tag{4.206}$$

where

$$I(x, y) = \exp\left(\int \left(\frac{1}{g}\frac{\partial g}{\partial y} - D\frac{\partial \phi}{\partial y}\right) dy\right). \tag{4.207}$$

Applying p_s to the second equation of (4.202) results in

$$\epsilon y \alpha p_s + \pi S_0 \frac{\partial p_s}{\partial y} = 0. \tag{4.208}$$

Using Eq. (4.199) and reorganizing the terms, the following equation is formulated:

$$\alpha(x,y) = \frac{\pi S_0}{y\epsilon}\left(D\frac{\partial \phi}{\partial y} - \frac{1}{g}\frac{\partial g}{\partial y}\right) = \frac{1}{y}\left(\frac{\partial \phi}{\partial y} - \frac{1}{Dg}\frac{\partial g}{\partial y}\right). \tag{4.209}$$

It is crucial to note that this formulation constitutes an extension of the previously introduced heuristic formulations. Recall the Eq. (4.150), with $U = {}^{Y^2}\!/_2$, which can be rewritten as

$$\ddot{X} - \epsilon\left(\frac{H_Y Y}{Y} f(H) - \frac{\pi S_0}{\epsilon}\left(\frac{H_{YY}}{Y H_Y} - \frac{1}{Y^2}\right)\right)\dot{X} + Y\frac{H_X}{H_Y} = W(t). \tag{4.210}$$

If $\phi(x,y) = \int f(H)dH$ and $g(x,y) = {}^{H_y}\!/_y$, then Eq. (4.210) is equivalent to (4.197).

Example 4.5.5. Revisiting the example of Eq. (4.260), direct calculations yield

$$\phi(x,y) = x^4 + y^4 + x^2y^2 = H, \quad f(H) = 1, \quad g(x,y) = x^2 + 2y^2. \tag{4.211}$$

Computing the derivatives results in

$$\frac{\partial g}{\partial x} = 2x, \quad \frac{\partial g}{\partial y} = 4y, \quad \frac{\partial \phi}{\partial x} = 4x^3 + 2xy^2, \quad \frac{\partial \phi}{\partial y} = 2x^2y + 4y^3. \tag{4.212}$$

This leads to a nonlinear system described by Eq. (4.260):

$$I(x,y) = \exp\left(\int\left(\frac{1}{g}\frac{\partial g}{\partial y} - D\frac{\partial \phi}{\partial y}\right)dy\right) = (x^2 + 2y^2)\exp\Big(-D\big(x^2y^2 + y^4\big)\Big), \tag{4.213}$$

which provides

$$\beta(x,y) = \frac{x(2x^2 + y^2)}{x^2 + 2y^2}, \quad \alpha(x,y) = 2x^2 + 4y^2 - \frac{4}{D(x^2 + 2y^2)}. \tag{4.214}$$

This outcome is identical to Eq. (4.260), signifying that the formulation presented in this section is an extension of the heuristic formulation previously presented.

The acquired result will be employed in Section 4.6.2 to determine the analytical stationary probability density densities of a new set of nonlinear oscillators.

4.6 Illustrative Examples of Randomization

In this section, the randomization of dynamical systems is applied to various examples, showcasing the effectiveness of the proposed method. The examples are divided into three categories: multiple equilibria, limit cycles, and bifurcation. Heuristic methods developed in Section 4.5.1 and 4.5.3 are extensively utilized to solve the diffusion equation.

4.6.1 Multiple Equilibrium Points

Two widely studied nonlinear oscillators, the Duffing equation and the damped pendulum equation, are considered. Particular focus is placed on the stability of their equilibria.

Duffing Equation

The present discussion encompasses the randomization of dynamical systems, focusing on the Duffing equation as a primary example. Introduced in Eq. (2.3), the unforced Duffing equation incorporates linear damping and nonlinear stiffness:

$$\ddot{x} + \epsilon\dot{x} + k_1 x + k_2 x^3 = 0, \qquad t > 0. \tag{4.215}$$

Incorporating randomness, the system is expressed as

$$\ddot{X} + \epsilon\dot{X} + k_1 X + k_2 X^3 = W(t), \tag{4.216}$$

where $X(0) = x_0$ and $\dot{X}(0) = \dot{x}_0$ denote the initial conditions, ϵ represents the coefficient associated with the nonlinear stiffness, and $W(t)$ refers to a stationary Gaussian white noise featuring a zero mean and a constant power spectral density S_0. This equation may be placed in state-space form as demonstrated in Eq. (4.217),

$$\dot{\mathbf{Z}} = \begin{bmatrix} Y \\ -\epsilon Y - k_1 X - k_2 X^3 \end{bmatrix} \mathbf{Z} + \begin{bmatrix} 0 \\ 1 \end{bmatrix} W(t), \tag{4.217}$$

where

$$\mathbf{Z}(0) = \mathbf{z}_0 = \begin{bmatrix} x_0 \\ \dot{x}_0 \end{bmatrix}.$$

Here, $\mathbf{Z} = \left[X, \dot{X}\right]^T = [X, Y]^T$. For the transitional probability of the system, represented by $p(x, y, t|x_0, y_0)$, the corresponding diffusion equation emerges as

$$\frac{\partial p}{\partial t} = -y\frac{\partial p}{\partial x} + \frac{\partial}{\partial y}\big((\epsilon y + k_1 x + k_2 x^3)p\big) + \pi S_0 \frac{\partial^2 p}{\partial y^2}. \tag{4.218}$$

The initial condition is defined as

$$p(x, y, 0|x_0, y_0) = \delta(x - x_0)\delta(y - y_0). \tag{4.219}$$

Furthermore, the stationary probability density is governed by

$$-y\frac{\partial p_s}{\partial x} + \frac{\partial}{\partial y}\big((\epsilon y + k_1 x + k_2 x^3)p_s\big) + \pi S_0 \frac{\partial^2 p_s}{\partial y^2} = 0. \tag{4.220}$$

This equation holds if

$$-y\frac{\partial p_s}{\partial x}+\frac{\partial}{\partial y}\big((k_1x+k_2x^3)p_s\big)=0 \tag{4.221}$$

and

$$\frac{\partial}{\partial y}(\epsilon y p_s)+\pi S_0\frac{\partial^2 p_s}{\partial y^2}=0. \tag{4.222}$$

Utilizing the method of characteristics to solve Eq. (4.221), the general solution takes the form

$$p_s=h\bigg(\frac{1}{2}k_1x^2+\frac{1}{4}k_2x^4+\frac{1}{2}y^2\bigg)=h(H). \tag{4.223}$$

In this instance, h denotes an arbitrary function. Additionally,

$$\frac{\partial}{\partial y}\bigg(\epsilon y p_s+\pi S_0\frac{\partial p_s}{\partial y}\bigg)=0, \tag{4.224}$$

and after integrating the above equation over y, it yields

$$\epsilon y p_s+\pi S_0\frac{\partial p_s}{\partial y}=e(x). \tag{4.225}$$

By defining $e(x)$ such that p_s and its first-order derivatives vanish as $|x|+|y|\to\infty$, it becomes evident that $e(x)=0$ and

$$\epsilon y p_s+\pi S_0\frac{\partial p_s}{\partial y}=0. \tag{4.226}$$

Substituting $p_s=h(H)$ in the above equation,

$$\epsilon y h+\pi S_0\frac{dh}{dH}y=0, \tag{4.227}$$

and upon integrating the above equation over y,

$$h=A\exp\bigg(-\frac{\epsilon H}{\pi S_0}\bigg), \tag{4.228}$$

where A is a normalization constant. Consequently, the stationary probability density is given by

$$p_s(x,y)=\frac{\exp\Big(-\frac{\epsilon}{\pi S_0}\big(\frac{1}{2}k_1x^2+\frac{1}{4}k_2x^4+\frac{1}{2}y^2\big)\Big)}{\int_{-\infty}^{\infty}\int_{-\infty}^{\infty}\exp\Big(-\frac{\epsilon}{\pi S_0}\big(\frac{1}{2}k_1x^2+\frac{1}{4}k_2x^4+\frac{1}{2}y^2\big)\Big)dxdy}. \tag{4.229}$$

This outcome aligns with the solution derived from the rationale provided in Section 4.4. For cases where $k_2>0$, Fig. 4.7 exhibits a typical graph of the stationary probability density.

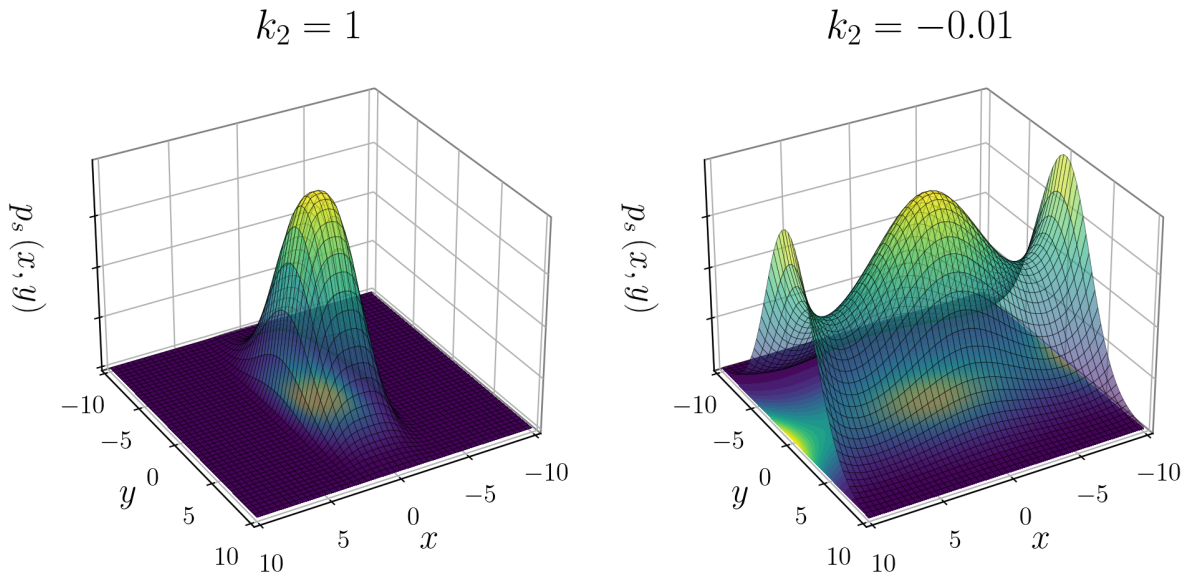

Figure 4.7: The stationary probability density function of the Duffing equation, $\epsilon = 0.1$, $k_1 = 1$, $S_0 = 1/\pi$, and $k_2 = \{1, -0.01\}$.

Notably, the stationary probability density $p_s(\mathbf{z})$ attains a maximum at $\mathbf{z} = \mathbf{0}$. However, for the case when $\epsilon > 0$, $k_1 > 0$, and $k_2 > 0$, the deterministic Duffing equation

$$\ddot{x} + \epsilon\dot{x} + k_1 x + k_2 x^3 = 0 \tag{4.230}$$

possesses a single equilibrium point at $(0, 0)$, which is classified as a stable focus. In general, the stationary probability density of a system exhibits a relative maximum at each stable equilibrium point. The stationary probability density associated with the response $x(t)$ can be expressed as

$$p_s(x) = \int_{-\infty}^{\infty} p_s(x, y)dy = A \exp\left(-\frac{\epsilon}{\pi S_0}\left(\frac{1}{2}k_1 x^2 + \frac{1}{4}k_2 x^4\right)\right). \tag{4.231}$$

In the scenario where $\epsilon = 0$, the stationary probability density cannot exist due to the origin functioning as a center. When $\epsilon > 0$, $k_1 > 0$, and $k_2 < 0$, three equilibrium points emerge, located at $(0, 0)$ and $(\pm\sqrt{-k_1/k_2}, 0)$. While the origin remains a stable focus, the other two equilibrium points act as saddle points. The majority of trajectories are unbounded, subsequently resulting in an absence of stationary probability density. Such probability density for $k_2 < 0$ can be observed in cases where a Brownian particle is constrained to a rectangle centered at the origin of the phase plane.

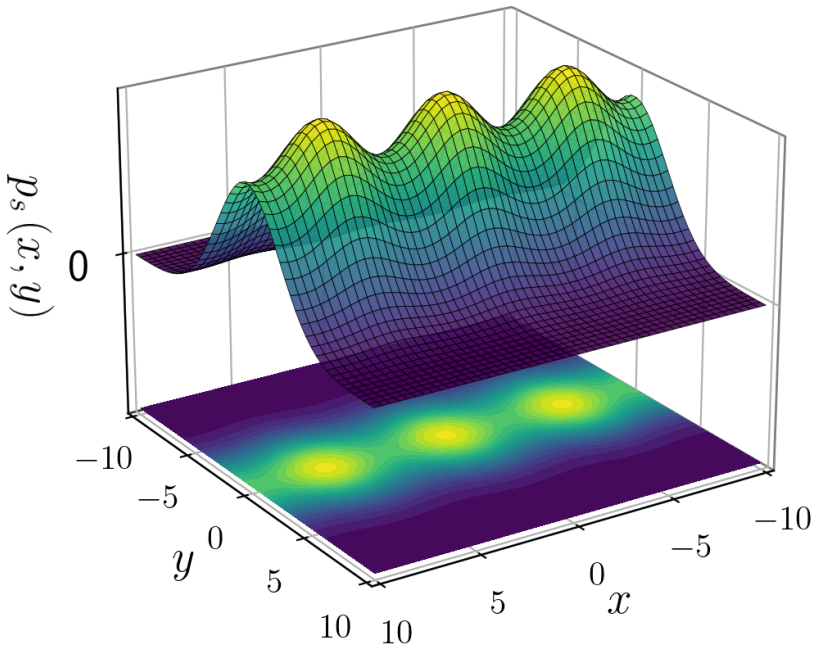

Figure 4.8: The stationary probability density of the damped pendulum, $\epsilon = 0.15$ and $S_0 = 1/\pi$

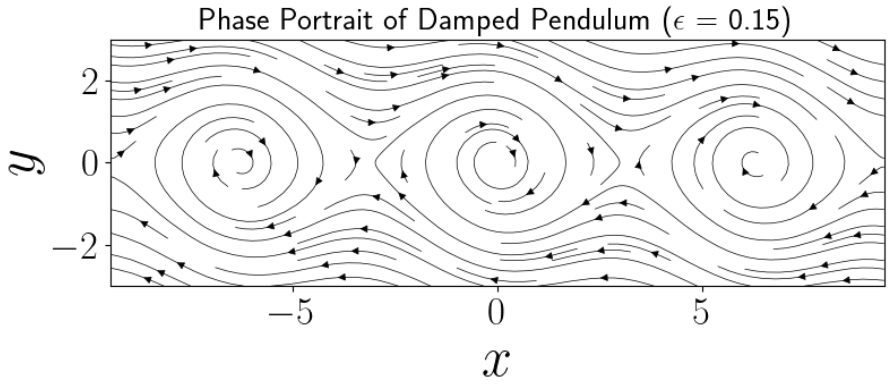

Figure 4.9: The phase portrait of a deterministic equation of damped pendulum with $\epsilon = 0.15$

Damped Pendulum

In Example 3.3.1, the qualitative behavior of the damped pendulum was analyzed using conventional deterministic methods. The present discussion pivots to an analysis via randomization. Recall that the deterministic damped pendulum equation is given by

$$\ddot{x} + \epsilon\dot{x} + \sin(x) = 0, \qquad t > 0.$$

When excited by white noise, the equation becomes

$$\ddot{X} + \epsilon\dot{X} + \sin(X) = W(t). \tag{4.232}$$

This is equivalent to Eq. (4.104) with $g(X) = \sin(X)$. Following the procedure outlined in Section 4.4, the stationary probability density can be expressed as

$$p_s(x,y) = \begin{cases} \frac{\exp\left(-\frac{\epsilon}{\pi S_0}\left(-\cos(x)+\frac{1}{2}y^2\right)\right)}{\int_{-b}^{b}\int_{-b}^{b}\exp\left(-\frac{\epsilon}{\pi S_0}\left(-\cos(x)+\frac{1}{2}y^2\right)\right)dxdy} & -b < x, \quad y < b \\ 0 & \text{otherwise} \end{cases}. \tag{4.233}$$

A typical graph of the stationary probability density is illustrated in Fig. 4.8. It should be noted that

$$\lim_{b\to\infty}\left(\int_{-b}^{b}\int_{-b}^{b}\exp\left(-\frac{\epsilon}{\pi S_0}\left(-\cos(x)+\frac{1}{2}y^2\right)\right)dxdy\right) \to \infty \tag{4.234}$$

Further scrutiny reveals that $p_s(\mathbf{z})$ attains a relative maximum at $(2n\pi, 0)$ and a saddle point at $\big((2n-1)\pi, 0\big)$, where n is an integer.

For the deterministic damped pendulum equation with $\epsilon > 0$, there are two types of equilibrium points. Stable equilibrium points are located at $(2n\pi, 0)$ and can be classified as stable foci. On the other hand, unstable equilibrium points are situated at $\big((2n-1)\pi, 0\big)$ and serve as saddle points. A phase portrait for $\epsilon = 0.15$ is presented in Fig. 4.9.

4.6.2 Limit Cycles

The current discussion focuses on the randomization of nonlinear systems that exhibit a limit cycle in their corresponding deterministic system.

The Van der Pol-Rayleigh Oscillator

Revisiting the nonlinear system with an existing limit cycle introduced in Eq. (3.13),

$$\ddot{x} - \epsilon\big(1 - x^2 - \dot{x}^2\big)\dot{x} + x = 0.$$

The system, excited by white noise, is expressed as

$$\ddot{X} - \epsilon\Big(1 - X^2 - \dot{X}^2\Big)\dot{X} + X = W(t), \tag{4.235}$$

where initial conditions are $X(0) = 0$ and $\dot{X}(0) = 0$. The stochastic forcing $W(t)$ is a Gaussian white noise with zero mean and spectral density S_0. Denoting $Y = \dot{X}$, the Eq. (4.235) becomes analogous to Eq. (4.122), where

$$g(X) = 1, \quad f(H) = -(1 - 2H), \quad H = \frac{1}{2}X^2 + \frac{1}{2}Y^2. \tag{4.236}$$

Following the procedure in Section 4.5, the solution is

$$p_s(x, y) = A \exp\left(\frac{\epsilon}{\pi S_0}\left(\int (1 - 2H)dH\right)\right) = A \exp\left(\frac{\epsilon(H - H^2)}{\pi S_0}\right). \tag{4.237}$$

Replacing H with ${}^{x^2}\!/_2 + {}^{y^2}\!/_2$ yields

$$p_s(x, y) = A \exp\left(\frac{\epsilon}{\pi S_0}\left(\frac{1}{2}x^2 + \frac{1}{2}y^2\right)\left(1 - \frac{1}{2}x^2 - \frac{1}{2}y^2\right)\right), \tag{4.238}$$

where

$$A = \frac{1}{\int_{-\infty}^{\infty}\int_{-\infty}^{\infty} \exp\Big(\frac{\epsilon}{\pi S_0}\big(\frac{1}{2}x^2 + \frac{1}{2}y^2\big)\big(1 - \frac{1}{2}x^2 - \frac{1}{2}y^2\big)\Big)dxdy}. \tag{4.239}$$

In a vector form,

$$p_s(\mathbf{z}) = \frac{\exp\Big(\frac{\epsilon}{\pi S_0}\big(\frac{1}{2}\mathbf{z}\cdot\mathbf{z}\big)\big(1 - \frac{1}{2}\mathbf{z}\cdot\mathbf{z}\big)\Big)}{\int_{-\infty}^{\infty}\int_{-\infty}^{\infty} \exp\Big(\frac{\epsilon}{\pi S_0}\big(\frac{1}{2}\mathbf{z}\cdot\mathbf{z}\big)\big(1 - \frac{1}{2}\mathbf{z}\cdot\mathbf{z}\big)\Big)d\mathbf{z}}. \tag{4.240}$$

The uniqueness of the solution implies that this is the only solution. Notably, x and y are correlated and not jointly normal. The stationary probability density $p_s(x, y)$ was derived by partitioning the stationary diffusion equation into two component equations, which proved effective as the stationary probability density is symmetric about the y-axis, illustrated in

$$p_s(x, y) = p_s(-x, y). \tag{4.241}$$

Consequently, the diffusion equation is satisfied upon substituting x with $-x$, resulting in

$$-y\frac{\partial p_s}{\partial x} + \frac{\partial}{\partial y}(xp_s) = 0, \tag{4.242}$$

which implies that

$$-\frac{\partial}{\partial y}\big(\epsilon(1 - x^2 - y^2)yp_s\big) + \pi S_0\frac{\partial^2 p_s}{\partial y^2} = 0. \tag{4.243}$$

Similarly, the symmetry about the y-axis yields the same stationary diffusion equations if

$$p_s(x,y) = p_s(x,-y). \tag{4.244}$$

Moreover, the two separated equations do not originate from radial symmetry of $p_s(x,y)$. This is visible in Fig. 4.3b, which displays the stationary probability density function $p_s(x,y)$ and the level curve of the Van der Pol-Rayleigh oscillator. By computing first-order partial derivatives,

$$\begin{aligned}
\frac{\partial p_s}{\partial x} &= \frac{dp_s}{dH}\frac{\partial H}{\partial x} = A\exp\left(\frac{\epsilon}{\pi S_0}H(H-1)\right)\frac{\epsilon}{\pi S_0}(1-2H)x = \frac{\epsilon}{\pi S_0}\big((1-2H)x\big)p_s, \\
\frac{\partial p_s}{\partial y} &= \frac{dp_s}{dH}\frac{\partial H}{\partial y} = A\exp\left(\frac{\epsilon}{\pi S_0}H(H-1)\right)\frac{\epsilon}{\pi S_0}(1-2H)y = \frac{\epsilon}{\pi S_0}\big((1-2H)y\big)p_s.
\end{aligned} \tag{4.245}$$

Through the analysis of Section 4.5.1, a limit cycle can be deduced from the stationary probability density $p_s(x,y)$ of the randomized Van der Pol-Rayleigh oscillator. For the limit cycle to be a level curve C, the projection of $p_s(x,y)$ onto a vertical plane must possess a relative maximum on C. This implies that

$$\frac{\partial p_s}{\partial x} = \frac{\partial p_s}{\partial y} = 0, \tag{4.246}$$

which leads to

$$(1-2H)x = (1-2H)y = 0. \tag{4.247}$$

The solution of Eq. (4.247) is either $(x,y) = (0,0)$ or $(1-2H) = 0$. This implies that the limit cycle is the unit circle:

$$x^2 + y^2 = 1.$$

The stationary probability density $p_s(x,y)$ has a relative minimum at the equilibrium point $(0,0)$, which is an unstable focus if $0 < \epsilon < 2$ or an unstable node if $\epsilon > 2$. At the origin,

$$p_s(0,0) = p_s(H=0) = A. \tag{4.248}$$

The limit cycle of the Van der Pol-Rayleigh oscillator is the unit circle for all positive values of ϵ, no matter how large. On the limit cycle,

$$p_s\left(H = \frac{1}{2}\right) = A\exp\left(\frac{\epsilon}{4\pi S_0}\right) > A = p_s(0,0). \tag{4.249}$$

It is impossible to determine the nature of any critical points on the limit cycle since $p_s(x,y)$ is constant on the limit cycle. This can be verified by calculating the determinant of the Hessian of $p_s(x,y)$ being zero:

$$\begin{aligned}
\frac{\partial^2 p_s}{\partial x^2} &= \frac{\partial}{\partial x}\left(\frac{\epsilon}{\pi S_0}\big((1-2H)x\big)p_s\right) = \left(\frac{\epsilon}{\pi S_0}\right)^2\Big((1-2H)^2x^2\Big)p_s + \frac{\epsilon}{\pi S_0}\big(1-3x^2-y^2\big)p_s, \\
\frac{\partial^2 p_s}{\partial y^2} &= \frac{\partial}{\partial y}\left(\frac{\epsilon}{\pi S_0}\big((1-2H)y\big)p_s\right) = \left(\frac{\epsilon}{\pi S_0}\right)^2\Big((1-2H)^2y^2\Big)p_s + \frac{\epsilon}{\pi S_0}\big(1-x^2-3y^2\big)p_s, \\
\frac{\partial^2 p_s}{\partial x \partial y} &= \frac{\partial}{\partial x}\left(\frac{\epsilon}{\pi S_0}\big((1-2H)y\big)p_s\right) = \left(\frac{\epsilon}{\pi S_0}\right)^2\Big((1-2H)^2xy\Big)p_s - \frac{2\epsilon}{\pi S_0}xyp_s.
\end{aligned}$$

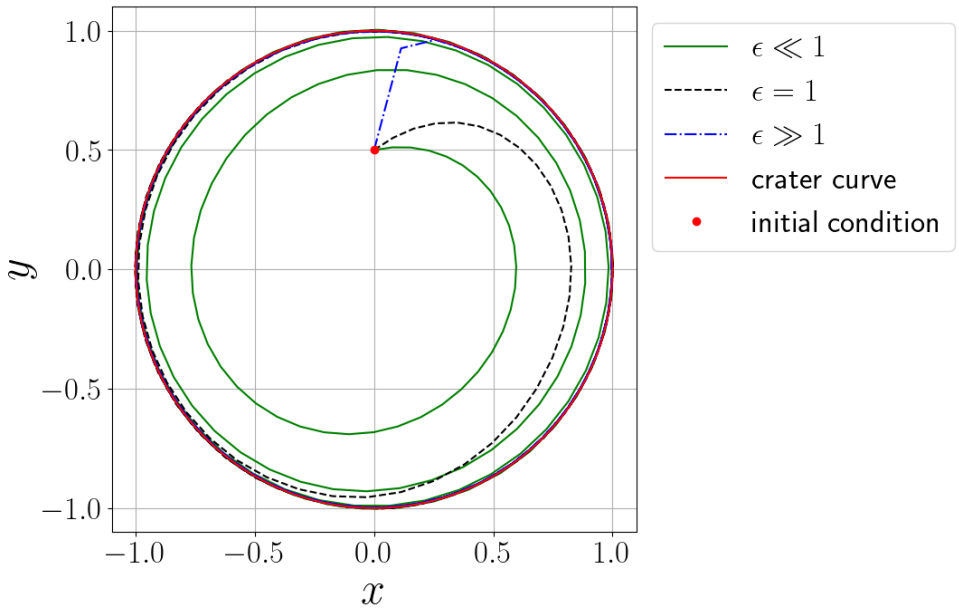

Figure 4.10: The limit cycle of the van der Pol-Rayleigh oscillator with different damping constants ϵ

On the limit cycle, however,

$$\begin{aligned}
\frac{\partial^2 p_s}{\partial x^2} &= \frac{\epsilon}{\pi S_0}\big(1 - 3x^2 - y^2\big)p_s = \frac{2\epsilon}{\pi S_0}(-2x^2)p_s < 0, \\
\frac{\partial^2 p_s}{\partial y^2} &= \frac{\epsilon}{\pi S_0}\big(1 - x^2 - 3y^2\big)p_s = \frac{2\epsilon}{\pi S_0}(-2y^2)p_s < 0, \\
\frac{\partial^2 p_s}{\partial x \partial y} &= -\frac{2\epsilon}{\pi S_0} xy p_s.
\end{aligned} \tag{4.250}$$

The determinant of the Hessian of $p_s(x, y)$ is

$$\det(\boldsymbol{H}) = \begin{vmatrix} \frac{\partial^2 p_s}{\partial x^2} & \frac{\partial^2 p_s}{\partial x \partial y} \\ \frac{\partial^2 p_s}{\partial y \partial x} & \frac{\partial^2 p_s}{\partial y^2} \end{vmatrix} = \frac{\epsilon^2}{\pi^2 S_0^2}\big((2x^2)(2y^2) - (2xy)^2\big)p_s^2 = 0. \tag{4.251}$$

The limit cycle is the unit circle $2H = 1$ for any ϵ. The directional derivative of $p_s(x, y)$ normal to a level curve is proportional to

$$\boldsymbol{\nabla} p_s \cdot \boldsymbol{\nabla} H = \frac{\partial p_s}{\partial x} g(x) + \frac{\partial p_s}{\partial y} y = \frac{\epsilon}{\pi S_0} p_s (1 - 2H)\big(g^2(x) + y^2\big). \tag{4.252}$$

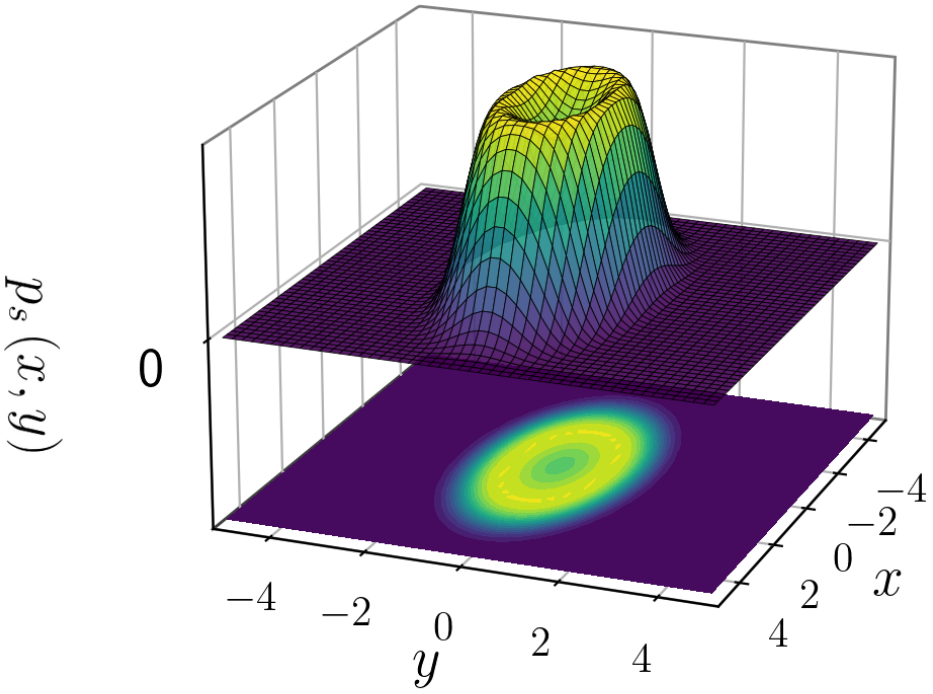

Figure 4.11: Stationary probability density of Eq. (4.255)

For points inside the limit cycle, $2H < 1$, and consequently, $p_s(x, y)$ increases towards the limit cycle. For points outside the limit cycle, $2H > 1$, and thus $p_s(x, y)$ decreases away from the limit cycle.

Elliptical Limit Cycle

The nonlinear oscillator with an elliptical limit cycle can be analyzed similarly. The randomized nonlinear equation of

$$\ddot{x} - \epsilon\left(1 - \frac{x^2}{a^2} - \frac{\dot{x}^2}{b^2}\right)\dot{x} + \frac{b^2}{a^2}x = 0$$

becomes

$$\ddot{X} - \epsilon\left(1 - \frac{X^2}{a^2} - \frac{\dot{X}^2}{b^2}\right)\dot{X} + \frac{b^2}{a^2}X = W(t), \tag{4.253}$$

where a, b, are constants. The Hamiltonian function is

$$H(X,Y) = \int g(X)dX + \frac{1}{2}Y^2 = \frac{b^2X^2}{2a^2} + \frac{Y^2}{2}, \quad f(H) = -\left(1 - \frac{2H}{b^2}\right). \tag{4.254}$$

The stationary probability density p_s becomes

$$p_s(x,y) = A\exp\left(\frac{\epsilon(H - \frac{H^2}{b^2})}{\pi S_0}\right) = A\exp\left(\frac{\epsilon}{\pi S_0}\left(\frac{x^2}{2a^2} + \frac{y^2}{2b^2}\right)\left(1 - \frac{x^2}{2a^2} - \frac{y^2}{2b^2}\right)\right), \tag{4.255}$$

where

$$A = \frac{1}{\int_{-\infty}^{\infty}\int_{-\infty}^{\infty}\exp\left(\frac{\epsilon}{\pi S_0}\left(\frac{x^2}{2a^2} + \frac{y^2}{2b^2}\right)\left(1 - \frac{x^2}{2a^2} - \frac{y^2}{2b^2}\right)\right)dxdy}. \tag{4.256}$$

The stationary probability density and level curves of the probability are shown in Fig. 4.11, which are ellipses. The limit cycle, for any value of ϵ, is the ellipse:

$$f(H) = -\left(1 - \frac{2H}{b^2}\right) = 0, \tag{4.257}$$

which is equivalent to

$$\frac{x^2}{a^2} + \frac{y^2}{b^2} = 1.$$

This result is consistent with the one obtained from the deterministic approach presented in Section 3.3.2.

Hamiltonian Function with Quartic Terms

For weakly non-linear systems, approximation methods can be employed to find solutions. However, such techniques become ineffective when strong nonlinearity is present. Consider the following differential equation

$$\ddot{x} + \epsilon\left(2x^2 + 4\dot{x}^2 - \frac{\pi S_0}{\epsilon}\left(\frac{4}{x^2 + 2\dot{x}^2}\right)\right)\dot{x} + \frac{2x^3 + x\dot{x}^2}{x^2 + 2\dot{x}^2} = 0. \tag{4.258}$$

Recall the Hamiltonian associated with the equation of motion of the stochastic system in Eq. (4.150):

$$\begin{aligned} &H = x^4 + y^4 + x^2y^2 = x^4 + 4u^2 + 2x^2u, \quad f(H) = 1, \\ &H_x = 4x^3 + 2xy^2 = 4x^3 + 4xu, \quad H_u = 2x^2 + 4y^2 = 8u + 2x^2. \end{aligned} \tag{4.259}$$

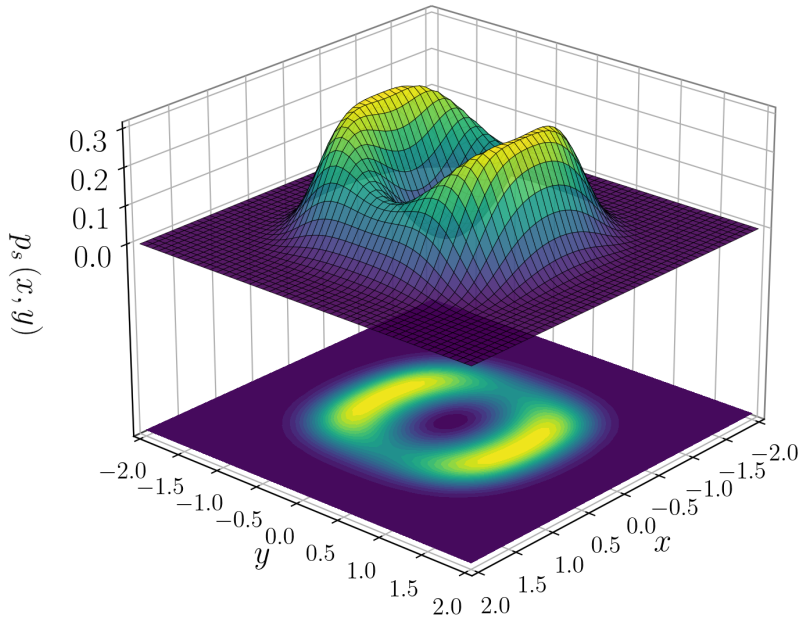

Figure 4.12: The stationary probability density function of the stochastic nonlinear system Eq. (4.260)

Randomizing (4.258)with white noise $W(t)$ results in

$$\ddot{X} + \epsilon\left(2X^2 + 4\dot{X}^2 - \frac{\pi S_0}{\epsilon}\left(\frac{4}{X^2 + 2\dot{X}^2}\right)\right)\dot{X} + \frac{2X^3 + X\dot{X}^2}{X^2 + 2\dot{X}^2} = W(t). \tag{4.260}$$

Assuming $0 < \epsilon \ll 1$ is not enough to reduce the strong nonlinearity observed in this system due to the presence of nonlinear stiffness and damping terms. The corresponding probability density is expressed as follows:

$$p_s(x, y) = A\exp\left(-\frac{\epsilon}{\pi S_0}\int f(H)dH\right)H_u = A\exp\left(\frac{\epsilon}{\pi S_0}\left(-x^4 - y^4 - x^2y^2\right)\right)\left(x^2 + 2y^2\right). \tag{4.261}$$

The stationary probability density function and the limit cycle of the nonlinear oscillator, with $\epsilon = \pi S_0$ and $S_0 = 1/\pi$, are illustrated in Fig. 4.12. The level curves of $p_s(x, y)$ are given by

$$-\frac{\epsilon}{\pi S_0}\int f(H)dH + \ln H_u = -\frac{\epsilon}{\pi S_0}\left(x^4 + y^4 + x^2y^2\right) + \ln\left(x^2 + 2y^2\right) = C. \tag{4.262}$$

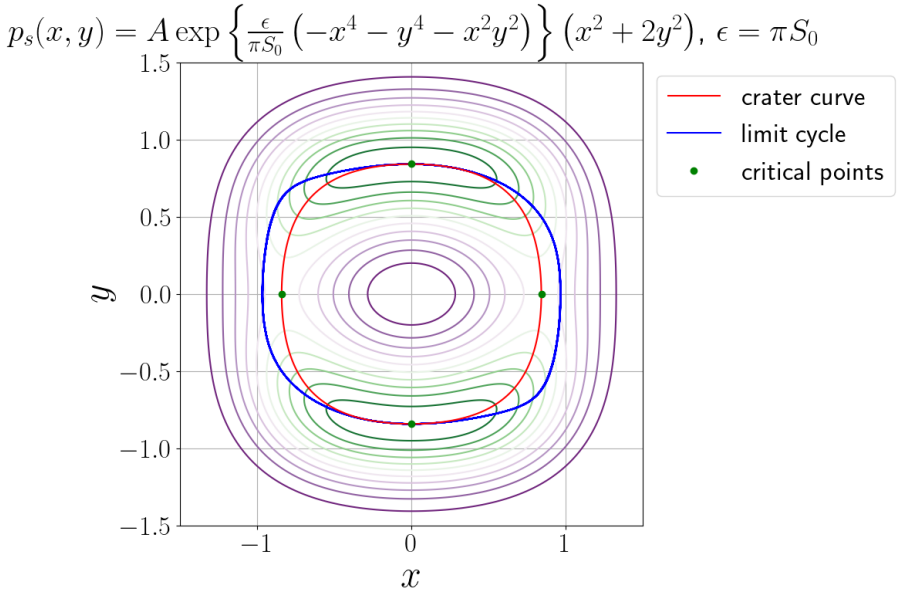

Figure 4.13: The critical points, limit cycle, and the projected crater curve of the nonlinear system Eq. (4.260)

Compared to the results obtained from the Van der Pol-Rayleigh oscillator and the nonlinear oscillator with an elliptical limit cycle, the limit cycle does not demonstrate an identical behavior to a level curve. It is notable that while the function $p_s(x, y)$ demonstrates symmetry about the coordinate axes, the limit cycle lacks symmetry with respect to the y-axis. Nonetheless, a degree of similarity exists between the crater curve of p_s and the limit cycle of the corresponding deterministic system, as supported by several studies [60, 79–83].

To ascertain the critical points of the stationary probability density, Eq. (4.142) is employed. The critical points are

$$(x, y) = \left(\pm\left(\frac{\pi S_0}{2\epsilon}\right)^{\frac{1}{4}}, 0\right), \quad \left(0, \pm\left(\frac{\pi S_0}{2\epsilon}\right)^{\frac{1}{4}}\right). \tag{4.263}$$

In the special case where $\epsilon = \pi S_0$,

$$\left(\frac{\pi S_0}{2\epsilon}\right)^{\frac{1}{4}}\Bigg|_{\epsilon=\pi S_0} = 0.8409. \tag{4.264}$$

The critical points are depicted in Fig. 4.13. It is important to note that the critical points along the x-axis do not reside on the limit cycle due to the asymmetry of the limit cycle about the y-axis.

The projected crater curve can be determined by the following expression:

$$\boldsymbol{\nabla} p_s(x,y) \cdot \boldsymbol{\nabla} l(x,y) = \boldsymbol{\nabla}\left(\frac{\epsilon}{\pi S_0}\left(x^2+2y^2\right)\exp\left(-4x^3-4y^3-2x^2y^2\right)\right)\cdot\boldsymbol{\nabla}\left(x^2+y^2\right)=0. \tag{4.265}$$

After computing the dot products and simplifying the equation, the projected crater curve takes on the form:

$$\frac{\epsilon}{\pi S_0}\left(-2x^6-6x^4y^2-6x^2y^4-4y^6\right)+x^2+2y^2=0. \tag{4.266}$$

By transforming Eq. (4.265) into polar coordinates, it becomes

$$\frac{\epsilon}{\pi S_0}\left(-2r^4\sin^6\theta-2r^4\right)+\sin^2\theta+1=0. \tag{4.267}$$

Nonlinear Oscillator with Tabular Functions

This section considers more complicated nonlinear oscillators specified by tabular functions, such as polynomial, Bessel, sine, cosine, and exponential functions.

Randomized System

The deterministic system is given by

$$\ddot{x}+\epsilon\alpha(x,\dot{x})\dot{x}+\beta(x,\dot{x})=0,$$

and its corresponding randomized system:

$$\ddot{X}+\epsilon\alpha(X,Y)Y+\beta(X,Y)=W(t).$$

The goal is to find $\alpha(x,y)$ and $\beta(x,y)$ such that the equivalent stationary probability density of the randomized system becomes

$$p_s(x,y)=A\exp\left(-\frac{\epsilon}{\pi S_0}\phi(x,y)\right)g(x,y),$$

where $\phi(x,y)=x^2+y^2+x^2y^2$, $g(x,y)=x^2+C_1y^2$, and C_1 is a free parameter. The resulting stationary probability density is identical to Eq. (4.197), and the contour of the stationary probability density is shown in Fig. 4.14.

Using the same procedure as the previous section, the first-order derivatives of g and ϕ are calculated:

$$\frac{\partial g}{\partial x}=2x,\quad \frac{\partial g}{\partial y}=2C_1y,\quad \frac{\partial \phi}{\partial x}=2x+2xy^2,\quad \frac{\partial \phi}{\partial y}=2y+2x^2y. \tag{4.268}$$

$$p_s(x,y) = A\exp\left\{\left(-x^2-y^2-x^2y^2\right)\right\}\left(x^2+2y^2\right)$$

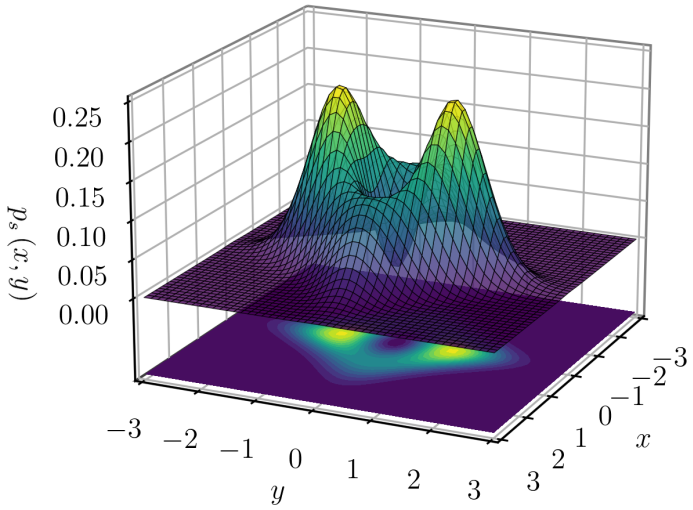

(a) The probability density function

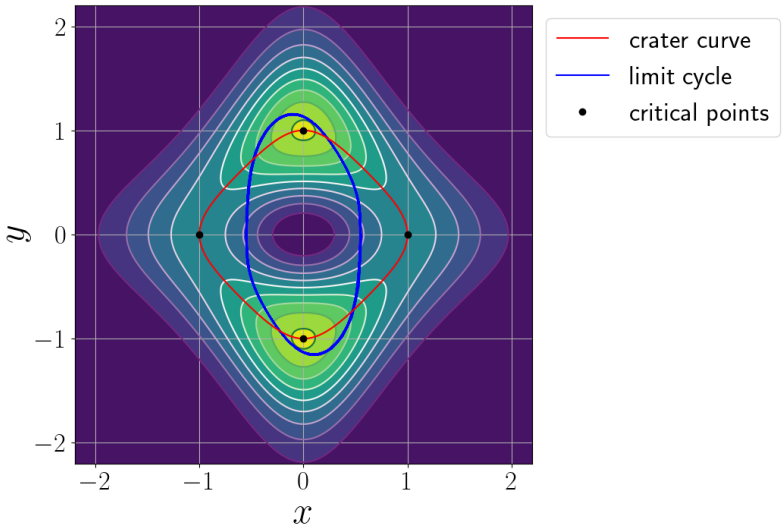

(b) A comparison between the limit cycle and the projected crater curve

Figure 4.14: $\phi(x,y) = x^2+y^2+x^2y^2$, $g(x,y) = x^2+2y^2$

Applying the same procedure of Section 4.5.3, $\alpha(x,y)$ and $\beta(x,y)$ are obtained through direct calculations:

$$\alpha(x,y) = \frac{1}{y}\left(\frac{\partial\phi}{\partial x} - \frac{1}{D}\frac{1}{g}\frac{\partial g}{\partial y}\right) = \frac{2\Big((x^2+1)(x^2+C_1y^2) - \frac{C_1}{D}\Big)}{x^2+C_1y^2}, \tag{4.269}$$

$$\begin{aligned}\beta(x,y) &= \int\left(I(x,y)y\left(\frac{1}{g}\frac{\partial g}{\partial x} - D\frac{\partial\phi}{\partial x}\right)\right)dy\Big/ I(x,y)\\ &= \frac{x\Big(x^6y^2 + x^6 + 2x^4y^2 + x^2y^2 + 2x^4 + x^2 - \frac{x^2+1}{D}\Big)}{(x^2+C_1y^2)(x^6+3x^4+3x^2+1)}\\ &\quad + \frac{xC_1\Big(x^4y^4 + x^4y^2 + x^4 + 2x^2y^4 + 2x^2y^2 + y^4 + y^2 + \frac{2x^2y^2+x^2+2y^2+1}{D} + \frac{2}{D^2}\Big)}{(x^2+C_1y^2)(x^6+3x^4+3x^2+1)},\end{aligned} \tag{4.270}$$

where

$$I(x,y) = \exp\left(\int\left(\frac{1}{g}\frac{\partial g}{\partial y} - D\frac{\partial\phi}{\partial y}\right)dy\right) = (x^2+C_1y^2)\exp\Big(-D\big(x^2+1\big)\Big). \tag{4.271}$$

Projected Crater Curves

The calculation of the projected crater curve for the nonlinear oscillator involves the equation $\boldsymbol{\nabla} p_s \cdot \boldsymbol{\nabla} l = 0$. This leads to the following $C(x,y)$ expression:

$$C_1\Big(-D\big(2x^2y^4 + x^2y^2 + y^4\big) + y^2\Big) - D\big(2x^4y^2 + x^4 + x^2y^2\big) + x^2 = 0. \tag{4.272}$$

In polar coordinates, deriving $C(r,\theta)$ with respect to r, using ${}^{\partial p_s(r,\theta)}/_{\partial r} = 0$, results in

$$-D\big(2r^4\sin^6\theta - 4r^4\sin^4\theta + 2r^4\sin^2\theta - r^2\sin^2\theta + r^2\big) - \sin^2\theta + 1 = 0. \tag{4.273}$$

To find the critical points, take the partial derivatives of p_s with respect to x and y, utilizing ${}^{\partial p_s}/_{\partial x} = 0$ and ${}^{\partial p_s}/_{\partial y} = 0$:

$$\begin{cases} -D(x^2+C_1y^2)(y^2+1) + 1 = 0\\ -D(x^2+C_1y^2)(x^2+1) + C_1 = 0 \end{cases}. \tag{4.274}$$

After determining the critical points, the following are obtained:

$$\begin{cases} x = 0, \quad y = \pm\big(\frac{1}{D}\big)^{\frac{1}{2}} = \pm\Big(\frac{S_0\pi}{\epsilon}\Big)^{\frac{1}{2}}\\ y = 0, \quad x = \pm\big(\frac{1}{D}\big)^{\frac{1}{2}} = \pm\Big(\frac{S_0\pi}{\epsilon}\Big)^{\frac{1}{2}} \end{cases}. \tag{4.275}$$

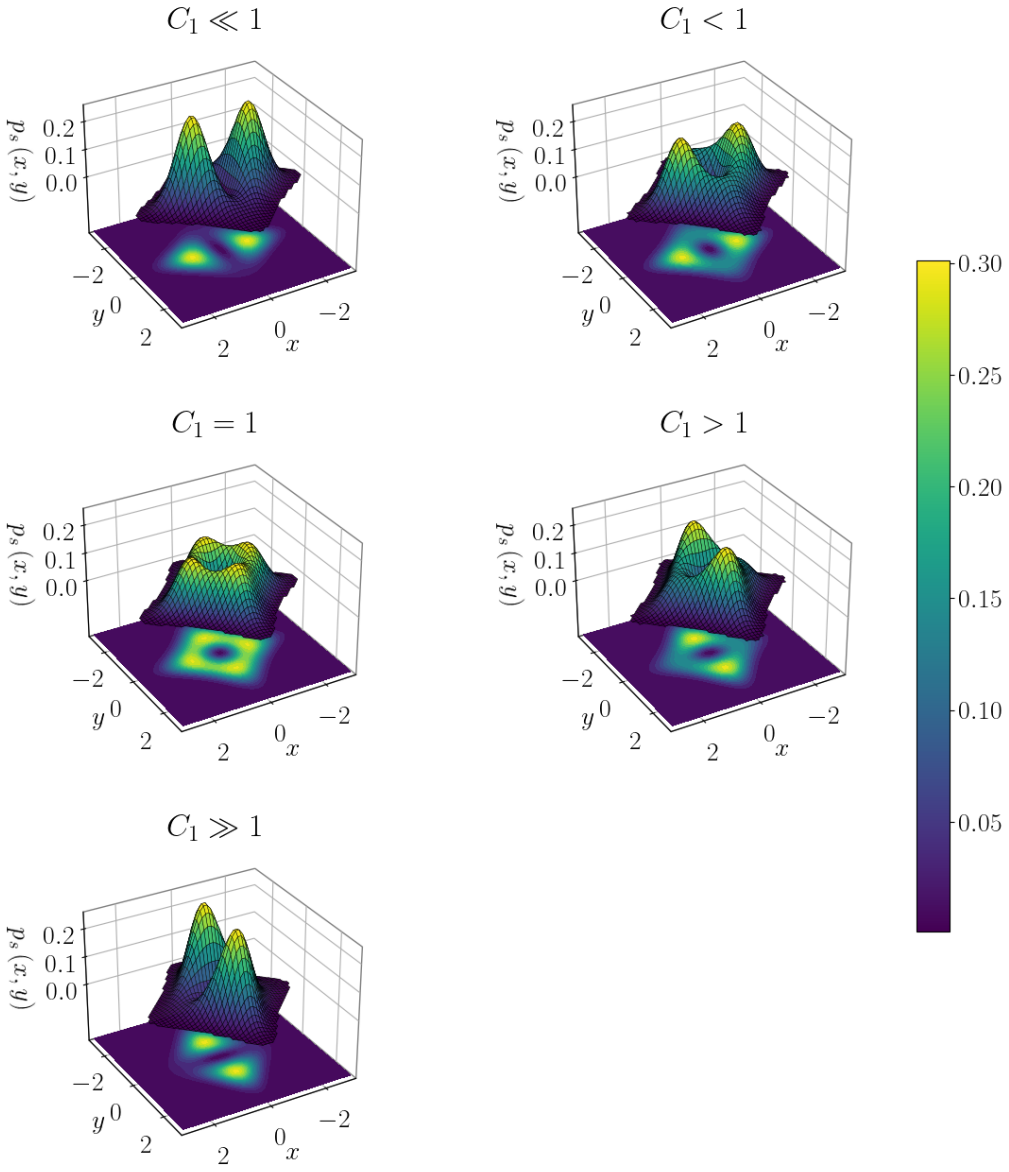

Figure 4.15: $p_s = A\exp\big(-D(x^2+y^2+x^2y^2)\big)(x^2+C_1y^2)$ with different coefficients C_1 and fixed $D = 1$

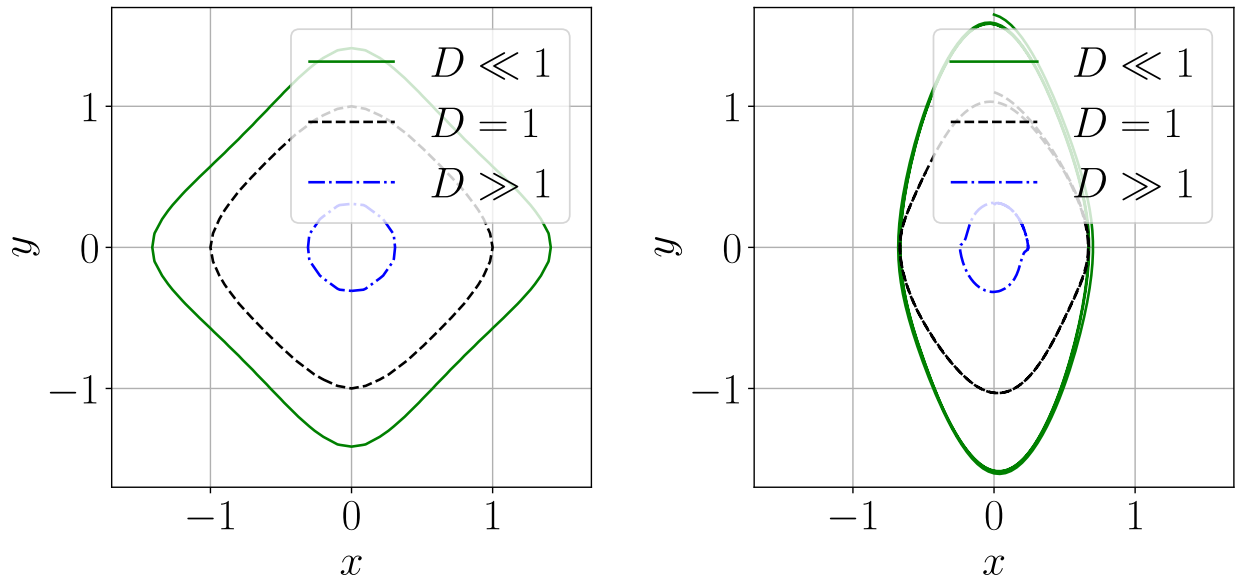

(a) Projected crater curves (b) Limit cycles

Figure 4.16: $p_s(x, y) = A \exp\big(-x^2 - y^2 - x^2y^2\big)(x^2 + C_1y^2)$, $C_1 < 1$

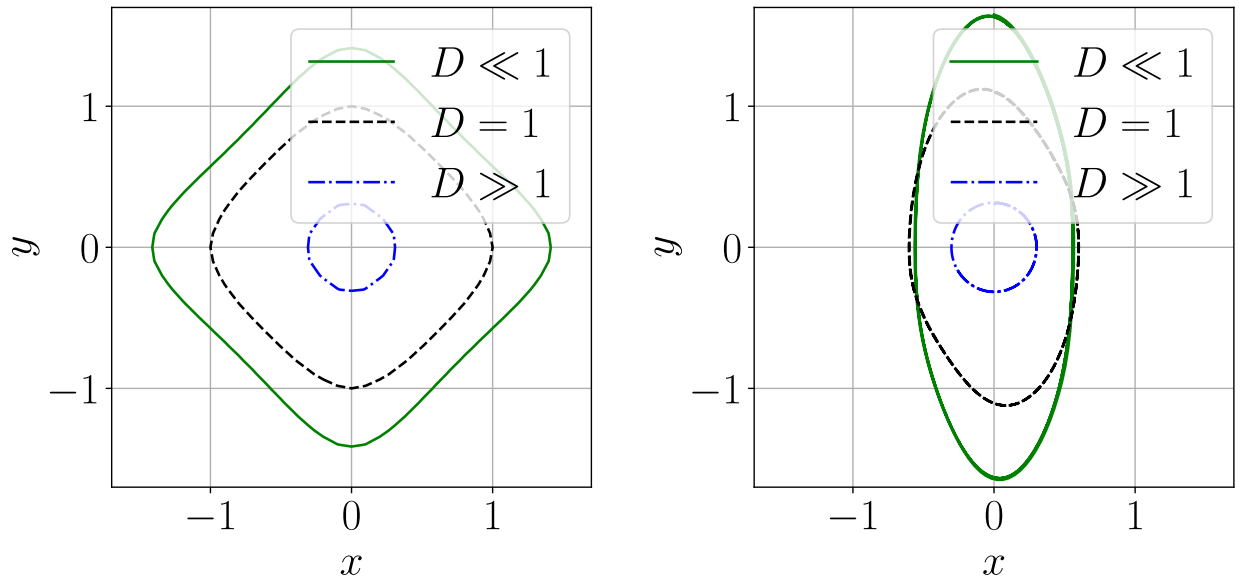

(a) Projected crater curves (b) Limit cycles

Figure 4.17: $p_s(x, y) = A \exp\big(-x^2 - y^2 - x^2y^2\big)(x^2 + C_1y^2)$, $C_1 = 1$

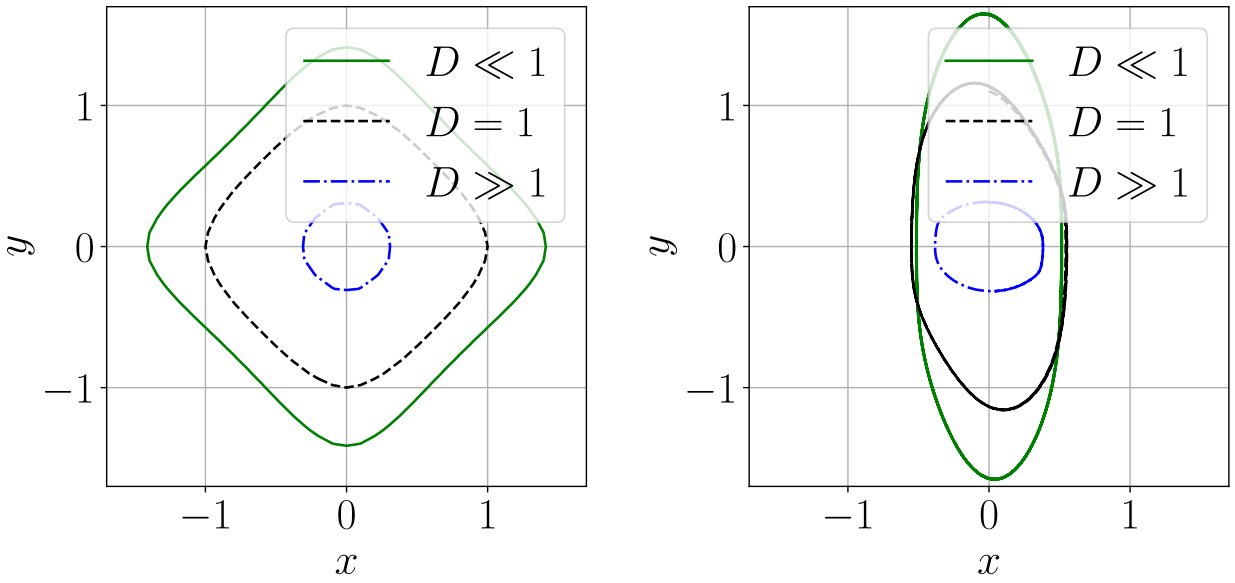

(a) Projected crater curves (b) Limit cycles

Figure 4.18: $p_s(x, y) = A \exp\left(-x^2 - y^2 - x^2y^2\right)(x^2 + C_1y^2)$, $C_1 > 1$

The limit cycle of the nonlinear oscillator alongside the projected crater curve (where $C_1 = 2$) is shown in Fig. 4.14. Mirroring the outcome depicted in Fig. 4.13, the discrepancy between the projected crater curve and the limit cycle intensifies considerably, a consequence of the additional nonlinearity introduced by the oscillator.

Effect of Damping Constant D and Free Parameter C_1

The effect of the constants C_1 and $D = \epsilon/\pi S_0$ on the projected crater curve is investigated, with $S_0 = 1/\pi$. The results for different values of C_1 are displayed in Fig. 4.15. It is observed that the crater curve exists for most values of C_1, except for very large positive or negative values. The critical points of the system described by Eq. (4.275) remain unchanged as they do not depend on C_1.

The projected crater curves for $C_1 > 1$, $C_1 = 1$, and $C_1 < 1$ are provided in Fig. 4.16, 4.17, and 4.18, respectively. Although the analytical expression of the projected crater curve Eq. (4.272) includes both C_1 and D, the trajectory of the projected curve remains the same when the value of D is fixed, as seen in the left column of these figures.

In contrast, the trajectory of limit cycles is significantly affected by changes in the value of C_1, as illustrated in the right column of the same figures. Moreover, the results for varying values of D are presented. When the value of D decreases, the trajectory of both the projected crater curve and the limit cycles become larger. This observation is consistent

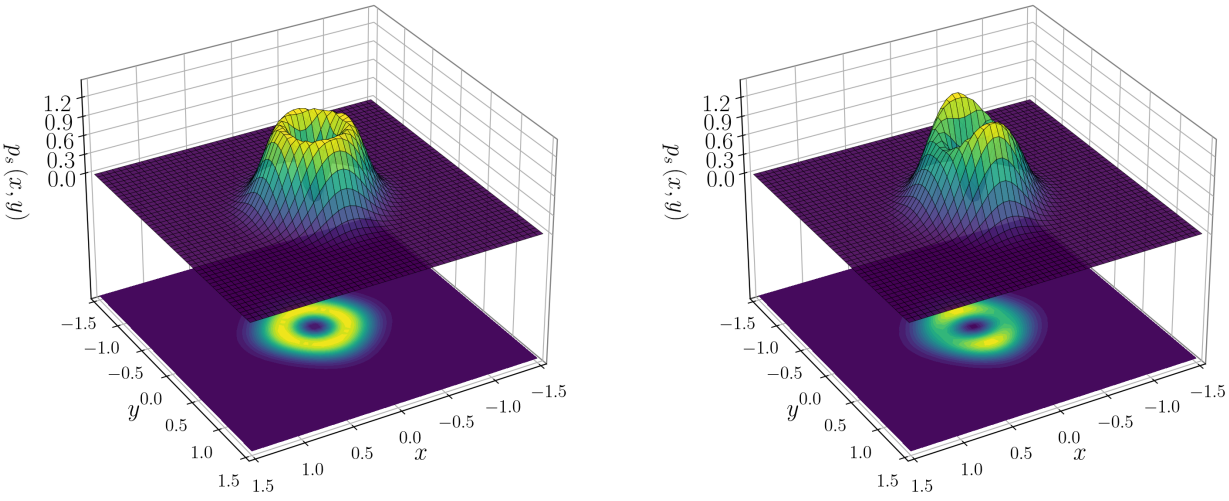

(a) $C_1 = 1$ (b) $C_1 < 1$

Figure 4.19: $p_s(x, y) = A \exp\big(D(-x^2 - y^2 - x^2y^2)\big)(x^2 + C_1y^2)$, $D \gg 1$

with the fact that the critical points of the stationary probability density increase with a larger value of D.

A noticeable deviation exists between the projected crater curve and the limit cycle, meaning that in most cases, the limit cycle is not the projected crater curve. However, when $C_1 = 1$ and $D \gg 1$, as shown in Fig. 4.17, the projected crater curve becomes identical to the limit cycle. This occurs because the crater curve turns into a level curve, as demonstrated in the example of the Van der Pol-Rayleigh oscillator.

Finally, a comparison is made with the case where $C_1 < 1$ and $D \gg 1$, as illustrated in Fig. 4.19. In this situation, the crater curve is no longer a level curve, resulting in a deviation between the projected crater curve and the limit cycle.

Nonlinear Oscillator with Non-Tabular Functions

The randomization is not limited to nonlinear systems with tabular functions; it can also be applied to non-tabular forms such as error functions.

Randomized System

Let $\phi(x, y) = x^4 + y^4 + x^4y^4$, $g(x, y) = x^2 + C_1y^2$, where C_1 is a free parameter. The stationary probability density is calculated using Eq. (4.197), and its contour is illustrated in Fig. 4.20.

$$p_s(x,y) = A \exp\left\{\left(-x^4 - y^4 - x^4y^4\right)\right\}\left(x^2 + y^2\right)$$

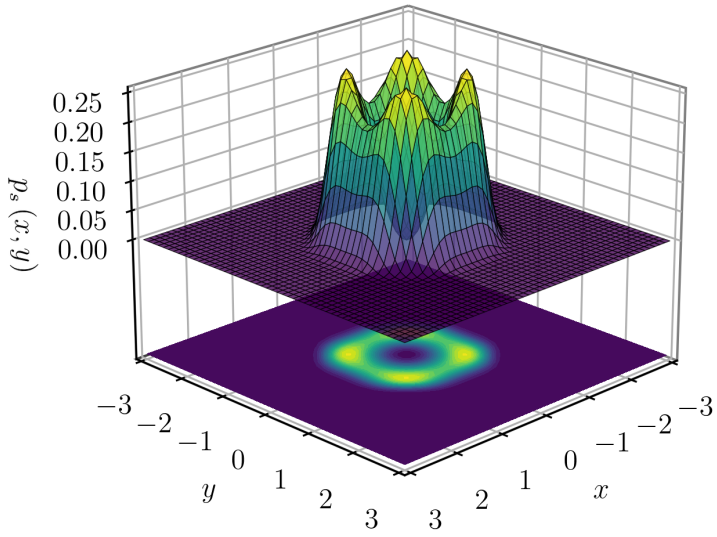

(a) The probability density function

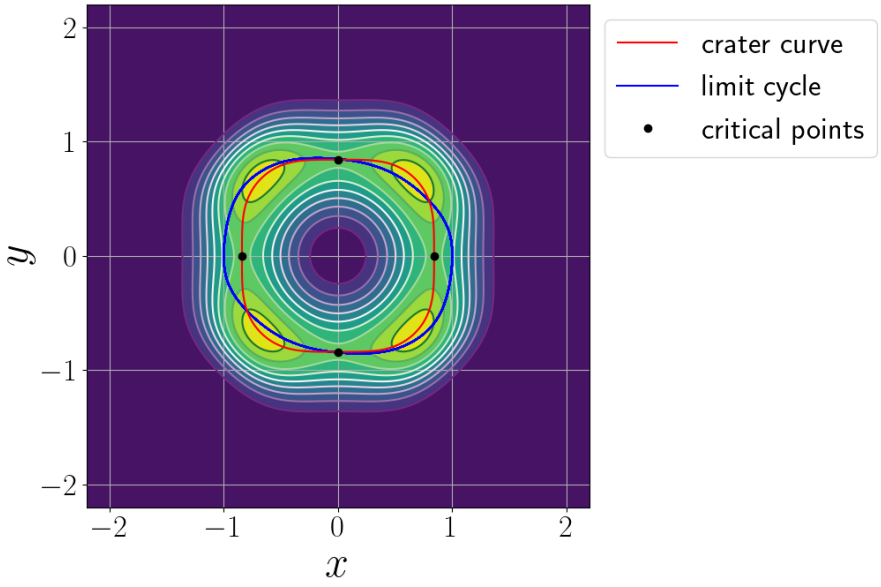

(b) A comparison between the limit cycle and the projected crater curve

Figure 4.20: $\phi(x,y) = x^4 + y^4 + x^4y^4$, $g(x,y) = x^2 + y^2$

Consequently, the resulting deterministic system is given by

$$\ddot{x} + \epsilon\alpha(x,\dot{x})\dot{x} + \beta(x,\dot{x}) = 0,$$

where

$$\begin{aligned}\alpha(x,\dot{x}) &= \frac{2\Big(-C_1 + 2D\dot{x}^2\big(x^4+1\big)\big(C_1\dot{x}^2+x^2\big)\Big)}{D(C_1\dot{x}^2+x^2)},\\ \beta(x,\dot{x}) &= \frac{N(x,\dot{x})}{2D^{\frac{3}{2}}(C_1x^8\dot{x}^2 + 2C_1x^4\dot{x}^2 + C_1\dot{x}^2 + x^{10} + 2x^6 + x^2)},\end{aligned} \tag{4.276}$$

and the numerator function $N(x,\dot{x})$ is

$$\begin{aligned}N(x,\dot{x}) = x\Bigg(&2C_1D^{\frac{3}{2}}x^6\dot{x}^4 + 2C_1D^{\frac{3}{2}}x^6 + 2C_1D^{\frac{3}{2}}x^2\dot{x}^4 + 2C_1D^{\frac{3}{2}}x^2 + 2C_1\sqrt{D}x^2 + 2D^{\frac{3}{2}}x^8\dot{x}^2\\ &+ 2D^{\frac{3}{2}}x^4\dot{x}^2 - 2\sqrt{\pi}D^2x^8\sqrt{x^4+1}\exp\Big(D\dot{x}^4\big(x^4+1\big)\Big)\operatorname{erf}\Big(\sqrt{D}\dot{x}^2\sqrt{x^4+1}\Big)\\ &- 2\sqrt{\pi}D^2x^4\sqrt{x^4+1}\exp\Big(D\dot{x}^4\big(x^4+1\big)\Big)\operatorname{erf}\Big(\sqrt{D}\dot{x}^2\sqrt{x^4+1}\Big)\\ &+ \sqrt{\pi}Dx^4\sqrt{x^4+1}\exp\Big(D\dot{x}^4\big(x^4+1\big)\Big)\\ &+ \sqrt{\pi}D\sqrt{x^4+1}\exp\Big(D\dot{x}^4\big(x^4+1\big)\Big)\operatorname{erf}\Big(\sqrt{D}\dot{x}^2\sqrt{x^4+1}\Big)\Bigg).\end{aligned}$$

Note that the error function is defined as

$$\operatorname{erf}(x) = \frac{2}{\sqrt{\pi}}\int_0^x e^{-t^2}dt, \tag{4.277}$$

which is a non-elementary mathematical function.

Projected Crater Curves

Using the same procedure as in Section 4.5.2, the projected crater curve is given by

$$\begin{aligned}\mathrm{C}(x,y) &= -4x^6y^4D - 2x^6D - 4x^4y^6C_1D - 2x^4y^2C_1D - 2x^2y^4D + x^2 - 2y^6C_1D + y^2C_1 = 0,\\ \mathrm{C}(r,\theta) &= r^2\big(-4C_1Dr^8\sin^6(\theta)\cos^4(\theta) - 2C_1Dr^4\sin^6(\theta) - 2C_1Dr^4\sin^2(\theta)\cos^4(\theta)\\ &\quad + C_1\sin^2(\theta) - 4Dr^8\sin^4(\theta)\cos^6(\theta) - 2Dr^4\sin^4(\theta)\cos^2(\theta) - 2Dr^4\cos^6(\theta)\\ &\quad + \cos^2(\theta)\big) = 0.\end{aligned} \tag{4.278}$$

The critical points are

$$(x_c,y_c) = \left(0, \pm\left(\frac{1}{2D}\right)^{\frac{1}{4}}\right), \quad \left(\pm\left(\frac{1}{2D}\right)^{\frac{1}{4}}, 0\right). \tag{4.279}$$

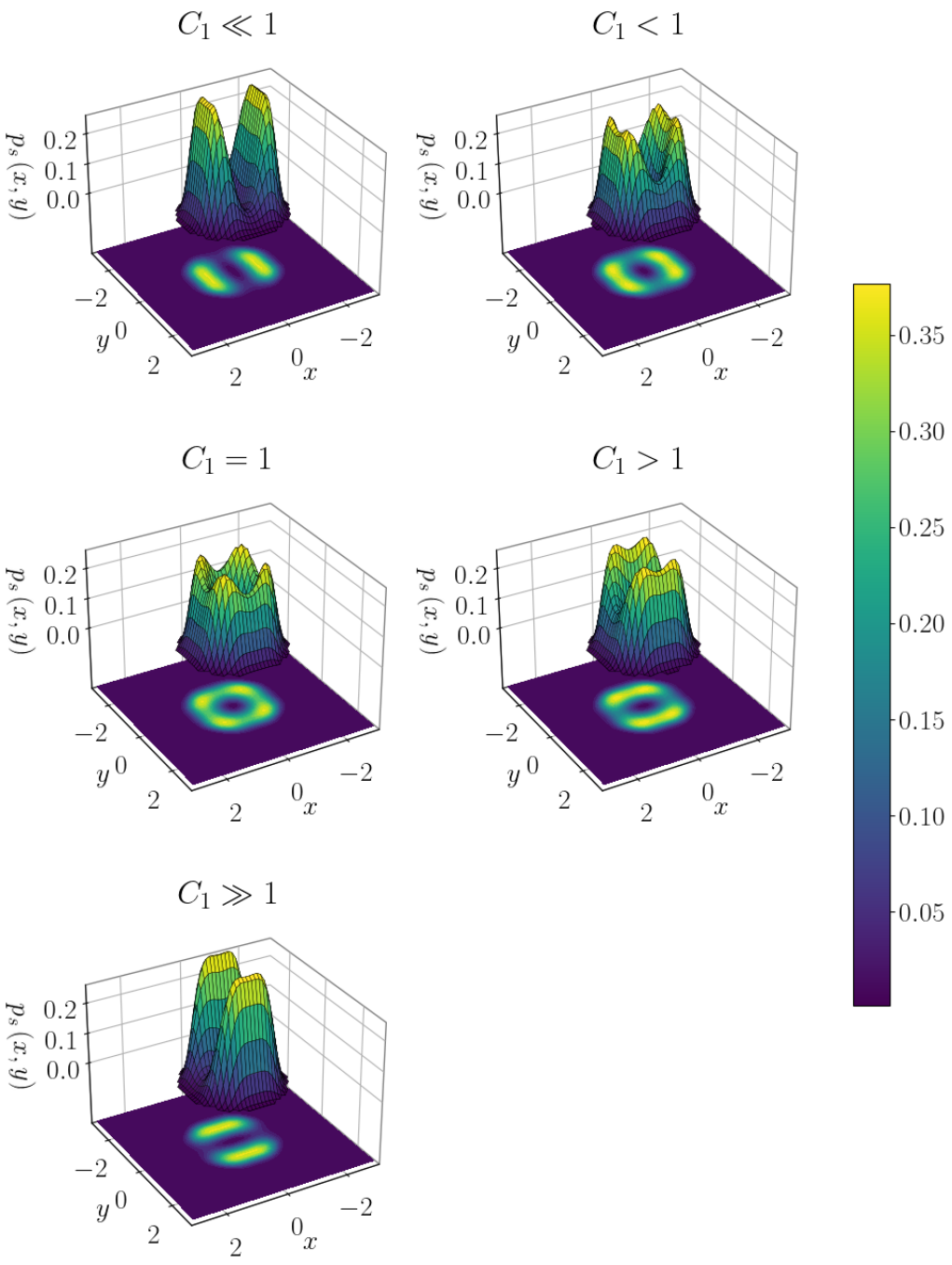

Figure 4.21: $p_s = A \exp\big(-D(x^4 + y^4 + x^4 y^4)\big)(x^2 + C_1 y^2)$ with different coefficients C_1 and fixed $D = 1$

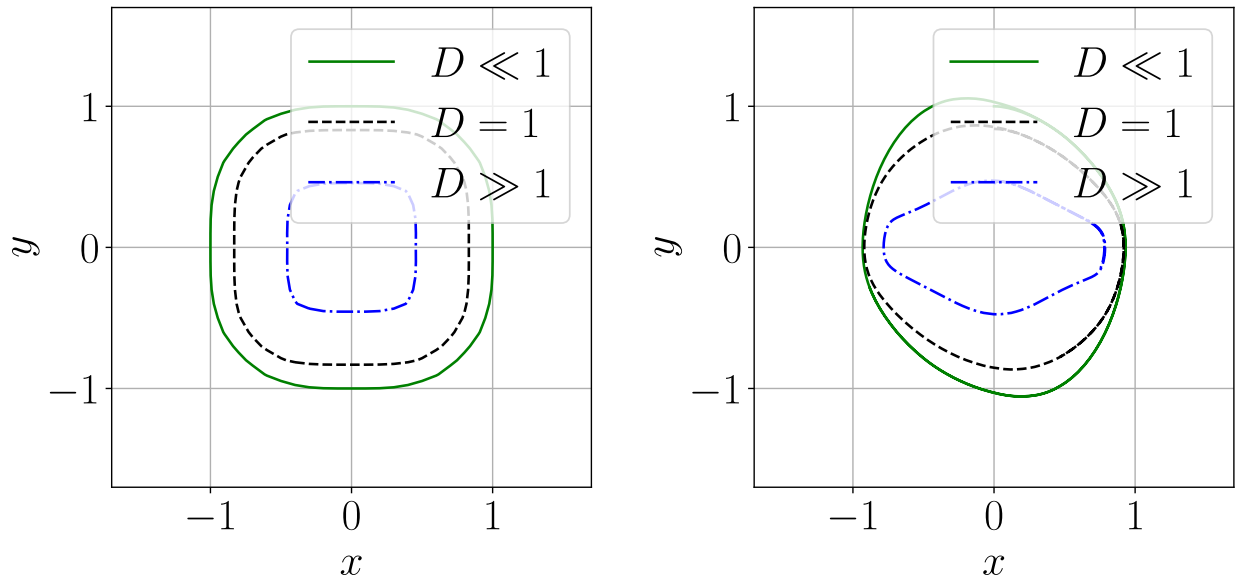

(a) Projected crater curves (b) Limit cycles

Figure 4.22: $p_s(x, y) = A \exp\big(-x^4 - y^4 - x^4 y^4\big)(x^2 + C_1 y^2)$, $C_1 < 1$

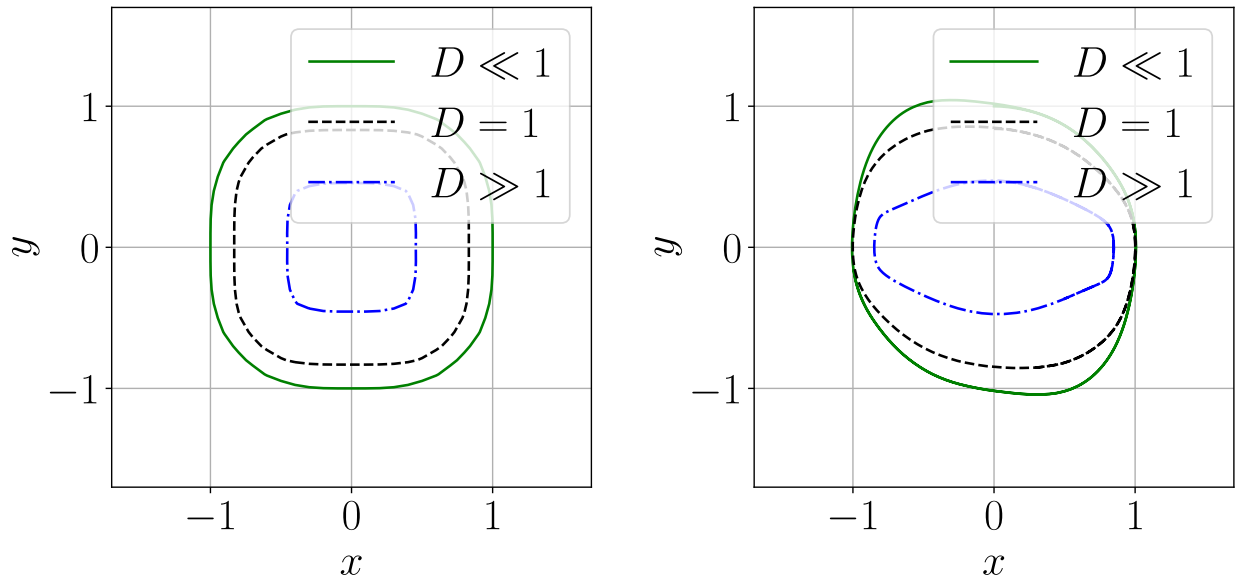

(a) Projected crater curves (b) Limit cycles

Figure 4.23: $p_s(x, y) = A \exp\big(-x^4 - y^4 - x^4 y^4\big)(x^2 + C_1 y^2)$, $C_1 = 1$

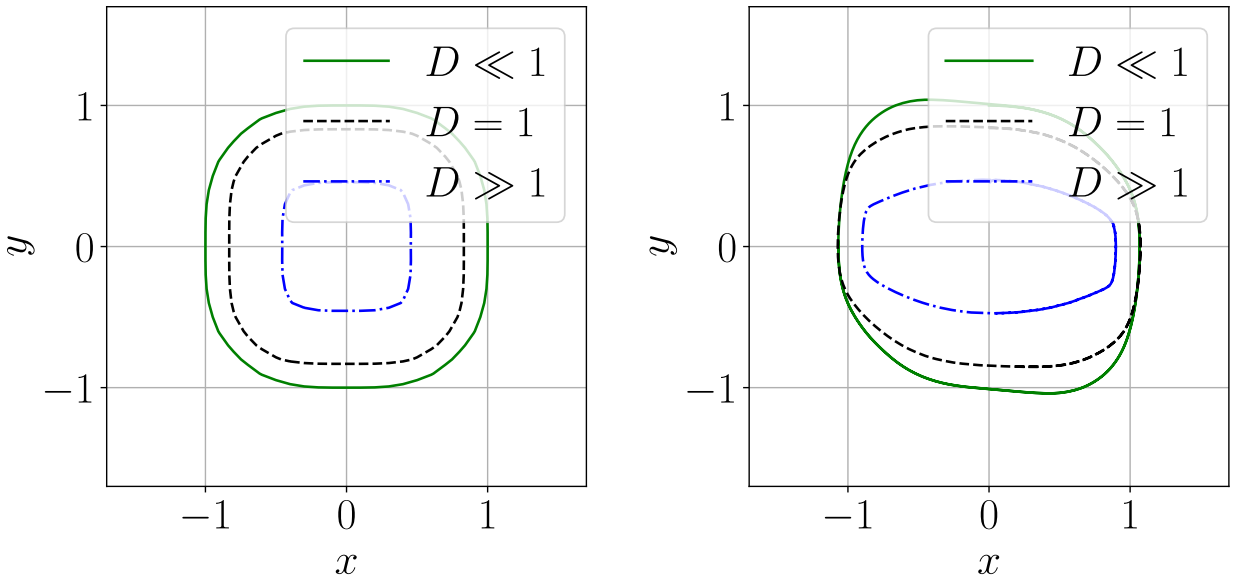

(a) Projected crater curves (b) Limit cycles

Figure 4.24: $p_s(x, y) = A \exp\big(-x^4 - y^4 - x^4y^4\big)(x^2 + C_1y^2)$, $C_1 > 1$

Figure 4.20 showcases the limit cycle of the nonlinear oscillator and the projected crater curve with $C_1 = 1$. Although the system has increased complexity, the deviation between the projected crater curve and the limit cycle is noticeably smaller compared to the previous example. This observation indicates that the complexity of the nonlinear system is not the main factor determining the magnitude of the deviation between the projected crater curve and the limit cycle. The primary factors affecting the deviation are the damping constant D and the free parameter C_1. Further discussion on these parameters will be provided in the following sections.

Effect of Damping Constant D and Free Parameter C_1

The stationary probability density functions, illustrated in Fig. 4.21, show the impact of varying free parameter C_1. It becomes evident that C_1 mainly affects the contour shape of p_s, while not altering the corresponding trajectory of the projected crater curve. As observed in the previous example, the crater curves vanish when $C_1 \gg 1$ or $C_1 \ll 1$. Additionally, a slight widening of the limit cycle with respect to the x-axis occurs as C_1 increases.

In contrast, the effect of damping constant D is more pronounced on the trajectories of both the limit cycle and projected crater curve, which supports the analysis from the previous example. Notably, the closest resemblance between the limit cycle shape and projected crater curve happens when $D \ll 1$ and $C_1 = 1$. This observation contradicts the conclusion drawn

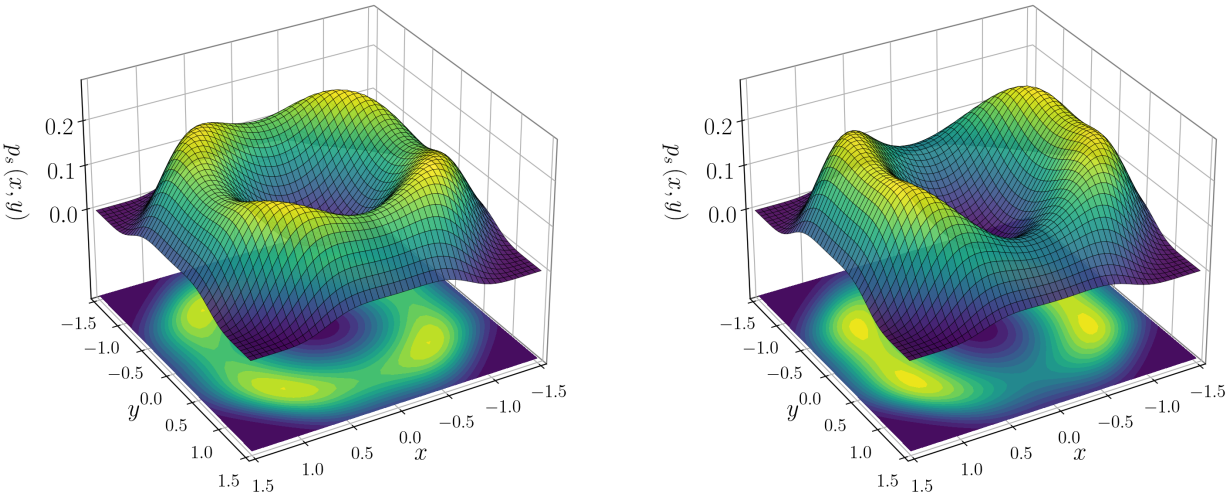

(a) $C_1 = 1$ (b) $C_1 < 1$

Figure 4.25: $p_s(x, y) = A \exp\big(D(-x^4 - y^4 - x^4y^4)\big)(x^2 + C_1y^2)$, $D \ll 1$

in the previous example, which can be attributed to the misalignment between the projected crater curve and a given p_s level curve.

4.6.3 Bifurcations

This example illustrates the use of the heuristic formulation, presented in Section 4.5.3, applied to a nonlinear oscillator exhibiting complex behavior. The characteristics of the oscillator include multiple limit cycles and homoclinic bifurcation, demonstrating the versatility and applicability of the proposed approach.

Reconsider the nonlinear oscillator of Eq. (3.34):

$$\ddot{x} + \epsilon\left(4y^2 + \left(\frac{x^2}{4} - 1\right)\left(\epsilon^2x^2\big(x^2 - 4\big) + 16\right)\right)y + x\left(\frac{3\epsilon^2x^4}{16} - \epsilon^2x^2 + \epsilon^2 + 1\right) = 0.$$

The qualitative behaviors have been investigated through traditional deterministic methods in Example 3.3.3 and 3.3.2, which exhibited their limitations. In this example, the randomization is applied to the system, revealing the effectiveness of the proposed formulation.

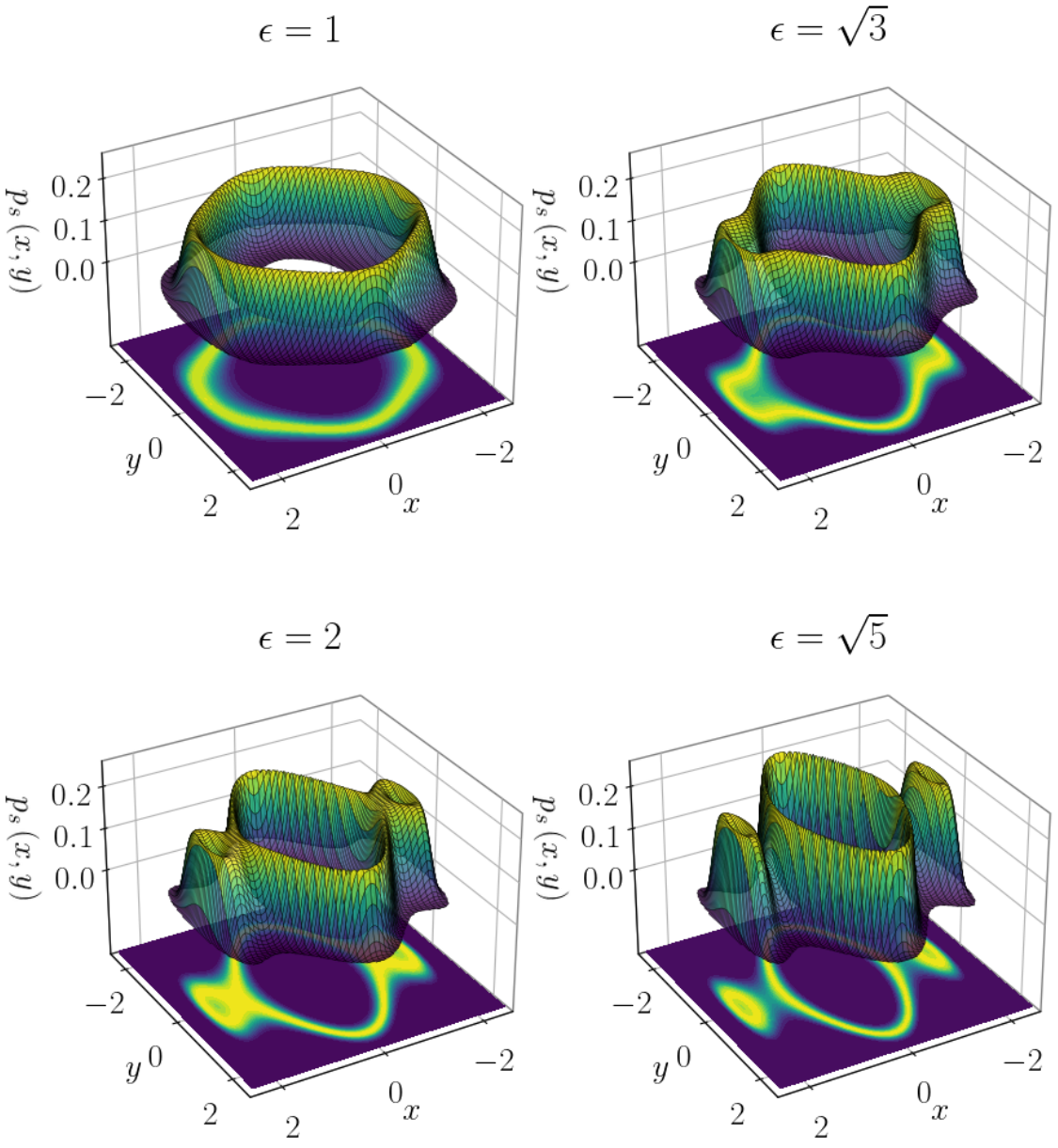

Figure 4.26: Stationary probability density of the nonlinear oscillator with complex qualitative behavior

Randomized System

The corresponding randomized system of the deterministic system is given by

$$\ddot{X} + \epsilon\left(4Y^2 + \left(\frac{X^2}{4} - 1\right)\left(\epsilon^2 X^2\big(X^2 - 4\big) + 16\right)\right)Y + X\left(\frac{3\epsilon^2 X^4}{16} - \epsilon^2 X^2 + \epsilon^2 + 1\right) = W(t), \tag{4.280}$$

where $W(t)$ is a white noise process with a zero mean and a constant power spectral density of S_0. By the virtue of the formulation presented in Section 4.5.3, the stationary probability density can be obtained in the form:

$$p_s(x, y) = A \exp\left(-\frac{\epsilon}{\pi S_0}\left(y^2 + \big(x^2 - 4\big)\left(\frac{\epsilon^2}{16}x^2\big(x^2 - 4\big) + 1\right)\right)^2\right). \tag{4.281}$$

By substituting

$$\phi(x, y) = \left(y^2 + \big(x^2 - 4\big)\left(\frac{\epsilon^2}{16}x^2\big(x^2 - 4\big) + 1\right)\right)^2, \quad g(x, y) = 1 \tag{4.282}$$

in Eq. (4.206) and (4.209), the following results are achieved:

$$\begin{aligned} \alpha(x, y) &= \frac{1}{y}\left(\frac{\partial \phi}{\partial x} - \frac{1}{D}\frac{1}{g}\frac{\partial g}{\partial y}\right) = 4y^2 + \left(\frac{x^2}{4} - 1\right)\Big(\epsilon^2 x^2\big(x^2 - 4\big) + 16\Big), \\ \beta(x, y) &= \int \left(I(x, y) y\left(\frac{1}{g}\frac{\partial g}{\partial x} - D\frac{\partial \phi}{\partial x}\right)\right) dy \Big/ I(x, y) = x\left(\frac{3\epsilon^2 x^4}{16} - \epsilon^2 x^2 + \epsilon^2 + 1\right). \end{aligned} \tag{4.283}$$

Projected Crater Curves

In this example the projected crater curves are identical to the level curves. Therefore, the projected crater curve analysis of Section 4.5.2 provides the exact analytical form of the limit cycles. The projected crater curve of the corresponding deterministic system can be calculated through $\boldsymbol{\nabla} p_s \cdot \boldsymbol{\nabla} l = 0$, leading to $C(x, y)$:

$$y^2 + \big(x^2 - 4\big)\left(\frac{\epsilon^2}{16}x^2\big(x^2 - 4\big) + 1\right) = 0. \tag{4.284}$$

After transforming the equation into polar coordinates, $C(r, \theta) = {}^{\partial p_s(r,\theta)}/_{\partial r} = 0$ yields

$$\frac{\epsilon^2 r^6 \cos^6\theta}{16} - \frac{\epsilon^2 r^4 \cos^4\theta}{2} + \epsilon^2 r^2 \cos^2\theta + r^2 - 4 = 0. \tag{4.285}$$

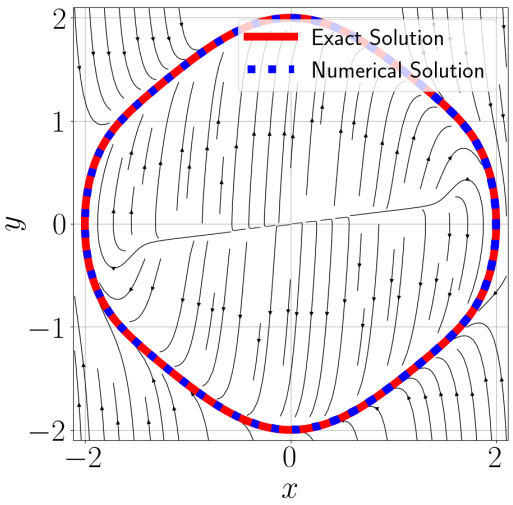

(a) $\epsilon = 1$

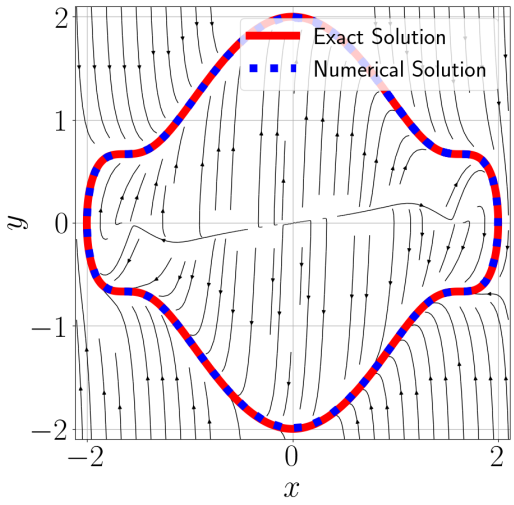

(b) $\epsilon = \sqrt{3}$

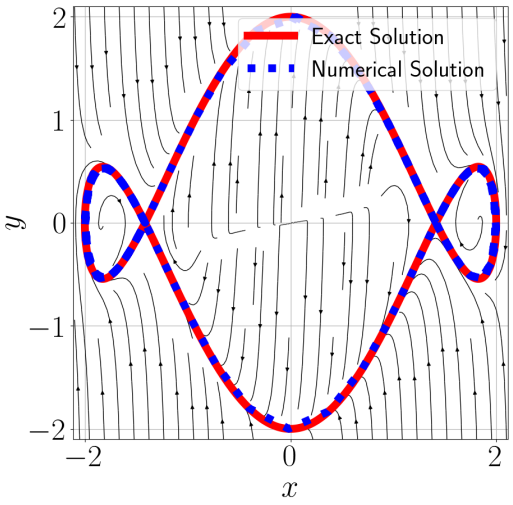

(c) $\epsilon = 2$

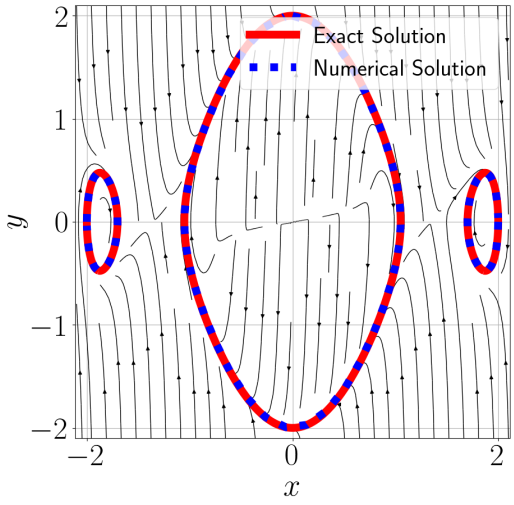

(d) $\epsilon = \sqrt{5}$

Figure 4.27: Exact solution of the limit cycles

This equation is identical to exact solution of the limit cycle, which can be demonstrated by Fig. 4.26. This is a significant advantage of the randomization, as obtaining the exact analytical form of the limit cycle is not readily available with traditional deterministic methods.

Effect of ϵ as a Bifurcation Parameter and the Existence of Limit Cycles

Example 3.3.3 reveals that the equilibrium points are given by

$$(x_{eq}, y_{eq}) = (0,0), \quad \text{and } (x_{eq}, y_{eq}) = \left(\frac{\pm\sqrt{3}\sqrt{8 \pm \frac{4\sqrt{\epsilon^2-3}}{\epsilon}}}{3}, 0 \right). \tag{4.286}$$

Examining the contour of p_s in Fig. 4.26, various qualitative behaviors emerge as ϵ changes. The detailed observations are as follows:

- $0 < \epsilon < \sqrt{3}$: A stable single limit cycle surrounds the unstable node at $(0,0)$.
- $\epsilon = \sqrt{3}$: The system retains a single limit cycle, while two additional non-hyperbolic points emerge within the cycle.
- $\sqrt{3} < \epsilon < 2$: The unstable foci shift away from the origin, yet the oscillator maintains its single limit cycle.
- $\epsilon = 2$: Marking a homoclinic bifurcation point, the saddle points spawn two homoclinic orbits, while the system still exhibits only one limit cycle.
- $\epsilon > 2$: As the unstable foci continue to drift away from the origin, the system develops two more limit cycles. Two saddle points appear between these additional cycles.

The analysis through randomization provides a comprehensive understanding of the qualitative behavior of the system, in contrast to conventional deterministic methods that face limitations when characterizing the intricate behavior of the oscillator. Displaying the contour of p_s allows for a more intuitive interpretation of limit cycle trajectories for the oscillator as the bifurcation parameter ϵ varies.

Chapter 5

Conclusions

This dissertation presents a novel investigation into the qualitative behaviors of deterministic dynamical systems using randomization. The emphasis has been on randomization of nonlinear autonomous equations of motion. Chapters 1 through 3 offer a comprehensive examination of the foundational principles underlying randomization in nonlinear systems. In particular, an extensive review of nonlinear systems and theory of Brownian motion, including the derivation of the diffusion equation, was discussed.

Chapter 4 outlines the framework of randomization, a novel approach to analyzing nonlinear dynamical systems. This method is based on the idea of transforming deterministic system state variables into stochastic state variables due to white noise excitations. The analysis of the resulting stochastic systems was performed by obtaining the exact solution of the diffusion equation, incorporating heuristic methods that were introduced for solving the equation. The proposed methodology was applied to well-known nonlinear oscillators and a newly discovered class of analyzable nonlinear oscillators.

The contributions of this work encompass:

1. Using randomization as an effective tool for investigating stability at equilibrium points of nonlinear systems, demonstrated through established oscillators like the Duffing equation and damped pendulum equation. Comparing stationary probability density functions with deterministic trajectories on the phase plane reveals strong connections between them. This comparison simplifies the understanding of stability at equilibrium points, providing a more straightforward approach than traditional Lyapunov stability analysis.

2. Applying the randomization method to new analyzable nonlinear oscillators, demonstrating its effectiveness in obtaining exact analytical solutions for limit cycles. Comparisons with existing techniques, such as the Poincare-Bendixson theorem, highlight the advantages of randomization.

3. Showcasing the benefits of randomization when strong nonlinearity appears in systems, such as extended Liénard-type oscillators, which exhibit non-hyperbolic equilibria and

multiple limit cycles as bifurcation parameters vary.

The importance of randomization methods in understanding complex nonlinear systems in engineering and science cannot be overstated. These methods are crucial for studying various fields, including nonlinear vibration, biology, trajectory planning, and control systems. One key aspect is the strong relationship between limit cycles and the projected crater curves of stationary probability density functions.

When finding exact expressions for limit cycles is challenging, obtaining accurate solutions for stationary probability density functions becomes especially valuable. The proposed framework offers more than just precise results; it also presents additional benefits. For example, it can help create obstacle avoidance algorithms in control systems by using the exact solution of the stationary probability density function to closely match a related deterministic system's limit cycle.

Future research in areas such as artificial intelligence is worthwhile, where exact solutions can benefit various diffusion models that are commonly used in image generation models. In summary, the framework presented not only provides exact solutions of stationary probability density functions but also opens up new possibilities for progress in different research fields.

Bibliography

[1] Sigalia Dostrovsky. "Early Vibration Theory: Physics and Music in the Seventeenth Century". *Archive for History of Exact Sciences* 14.3 (1975). Publisher: Springer, pp. 169–218. ISSN: 0003-9519.

[2] John William Strutt. *The Theory of Sound*. Vol. 1. Cambridge Library Collection - Physical Sciences. Cambridge: Cambridge University Press, 2011. ISBN: 978-1-108-03220-9. DOI: 10.1017/CBO9781139058087.

[3] Paul H. Wirsching, Thomas L. Paez, and Keith Ortiz. *Random Vibrations: Theory and Practice*. Courier Corporation, Jan. 2006. ISBN: 978-0-486-45015-5.

[4] Alexandre J. Chorin and Ole H Hald. *Stochastic Tools in Mathematics and Science*. Vol. 58. Texts in Applied Mathematics. New York, NY: Springer New York, 2013. ISBN: 978-1-4614-6979-7 978-1-4614-6980-3. DOI: 10.1007/978-1-4614-6980-3.

[5] Albert Einstein. *Investigations on the Theory of the Brownian Movement*. Courier Corporation, Jan. 1956. ISBN: 978-0-486-60304-9.

[6] Thomas L. Paez. "The history of random vibrations through 1958". *Mechanical Systems and Signal Processing* 20.8 (Nov. 2006), pp. 1783–1818. ISSN: 0888-3270. DOI: 10.1016/j.ymssp.2006.07.001.

[7] Parham Radpay. "Langevin Equation and Fokker-Planck Equation" (July 2020).

[8] Don S. Lemons and Anthony Gythiel. "Paul Langevin's 1908 paper "On the Theory of Brownian Motion" ["Sur la théorie du mouvement brownien," C. R. Acad. Sci. (Paris) **146** , 530–533 (1908)]". *American Journal of Physics* 65.11 (Nov. 1997), pp. 1079–1081. ISSN: 0002-9505, 1943-2909. DOI: 10.1119/1.18725.

[9] A. D. Fokker. "Die mittlere Energie rotierender elektrischer Dipole im Strahlungsfeld". *Annalen der Physik* 348.5 (1914), pp. 810–820. ISSN: 1521-3889. DOI: 10.1002/andp.19143480507.

[10] G. E. Uhlenbeck and L. S. Ornstein. "On the Theory of the Brownian Motion". *Physical Review* 36.5 (Sept. 1930), pp. 823–841. ISSN: 0031-899X. DOI: 10.1103/PhysRev.36.823.

[11] Ming Chen Wang and G. E. Uhlenbeck. "On the Theory of the Brownian Motion II". *Reviews of Modern Physics* 17.2-3 (Apr. 1945), pp. 323–342. ISSN: 0034-6861. DOI: 10.1103/RevModPhys.17.323.

[12] T.K. Caughey. "Nonlinear Theory of Random Vibrations". *Advances in Applied Mechanics*. Vol. 11. Elsevier, 1971, pp. 209–253. ISBN: 978-0-12-002011-9. DOI: 10.1016/S0065-2156(08)70343-0.

[13] G. W. Hill. "Researches in the Lunar Theory". *American Journal of Mathematics* 1.1 (1878). Publisher: Johns Hopkins University Press, pp. 5–26. ISSN: 0002-9327. DOI: 10.2307/2369430.

[14] June Elizabeth Barrow-Green. "Poincaré and the Three Body Problem" (1993). Publisher: The Open University. DOI: 10.21954/OU.RO.0000E03B.

[15] Jean-Marc Ginoux. *Scholarpedia: Poincaré's Limit Cycles*. 2011.

[16] D.D. Nolte. *Georg Duffing's Equation*. Mar. 2019.

[17] Georg Duffing. *Erzwungene Schwingungen bei veränderlicher Eigenfrequenz und ihre technische Bedeutung*. Vieweg, 1918.

[18] C. Pezeshki and E. H. Dowell. "An examination of initial condition maps for the sinusoidally excited buckled beam modeled by the Duffing's equation". *Journal of Sound and Vibration* 117.2 (Sept. 1987), pp. 219–232. ISSN: 0022-460X. DOI: 10.1016/0022-460X(87)90535-9.

[19] Roberto Zivieri, Silvano Vergura, and Mario Carpentieri. "Analytical and numerical solution to the nonlinear cubic Duffing equation: An application to electrical signal analysis of distribution lines". *Applied Mathematical Modelling* 40.21 (Nov. 2016), pp. 9152–9164. ISSN: 0307-904X. DOI: 10.1016/j.apm.2016.05.043.

[20] E. C. Zeeman. "Brain modelling". *Structural Stability, the Theory of Catastrophes, and Applications in the Sciences*. Ed. by Peter Hilton. Lecture Notes in Mathematics. Berlin, Heidelberg: Springer, 1976, pp. 367–372. ISBN: 978-3-540-38254-6. DOI: 10.1007/BFb0077855.

[21] Philip Holmes. "History of dynamical systems". *Scholarpedia* 2.5 (May 2007), p. 1843. ISSN: 1941-6016. DOI: 10.4249/scholarpedia.1843.

[22] Balth. van der Pol. "LXXXVIII. *On "relaxation-oscillations"*". *The London, Edinburgh, and Dublin Philosophical Magazine and Journal of Science* 2.11 (Nov. 1926), pp. 978–992. ISSN: 1941-5982, 1941-5990. DOI: 10.1080/14786442608564127.

[23] Balth Van Der Pol and J. Van Der Mark. "Frequency Demultiplication". *Nature* 120.3019 (Sept. 1927). Number: 3019 Publisher: Nature Publishing Group, pp. 363–364. ISSN: 1476-4687. DOI: 10.1038/120363a0.

[24] Balth. van der Pol and J. van der Mark. "LXXII. *The heartbeat considered as a relaxation oscillation, and an electrical model of the heart*". *The London, Edinburgh, and Dublin Philosophical Magazine and Journal of Science* 6.38 (Nov. 1928), pp. 763–775. ISSN: 1941-5982, 1941-5990. DOI: 10.1080/14786441108564652.

[25] Jack K Hale. "Remarks on Bifurcation Theory in Differential Equations." (1979).

[26] Christian Oestreicher. "A history of chaos theory". *Dialogues in Clinical Neuroscience* 9.3 (Sept. 2007), pp. 279–289. ISSN: 1294-8322.

[27] Jaeseung Byun et al. "Predictive Control for Chasing a Ground Vehicle using a UAV". *arXiv* (May 2019).

[28] Jaeseung Byun, Simo A. Mäkiharju, and Mark W. Mueller. "A flow disturbance estimation and rejection strategy for multirotors with round-trip trajectories". *2021 International Conference on Unmanned Aircraft Systems (ICUAS)*. ISSN: 2575-7296. June 2021, pp. 1314–1320. DOI: 10.1109/ICUAS51884.2021.9476842.

[29] Yujiao Huang, Huaguang Zhang, and Zhanshan Wang. "Dynamical stability analysis of multiple equilibrium points in time-varying delayed recurrent neural networks with discontinuous activation functions". *Neurocomputing* Complete.91 (2012), pp. 21–28. ISSN: 0925-2312. DOI: 10.1016/j.neucom.2012.02.016.

[30] Huaguang Zhang, Zhanshan Wang, and Derong Liu. "Global Asymptotic Stability of Recurrent Neural Networks With Multiple Time-Varying Delays". *IEEE Transactions on Neural Networks* 19.5 (May 2008). Conference Name: IEEE Transactions on Neural Networks, pp. 855–873. ISSN: 1941-0093. DOI: 10.1109/TNN.2007.912319.

[31] Miao Feng and Chen Zhang. "On Periodic Oscillation and Its Period of a Circadian Rhythm Model". *Communications on Applied Mathematics and Computation* 4.3 (Sept. 2022), pp. 1131–1157. ISSN: 2096-6385, 2661-8893. DOI: 10.1007/s42967-021-00146-1.

[32] Alfred J. Lotka. "Analytical Note on Certain Rhythmic Relations in Organic Systems". *Proceedings of the National Academy of Sciences* 6.7 (July 1920). Publisher: Proceedings of the National Academy of Sciences, pp. 410–415. DOI: 10.1073/pnas.6.7.410.

[33] V. Volterra. "Variations and Fluctuations of the Number of Individuals in Animal Species living together". *ICES Journal of Marine Science* 3.1 (Apr. 1928), pp. 3–51. ISSN: 1054-3139, 1095-9289. DOI: 10.1093/icesjms/3.1.3.

[34] Ambarish Goswami, Benoit Thuilot, and Bernard Espiau. "Compass-Like Biped Robot Part I : Stability and Bifurcation of Passive Gaits". *Bulletin of Sociological Methodology/Bulletin de Méthodologie Sociologique* 37.1 (Dec. 1992), pp. 55–57. ISSN: 0759-1063, 2070-2779. DOI: 10.1177/075910639203700105.

[35] Tad McGeer. "Passive Dynamic Walking" (Apr. 1990), p. 21.

[36] Fumihiko Asano. "Limit Cycle Gaits". *Humanoid Robotics: A Reference*. Ed. by Ambarish Goswami and Prahlad Vadakkepat. Dordrecht: Springer Netherlands, 2018, pp. 1–30. ISBN: 978-94-007-7194-9. DOI: 10.1007/978-94-007-7194-9_44-2.

[37] Daan G.E. and Martijn Wisse. "Limit Cycle Walking". *Humanoid Robots, Human-like Machines*. Ed. by Matthias Hackel. I-Tech Education and Publishing, June 2007. ISBN: 978-3-902613-07-3. DOI: 10.5772/4808.

[38] D.G.E. Hobbelen and M. Wisse. "Controlling the Walking Speed in Limit Cycle Walking". *The International Journal of Robotics Research* 27.9 (Sept. 2008), pp. 989–1005. ISSN: 0278-3649, 1741-3176. DOI: 10.1177/0278364908095005.

[39] Ambarish Goswami, Benoit Thuilot, and Bernard Espiau. "A study of the passive gait of a compass-like biped robot: symmetry and chaos" (Dec. 1998), p. 29.

[40] Florian Dörfler and Francesco Bullo. "Synchronization in complex networks of phase oscillators: A survey". *Automatica* 50.6 (June 2014), pp. 1539–1564. ISSN: 0005-1098. DOI: 10.1016/j.automatica.2014.04.012.

[41] Ahmed Benzerrouk, Lounis Adouane, and Philippe Martinet. "Dynamic Obstacle Avoidance Strategies using Limit Cycle for the Navigation of Multi-Robot System". *2012 IEEE/RSJ IROS'12, 4th Workshop on Planning, Perception and Navigation for Intelligent Vehicles*. Vilamoura, Algarve, Portugal, Oct. 2012.

[42] Pedro Castillo-García, Laura Elena Muñoz Hernandez, and Pedro García Gil. "Indoor Navigation Strategies for Aerial Autonomous Systems". *Indoor Navigation Strategies for Aerial Autonomous Systems*. Ed. by Pedro Castillo-García, Laura Elena Muñoz Hernandez, and Pedro García Gil. Butterworth-Heinemann, Jan. 2017, pp. 243–261. ISBN: 978-0-12-805189-4. DOI: 10.1016/B978-0-12-805189-4.00013-5.

[43] Dong-Han Kim and Jong-Hwan Kim. "A real-time limit-cycle navigation method for fast mobile robots and its application to robot soccer". *Robotics and Autonomous Systems* 42.1 (Jan. 2003), pp. 17–30. ISSN: 0921-8890. DOI: 10.1016/S0921-8890(02)00311-1.

[44] Manuel Boldrer et al. "Socially-Aware Reactive Obstacle Avoidance Strategy Based on Limit Cycle". *IEEE Robotics and Automation Letters* 5.2 (Apr. 2020). Conference Name: IEEE Robotics and Automation Letters, pp. 3251–3258. ISSN: 2377-3766. DOI: 10.1109/LRA.2020.2976302.

[45] JC Wilson. "Algebraic periodic solutions of Liénard equations". *Contributions to Differential Equations* 3 (1964), pp. 1–20.

[46] Amos Nathan. "The Rayleigh-van der Pol harmonic oscillator". *International Journal of Electronics* 43.6 (Dec. 1977), pp. 609–614. ISSN: 0020-7217, 1362-3060. DOI: 10.1080/00207217708900770.

[47] D.e. Panayotounakos, N.d. Panayotounakou, and A.f. Vakakis. "On the lack of analytic solutions of the Van der Pol oscillator". *ZAMM - Journal of Applied Mathematics and Mechanics / Zeitschrift für Angewandte Mathematik und Mechanik* 83.9 (2003), pp. 611–615. ISSN: 1521-4001. DOI: 10.1002/zamm.200310040.

[48] K. Odani. "The Limit Cycle of the van der Pol Equation Is Not Algebraic". *Journal of Differential Equations* 115.1 (Jan. 1995), pp. 146–152. ISSN: 0022-0396. DOI: 10.1006/jdeq.1995.1008.

[49] Marc Delphin Monsia, Judith Akande, and Kolawolé Kêgnidé Damien Adjaï. *On the non-existence of limit cycles of the Duffing-Van der Pol type equations*. May 2021.

[50] Murilo R. Cândido, Jaume Llibre, and Claudia Valls. "Non-existence, existence, and uniqueness of limit cycles for a generalization of the Van der Pol–Duffing and the Rayleigh–Duffing oscillators". *Physica D: Nonlinear Phenomena* 407 (June 2020). ISSN: 0167-2789. DOI: 10.1016/j.physd.2020.132458.

[51] Jordi Sorolla Bardají. "On the algebraic limit cycles of quadratic systems" (2004), p. 100.

[52] Ting Chen, Lihong Huang, and Pei Yu. "Center condition and bifurcation of limit cycles for quadratic switching systems with a nilpotent equilibrium point". *Journal of Differential Equations* 303 (Dec. 2021), pp. 326–368. ISSN: 0022-0396. DOI: 10.1016/j.jde.2021.09.030.

[53] Panagiotis Papafragkos et al. "Optimizing energy dissipation in gas foil bearings to eliminate bifurcations of limit cycles in unbalanced rotor systems". *Nonlinear Dynamics* 111.1 (Jan. 2023), pp. 67–95. ISSN: 1573-269X. DOI: 10.1007/s11071-022-07837-1.

[54] J. K. Wang and M. M. Khonsari. "Bifurcation Analysis of a Flexible Rotor Supported by Two Fluid-Film Journal Bearings". *Journal of Tribology* 128.3 (Mar. 2006), pp. 594–603. ISSN: 0742-4787. DOI: 10.1115/1.2197842.

[55] T. K. Caughey and H. J. Payne. "On the response of a class of self-excited oscillators to stochastic excitation". *International Journal of Non-Linear Mechanics* 2.2 (June 1967), pp. 125–151. ISSN: 0020-7462. DOI: 10.1016/0020-7462(67)90010-8.

[56] T. K. Caughey. "Some Exact Solutions in the Theory of Nonlinear Random Oscillations". *Nonlinear Dynamics and Stochastic Mechanics*. Ed. by Wolfgang Kliemann and N. Namachchivaya. 1st ed. CRC Press, 1995, pp. 283–292. ISBN: 978-1-351-07505-3. DOI: 10.1201/9781351075053-11.

[57] TK Caughey and Fai Ma. "The steady-state response of a class of dynamical systems to stochastic excitation". *Journal of Applied Mechanics* 104.3 (1982), pp. 629–632.

[58] G. Q. Cai and Y. K. Lin. "On exact stationary solutions of equivalent non-linear stochastic systems". *International Journal of Non-Linear Mechanics* 23.4 (Jan. 1988), pp. 315–325. ISSN: 0020-7462. DOI: 10.1016/0020-7462(88)90028-5.

[59] Zhu Wei-qui. "Exact solutions for stationary responses of several classes of nonlinear systems to parametric and/or external white noise excitations". *Applied Mathematics and Mechanics* 11.2 (Feb. 1990), pp. 165–175. ISSN: 0253-4827, 1573-2754. DOI: 10.1007/BF02014541.

[60] Y. K. Lin and Guoqiang Cai. "Exact Stationary Response Solution for Second Order Nonlinear Systems Under Parametric and External White Noise Excitations: Part II". *Journal of Applied Mechanics* 55.3 (Sept. 1988), pp. 702–705. ISSN: 0021-8936, 1528-9036. DOI: 10.1115/1.3125852.

[61] M.F. Dimentberg. "An exact solution to a certain non-linear random vibration problem". *International Journal of Non-Linear Mechanics* 17.4 (Jan. 1982), pp. 231–236. ISSN: 00207462. DOI: 10.1016/0020-7462(82)90023-3.

[62] Lincong Chen and Jian-Qiao Sun. "The closed-form solution of the reduced Fokker Planck Kolmogorov equation for nonlinear systems". *Communications in Nonlinear Science and Numerical Simulation* 41 (Dec. 2016), pp. 1–10. ISSN: 10075704. DOI: 10.1016/j.cnsns.2016.03.015.

[63] Lincong Chen and Jian-Qiao Sun. "The Closed-Form Steady-State Probability Density Function of van der Pol Oscillator under Random Excitations". *Journal of Applied Nonlinear Dynamics* 5.4 (Dec. 2016), pp. 495–502. ISSN: 21646457, 21646473. DOI: 10.5890/JAND.2016.12.009.

[64] G. Q. Cai. "Response probability estimation for randomly excited quasi-linear systems using a neural network approach". *Probabilistic Engineering Mechanics* 18.3 (July 2003), pp. 235–240. ISSN: 0266-8920. DOI: 10.1016/S0266-8920(03)00027-4.

[65] Xi Wang et al. "Radial basis function neural networks solution for stationary probability density function of nonlinear stochastic systems". *Probabilistic Engineering Mechanics* 71 (Jan. 2023), p. 103408. ISSN: 02668920. DOI: 10.1016/j.probengmech.2022.103408.

[66] Xi Wang et al. "Random vibration analysis with radial basis function neural networks". *International Journal of Dynamics and Control* 10.5 (Oct. 2022), pp. 1385–1394. ISSN: 2195-268X, 2195-2698. DOI: 10.1007/s40435-021-00893-2.

[67] Yong Xu et al. "Solving Fokker-Planck equation using deep learning". *Chaos: An Interdisciplinary Journal of Nonlinear Science* 30.1 (Jan. 2020), p. 013133. ISSN: 1054-1500. DOI: 10.1063/1.5132840.

[68] Herbert Goldstein. *Classical Mechanics*. Pearson Education, Sept. 2002. ISBN: 978-81-7758-283-3.

[69] Eugene M. Izhikevich. "Equilibrium". *Scholarpedia* 2.10 (Oct. 2007), p. 2014. ISSN: 1941-6016. DOI: 10.4249/scholarpedia.2014.

[70] Barbara D. MacCluer, Paul Bourdon, and Thomas L. Kriete. *Differential equations: techniques, theory, and applications*. Providence, Rhode Island: American Mathematical Society, 2019. ISBN: 978-1-4704-4797-7.

[71] Russ Tedrake. *Underactuated Robotics: Algorithms for Walking, Running, Swimming, Flying, and Manipulation*. Course Notes for MIT 6.832. 2023.

[72] G. Habib and G. Kerschen. "Suppression of limit cycle oscillations using the nonlinear tuned vibration absorber". *Proceedings of the Royal Society A: Mathematical, Physical and Engineering Sciences* 471.2176 (Apr. 2015). Publisher: Royal Society, p. 20140976. DOI: 10.1098/rspa.2014.0976.

[73] Steven H. Strogatz. *Nonlinear dynamics and chaos: with applications to physics, biology, chemistry, and engineering*. Second edition. OCLC: ocn842877119. Boulder, CO: Westview Press, a member of the Perseus Books Group, 2015. ISBN: 978-0-8133-4910-7.

[74] Hassan K. Khalil. *Nonlinear Systems*. Prentice Hall, 2002. ISBN: 978-0-13-122740-8.

[75] D. W. Jordan and Peter Smith. *Nonlinear ordinary differential equations: an introduction for scientists and engineers*. 4th ed. New York : Oxford University Press, 2007. ISBN: 978-0-19-920824-1 978-0-19-920825-8.

[76] J. L. Doob. "The Brownian Movement and Stochastic Equations". *Annals of Mathematics* 43.2 (1942). Publisher: Annals of Mathematics, pp. 351–369. ISSN: 0003-486X. DOI: 10.2307/1968873.

[77] TK Caughey and Fai Ma. "The exact steady-state solution of a class of non-linear stochastic systems". *International Journal of Non-Linear Mechanics* 17.3 (1982). Publisher: Elsevier, pp. 137–142.

[78] Andrei D Polyanin and Valentin F Zaitsev. "Handbook of Ordinary Differential Equations". *Ordinary Differential Equations* (Nov. 2017), p. 1487.

[79] M. San Miguel and S. Chaturvedi. "Limit cycles and detailed balance in Fokker-Planck equations". *Zeitschrift für Physik B Condensed Matter* 40.1-2 (Mar. 1980), pp. 167–174. ISSN: 0340-224X, 1434-6036. DOI: 10.1007/BF01295086.

[80] Mark Dykman, Xiaolin Chu, and John Ross. "Stationary probability distribution near stable limit cycles far from Hopf bifurcation points". *Physical Review E* 48.3 (Sept. 1993). Publisher: American Physical Society, pp. 1646–1654. DOI: 10.1103/PhysRevE.48.1646.

[81] A. Bezen and F. C. Klebaner. "Stationary solutions and stability of second order random differential equations". *Physica A: Statistical Mechanics and its Applications* 233.3 (Dec. 1996), pp. 809–823. ISSN: 0378-4371. DOI: 10.1016/S0378-4371(96)00205-1.

[82] K. I. Mamis and G. A. Athanassoulis. "Exact stationary solutions to Fokker Planck Kolmogorov equation for oscillators using a new splitting technique and a new class of stochastically equivalent systems". *Probabilistic Engineering Mechanics* 45 (July 2016), pp. 22–30. ISSN: 0266-8920. DOI: 10.1016/j.probengmech.2016.02.003.

[83] Marc Mendler, Johannes Falk, and Barbara Drossel. "Analysis of stochastic bifurcations with phase portraits". *PLOS ONE* 13.4 (Apr. 2018). Ed. by Ramon Grima, e0196126. ISSN: 1932-6203. DOI: 10.1371/journal.pone.0196126.

[84] S. S. Demidov. "The Study of Partial Differential Equations of the First Order in the 18th and 19th Centuries". *Archive for History of Exact Sciences* 26.4 (1982). Publisher: Springer, pp. 325–350. ISSN: 0003-9519.

[85] Robert McOwen. *Partial Differential Equations: Methods and Applications*. 2nd edition. Upper Saddle, N.J: Pearson, Oct. 2002. ISBN: 978-0-13-009335-6.

[86] Lawrence C. Evans. *Partial Differential Equations*. American Mathematical Society, Mar. 2022. ISBN: 978-1-4704-6942-9.

[87] Julie Levandosky. *Partial Differential Equations of Applied Mathematics (Math 220A) Lecture Notes*. 2002.

[88] Haym Benaroya, Seon Mi Han, and Mark Nagurka. *Probabilistic Models for Dynamical Systems*. 0th ed. CRC Press, May 2013. ISBN: 978-0-429-10761-0. DOI: 10.1201/b14880.

[89] Haym Benaroya and Seon MI Han. "Probability Models in Engineering and Science" (2005).

[90] Guo-qiang Cai and Weiqiu Zhu. *Elements Of Stochastic Dynamics*. World Scientific Publishing Company, Aug. 2016. ISBN: 978-981-4723-34-3.

[91] Michael D. Greenberg. *Advanced Engineering Mathematics*. Pearson Education, Sept. 1998. ISBN: 978-81-7758-546-9.

Appendix A

Basic Theories of Differential Equations

This chapter offers a succinct overview of the basic theories pertaining to ordinary differential equations and partial differential equations, with an emphasis on nonlinear dynamical systems.

A.1 Nonlinear Dynamical Systems

The nth-order nonlinear system can be described by the following equation [74]:

$$\begin{aligned}
\dot{x}_1 &= a_1(t, x_1, x_2, \ldots, x_n, u_1, u_2, \ldots, u_m), \\
\dot{x}_2 &= a_2(t, x_1, x_2, \ldots, x_n, u_1, u_2, \ldots, u_m), \\
&\vdots \\
\dot{x}_n &= a_n(t, x_1, x_2, \ldots, x_n, u_1, u_2, \ldots, u_m),
\end{aligned} \tag{A.1}$$

where t is the time, x_i, $i = 1, \ldots, n$ is the state variable, $\dot{x}_i = {}^{\partial x_i}/_{\partial t}$, u_j, $j = 1 \ldots m$ is the input variable, and a_i is the ith nonlinear function. In vector notation, (A.1) can be written as

$$\dot{\boldsymbol{x}} = \boldsymbol{a}(t, \boldsymbol{x}, \boldsymbol{u}), \tag{A.2}$$

where $\boldsymbol{x} = [x_1, x_2, \ldots, x_n]^T$, $\boldsymbol{u} = [u_1, u_2, \ldots, u_m]^T$, and $\boldsymbol{a} = [a_1, a_2, \ldots, a_n]^T$. The system can be simplified by several assumptions, two of which hold prime importance in this thesis:

- *Unforced*: Implying that the dynamics $\boldsymbol{a}$ do not depend on the input vector $\boldsymbol{u}$,

$$\dot{\boldsymbol{x}} = \boldsymbol{a}(t, \boldsymbol{x}). \tag{A.3}$$

- *Autonomous*: Implying that the dynamics $\boldsymbol{a}$ do not contain the dependence of the time variable t,

$$\dot{\boldsymbol{x}} = \boldsymbol{a}(\boldsymbol{x}). \tag{A.4}$$

Nonlinear dynamical systems display a wide range of behaviors which are not present in linear systems, such as limit cycles, finite escape times, bifurcations, and multiple isolated equilibrium points. Some of these behaviors will be briefly discussed.

- Limit cycle: An isolated, periodic orbit of the system. Further information can be found in Section 3.3.2.
- Finite escape time: The system can reach infinity in finite time. As an example, consider the following nonlinear differential equation

$$\dot{x} = -x + x^2, \tag{A.5}$$

whose solution is

$$x(t) = \frac{x_0 \exp(-t)}{1 - x_0 + x_0 \exp(-t)}, \tag{A.6}$$

where x_0 is the initial condition. The system can reach infinity in finite time if $t = \ln\big(x_0 \,/\, (x_0 - 1)\big)$ and $x_0 > 1$.

- Multiple isolated equilibrium points: The system can feature multiple isolated equilibrium points. For instance, consider the nonlinear differential equation $\dot{x} = -x + x^2$ again. This system showcases two equilibrium points, $x = 0$ and $x = 1$. The system can be stable or unstable depending on the initial condition; if $x_0 < 1$, the system is stable at $x = 0$.
- Bifurcation: A phenomenon that occurs when a system undergoes a transition from one system response to another. Further information can be found in Section 3.3.3.
- Non-uniqueness/non-existence of the solution: In linear systems, the solution is unique and exists for all initial conditions. However, in nonlinear systems, the solution may not be unique and may not even exist for all initial conditions. The following nonlinear differential equation

$$\dot{x} = 3x^{\frac{2}{3}}, \quad x(0) = 0 \tag{A.7}$$

features two solutions, $x(t) = t^3$ and $x(t) = 0$. Similarly, the following nonlinear differential equation

$$\dot{x} = \frac{1}{x}, \quad x(0) = 0 \tag{A.8}$$

also presents two solutions:

$$x(t) = \pm 2t^{\frac{1}{2}}. \tag{A.9}$$

A.2 Partial Differential Equations

In this section, the key concepts involved in solving partial differential equations are reviewed. The focus is on second order partial differential equations, which are essential components for solving diffusion equations.

A.2.1 Classification of Partial Differential Equations

A partial differential equation can be classified by several criteria: linearity, the number of independent variables, the order of the partial derivatives, boundary conditions, and initial conditions. In this section, the focus will be on the linearity of the partial differential equation and the order of the partial derivatives. In the realm of solving the diffusion equation, second-order partial differential equations with two independent variables, x and y, are the most commonly encountered type of equations.

Due to the limited solvability of full nonlinear partial differential equations, often some simplifications are used to induce partial linearity into the equation. One example is a quasi-linear partial differential equation, which is given by

$$\begin{aligned} A\left(\frac{\partial u}{\partial x}, \frac{\partial u}{\partial y}, u, x, y\right)\frac{\partial^2 u}{\partial x^2} + 2B\left(\frac{\partial u}{\partial x}, \frac{\partial u}{\partial y}, u, x, y\right)\frac{\partial^2 u}{\partial x \partial y} + C\left(\frac{\partial u}{\partial x}, \frac{\partial u}{\partial y}, u, x, y\right)\frac{\partial^2 u}{\partial y \partial x} \\ + D\left(\frac{\partial u}{\partial x}, \frac{\partial u}{\partial y}, u, x, y\right)\frac{\partial^2 u}{\partial y^2} = f\left(\frac{\partial u}{\partial x}, \frac{\partial u}{\partial y}, u, x, y\right). \end{aligned} \tag{A.10}$$

By further assuming the form represented in (A.11), one obtains a semi-linear partial differential equation:

$$\begin{aligned} A\left(\frac{\partial u}{\partial x}, \frac{\partial u}{\partial y}, u, x, y\right) = A(x, y), \quad B\left(\frac{\partial u}{\partial x}, \frac{\partial u}{\partial y}, u, x, y\right) = B(x, y), \\ C\left(\frac{\partial u}{\partial x}, \frac{\partial u}{\partial y}, u, x, y\right) = C(x, y), \quad D\left(\frac{\partial u}{\partial x}, \frac{\partial u}{\partial y}, u, x, y\right) = D(x, y). \end{aligned} \tag{A.11}$$

Finally, a linear partial differential equation of a function $u(x, y)$ takes the following form:

$$\begin{aligned} A(x, y)\frac{\partial^2 u}{\partial x^2} + 2B(x, y)\frac{\partial^2 u}{\partial x \partial y} + C(x, y)\frac{\partial^2 u}{\partial y^2} \\ + D_1(x, y)\frac{\partial u}{\partial x} + D_2(x, y)\frac{\partial u}{\partial y} + D_3(x, y)u = f(x, y). \end{aligned} \tag{A.12}$$

The first three coefficient functions A, B, and C play an important role in determining the type of the partial differential equation. These coefficients can be used to calculate the characteristic polynomial, $B^2 - AC$, which can then be used to classify the partial differential equation as either *elliptic*, *hyperbolic* or *parabolic*. This classification can also be extended to n dimensional independent variables, where the eigenvalues of the coefficient matrix are used to determine the type of the partial differential equation. The partial differential equation is called *elliptic* if all its eigenvalues are negative, *hyperbolic* if they are positive, and *parabolic* if all eigenvalues are zero.

Example A.2.1. Consider the following example of a linear partial differential equation of stationary diffusion described in Eq. (1.4):

$$-y\frac{\partial p_s}{\partial x} + \frac{\partial}{\partial y}\Big(\big(\epsilon\alpha y + \beta\big)p_s\Big) + \pi S_0 \frac{\partial^2 p_s}{\partial y^2} = 0.$$

The partial differential equation can be categorized as linear since its coefficient functions are all linear functions of x and y. Furthermore, the characteristic polynomial is zero, indicating that it is a parabolic partial differential equation.

A.2.2 Method of Characteristics

The Method of Characteristics, also known as the Lagrange-Charpit method [84], effectively solves quasi-linear partial differential equations of the first order:

$$a_1\frac{\partial u}{\partial x_1} + a_2\frac{\partial u}{\partial x_2} + \cdots + a_n\frac{\partial u}{\partial x_n} = f(x_1, x_2, \ldots, x_n, u), \tag{A.13}$$

where $a_i = a_i(x_1, x_2, \ldots, x_n, u)$. In this context, the graph of $z = u(x_1, x_2, \ldots, x_n)$ forms an n-dimensional manifold S:

$$S = \Big\{\big(x_1, x_2, \ldots, x_n, z(x_1, x_2, \ldots, x_n)\big)\Big\}. \tag{A.14}$$

This manifold S is referred to as the integral manifold and serves as a solution to Eq. (A.13). The method of characteristics constructs characteristic curves along which the partial differential equation is reduced to a system of ordinary differential equations known as characteristic equations [85, 86]:

$$\begin{aligned} \frac{dx_i}{dt} &= a_i(x_1, x_2, \ldots, x_n, z), \quad i = 1, 2, \ldots, n, \\ \frac{dz}{dt} &= f(x_1, x_2, \ldots, x_n, z). \end{aligned} \tag{A.15}$$

Here, t is the parameter along the characteristic curves, which take the form:

$$\chi = \Big\{\big(x_1(t), x_2(t), \ldots, x_n(t), z(t)\big)\Big\}. \tag{A.16}$$

Additionally, the characteristic equations can be expressed in the form of auxiliary equations or Lagrange-Charpit equations:

$$\frac{dx_1}{a_1} = \frac{dx_2}{a_2} = \cdots = \frac{dx_n}{a_n} = \frac{dz}{f}. \tag{A.17}$$

The integral manifold is constructed by the smooth union of characteristic curves emanating from every point on the $(n-1)$-dimensional manifold, referred to as the non-characteristic. This manifold is represented by the graph of a function Γ, parameterized by $\mathbf{s} = (s_1, \ldots, s_{n-1})$:

$$\Gamma = \Big\{\big(g_1(\mathbf{s}), g_2(\mathbf{s}), \ldots, g_n(\mathbf{s}), \eta(\mathbf{s})\big)\Big\}. \tag{A.18}$$

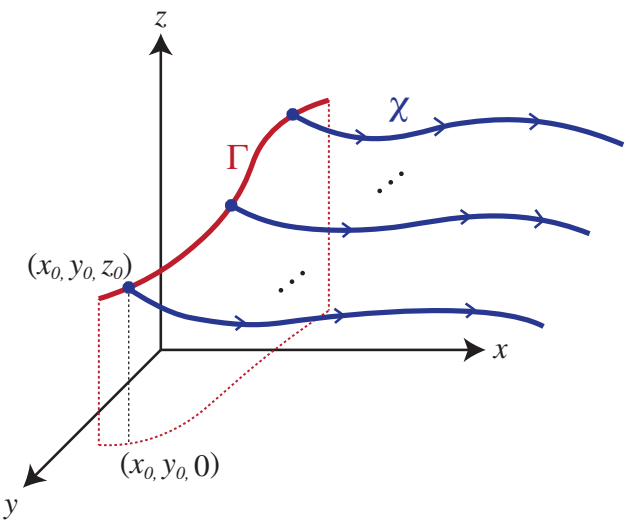

Figure A.1: An illustrative example of characteristic curves χ and non-characteristic Γ in a two-dimensional linear partial differential equation of first order.

The initial conditions are given by the functions $g_i(\mathbf{s})$ and $\eta(\mathbf{s})$:

$$\begin{aligned} x_i(\mathbf{s}, 0) &= g_i(\mathbf{s}), \quad i = 1, 2, \ldots, n, \\ z(\mathbf{s}, 0) &= \eta(\mathbf{s}). \end{aligned} \tag{A.19}$$

By solving Eq. (A.15) and applying corresponding initial conditions the solution of Eq. (A.13) is obtained.

When the dimension of the variable is reduced to two, the integral manifold is represented by a surface, and the non-characteristic Γ takes the form of a space curve (Fig. A.1 [85]). Consider the two-dimensional, linear formulation of Eq. (A.13):

$$a_1(x, y)\frac{\partial u}{\partial x} + a_2(x, y)\frac{\partial u}{\partial y} = f(x, y). \tag{A.20}$$

The characteristic equations are

$$\frac{dx}{dt} = a_1(x, y), \quad \frac{dy}{dt} = a_2(x, y), \quad \frac{dz}{dt} = f(x, y) \tag{A.21}$$

accompanied by the initial conditions:

$$x(s, 0) = g_1(s), \quad y(s, 0) = g_2(s), \quad z(s, 0) = \eta(s), \tag{A.22}$$

where g_1, g_2, and η are arbitrary functions. By solving Eq. (A.21) and subsequently substituting the variables (s, t) according to Eq. (A.22), the integral surface represented by $z = u(x, y)$ is derived. This surface, expressed in terms of (x, y), is the solution to Eq. (A.20).

Example A.2.2. Take the first-order linear partial differential equation of the form [87]:

$$x\frac{\partial u}{\partial x}+\frac{\partial u}{\partial y}=0,$$

with initial condition $u(x,0)=h(x)$. The associated characteristic equations are

$$\frac{dx}{dt}=x,\quad \frac{dy}{dt}=1,\quad \frac{dz}{dt}=0,$$

complemented by the initial state of the system:

$$x(s,0)=g_1(s)=s,\quad y(s,0)=g_2(s)=0,\quad z(s,0)=\eta(s).$$

Solving this system generates the following relations:

$$x(s,t)=c_1(s)e^t,\quad y(s,t)=t+c_2(s),\quad z(s,t)=c_3(s),$$

where $c_1(s)$, $c_2(s)$, and $c_3(s)$ are functions unveiled by utilizing the initial conditions. This leads to

$$x(s,t)=se^t,\quad y(s,t)=t,\quad z(s,t)=\eta(s).$$

After substituting from (s,t) to (x,y):

$$s(x,y)=xe^{-y},\quad t(x,y)=y.$$

The solution to the differential equation is consequently expressed by

$$u(x,y)=z\big(s(x,y),t(x,y)\big)=\eta\big(xe^{-y}\big).$$

Example A.2.3. Regarding Eq. (4.128):

$$-y\frac{\partial p_s}{\partial x}+g(x)\frac{\partial p_s}{\partial y}=0,$$

this can be represented in an alternative formulation:

$$-\frac{y}{g(x)}\frac{\partial p_s}{\partial x}+\frac{\partial p_s}{\partial y}=0.$$

The resulting characteristic equations are

$$\frac{dx}{dt}=-\frac{y}{g(x)},\quad \frac{dy}{dt}=1,\quad \frac{dz}{dt}=0.$$

The initial conditions are noted as

$$x(s,0)=s,\quad y(s,0)=0,\quad z(s,0)=\eta(s).$$

Integration with respect to these initial conditions yields

$$G(x) + \int y\,dt = c_1(s), \quad y(s,t) = t + c_2(s), \quad z(s,t) = c_3(s),$$

where $G(x) = \int g(x)\,dx$. Upon applying the initial conditions, the solutions become

$$G(x) + \frac{1}{2}y^2 = G(s), \quad y(s,t) = t, \quad z(s,t) = \eta(s).$$

The change from (s,t) to (x,y) enables the solutions to be written as

$$s(x,y) = G^{-1}\bigg(G(x) + \frac{1}{2}y^2\bigg), \quad t(x,y) = y.$$

The solution is therefore given by

$$p_s(x,y) = \eta\big(s(x,y)\big) = h\bigg(G(x) + \frac{1}{2}y^2\bigg),$$

where h is an arbitrary function.

Example A.2.4. Examining Eq. (4.156)

$$-H_u\frac{\partial\phi}{\partial x} + H_x\frac{\partial\phi}{\partial u} = 0,$$

after rearranging the terms, the equation becomes

$$-\frac{H_u}{H_x}\frac{\partial\phi}{\partial x} + \frac{\partial\phi}{\partial u} = 0.$$

The corresponding characteristic equations are

$$\frac{dx}{dt} = -\frac{H_u}{H_x}, \quad \frac{du}{dt} = 1, \quad \frac{dz}{dt} = 0.$$

The initial conditions outlined are

$$x(s,0) = s, \quad u(s,0) = 0, \quad z(s,0) = \eta(s).$$

From the similar procedure of Example A.2.3, integration while considering the initial conditions produces

$$\int H_x\,dx + \int H_u\,du = H = c_1(s), \quad u(s,t) = t, \quad z(s,t) = \eta(s).$$

The transformation from (s,t) to (x,u) results in

$$s(x,u) = c_1^{-1}(H), \quad t(x,u) = u,$$

where $c_1(s) = H(s,0)$. The solution is therefore given by

$$\phi(x,u) = \eta\big(s(x,u)\big) = h(H),$$

with the function h chosen such that it conforms to the boundary or initial conditions.

Appendix B

Basic Theories of Stochastic Processes

A stochastic process/random process [88] is a physical/mathematical model of a system that evolves randomly over time. It is typically defined as a collection of time-dependent random variables, such as $X(t_1), X(t_2), \ldots$, with t_i (Fig. B.1 [89]). In stochastic processes, upper case letters represent random variables while lower case denotes specific realizations of those variables. For example, $X(t_i)$ could represent the possible position of a particle at time i, and $x(t_i)$ would be the actual value of the position.

Consider the measured values of $X(t_1) = x_1, \ldots, X(t_n) = x_n$ at discrete times $t_1, \ldots, t_n$, where $t_1 < \cdots < t_n$. The joint probability density which describes the system is given by

$$p(x_1, t_1; x_2, t_2; \ldots; x_n, t_n). \tag{B.1}$$

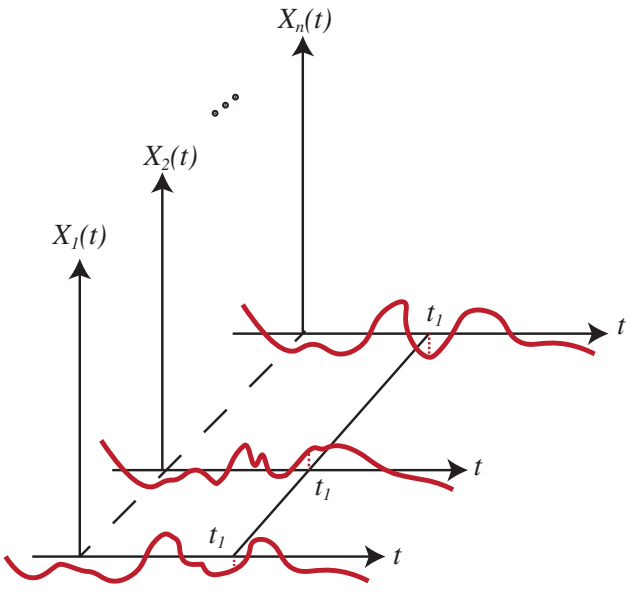

Figure B.1: A stochastic process

If the independence is assumed, the joint probability density can be written as

$$p(x_1, t_1; x_2, t_2; \ldots; x_n, t_n) = p(x_1, t_1)p(x_2, t_2) \ldots p(x_n, t_n). \tag{B.2}$$

If further measurements $y_1, y_2, \ldots, y_m$ are defined at s_1, s_2, ..., s_m, where $s_1 < \cdots < s_m < t_1 < \cdots < t_n$, the conditional probability density becomes:

$$p(x_1, t_1; x_2, t_2; \ldots; x_n, t_n | y_1, s_1; y_2, s_2; \ldots; y_m, s_m) = \frac{p(x_1, t_1; \ldots; x_n, t_n, y_1, s_1; \ldots; y_m, s_m)}{p(y_1, s_1; \ldots; y_m, s_m)}. \tag{B.3}$$

Another way to define a stochastic process is by its moments [90]

$$\begin{aligned} \mathbb{E}\big[X(t)\big] &= \int x p(x,t) dx, \\ \mathbb{E}\big[X(t_1)X(t_2)\big] &= \int x_1 x_2 p(x_1, t_1; x_2, t_2) dx_1 dx_2, \\ \ldots &= \ldots, \\ \mathbb{E}\big[X(t_1)X(t_2)\ldots X(t_n)\big] &= \int x_1 x_2 \ldots x_n p(x_1, t_1; x_2, t_2; \ldots; x_n, t_n) dx_1 dx_2 \ldots dx_n. \end{aligned} \tag{B.4}$$

The first and second moment of a stochastic process are also called mean and auto-correlation function, respectively:

$$\begin{aligned} \mu_X(t) = \mu\big[X(t)\big] &= \mathbb{E}\big[X(t)\big], \\ \mathrm{Cor}\big[X(t_1), X(t_2)\big] &= \mathbb{E}\big[X(t_1)X(t_2)\big]. \end{aligned} \tag{B.5}$$

Similarly, auto-covariance and variance function are written as

$$\begin{aligned} \mathrm{Cov}\big[X(t_1), X(t_2)\big] &= \mathbb{E}\Big[\big(X(t_1) - \mu_X(t_1)\big)\big(X(t_2) - \mu_X(t_2)\big)\Big], \\ \mathrm{Var}_X(t) = \mathrm{Var}\big[X(t)\big] &= \mathbb{E}\Big[\big(X(t) - \mu_X(t)\big)^2\Big]. \end{aligned} \tag{B.6}$$

For two stochastic processes $X(t)$ and $Y(t)$, cross-correlation and cross-covariance functions can be defined as follows:

$$\begin{aligned} \mathrm{Cor}\big[X(t_1), Y(t_2)\big] &= \mathbb{E}\big[X(t_1)Y(t_2)\big], \\ \mathrm{Cov}\big[X(t_1), Y(t_2)\big] &= \mathbb{E}\Big[\big(X(t_1) - \mu_X(t_1)\big)\big(Y(t_2) - \mu_Y(t_2)\big)\Big]. \end{aligned} \tag{B.7}$$

For simplicity, the auto-correlation/covariance and cross-correlation/covariance functions will be referred to as correlation/covariance functions in subsequent sections. The meaning of the function can be inferred from the notations.

A property of the correlation function is its symmetry. Consider two stochastic processes with a set of two random variables, $\big\{X(t_1), X(t_2)\big\}$ and $\big\{Y(t_1), Y(t_2)\big\}$, the following property holds:

$$\begin{aligned} \mathrm{Cor}\big[X(t_1), Y(t_2)\big] &= \mathrm{Cor}\big[Y(t_2), X(t_1)\big], \\ \mathrm{Cor}\big[X(t_1), X(t_2)\big] &= \mathrm{Cor}\big[X(t_2), X(t_1)\big]. \end{aligned} \tag{B.8}$$

Covariance function also exhibits the symmetry property

$$\begin{aligned} \mathrm{Cov}\big[X(t_1), Y(t_2)\big] &= \mathrm{Cov}\big[Y(t_2), X(t_1)\big], \\ \mathrm{Cov}\big[X(t_1), X(t_2)\big] &= \mathrm{Cov}\big[X(t_2), X(t_1)\big], \end{aligned} \tag{B.9}$$

which can be shown by Eq. (B.8) and

$$\mathrm{Cov}\big[X(t_1), Y(t_2)\big] = \mathrm{Cor}\big[X(t_1), Y(t_2)\big] - \mu_X(t_1)\mu_Y(t_2). \tag{B.10}$$

Notable stochastic processes include Markov, Wiener, and Ornstein-Uhlenbeck processes. Markov processes are essential when deriving the diffusion equation in Section 3.4.3. Other important concepts include stationary stochastic processes and power spectral density, which will be discussed in the following sections.

B.1 Stationary Processes

Consider an m-th order probability density function of the form

$$p(x_1, x_2, \ldots, x_m; t_1, t_2, \ldots, t_m). \tag{B.11}$$

The stochastic process is said to be stationary if the probability density function is invariant under time translation τ, i.e.:

$$p(x_1, x_2, \ldots, x_m; t_1, t_2, \ldots, t_m) = p(x_1, x_2, \ldots, x_m; t_1 + \tau, t_2 + \tau, \ldots, t_m + \tau). \tag{B.12}$$

Furthermore, the stochastic process is said to be stationary in the strong sense if Eq. (B.12) holds for all m, and stationary in the weak sense if Eq. (B.12) holds for $m = 1$ and $m = 2$. The weak sense of stationary stochastic process, with zero mean is used throughout this thesis unless stated otherwise.

Let $X(t)$ and $Y(t)$ be the weakly stochastic process with a set of two random variables, i.e, $X(t)$, $X(t+\tau)$ and $Y(t)$, $Y(t+\tau)$. Direct consequence of the definition of the weakly stationary stochastic process yields the following properties [90]:

1. The mean and moment of the stochastic process is constant over time:

$$\mu\big[X(t)\big] = \mu_X, \ \mathbb{E}\big[X^n(t)\big] = \mathbb{E}[X^n], \tag{B.13}$$

2. The correlation/covariance function of a single stochastic process $X(t)$ is a function of time shift τ only:

$$\begin{aligned} \mathrm{Cor}\big[X(t), X(t+\tau)\big] &= \mathrm{Cor}\big[X(\tau), X(\tau)\big] := \mathrm{Cor}\big[X(\tau)\big], \\ \mathrm{Cov}\big[X(t), X(t+\tau)\big] &= \mathrm{Cov}\big[X(\tau), X(\tau)\big] := \mathrm{Cov}\big[X(\tau)\big]. \end{aligned} \tag{B.14}$$

3. The correlation/covariance function of two stochastic processes $X(t)$ is a function of time shift τ only:

$$\begin{aligned} \mathrm{Cor}\big[X(t), Y(t+\tau)\big] &= \mathrm{Cor}\big[X(\tau), Y(\tau)\big], \\ \mathrm{Cov}\big[X(t), Y(t+\tau)\big] &= \mathrm{Cov}\big[X(\tau), Y(\tau)\big]. \end{aligned} \tag{B.15}$$

B.2 Power Spectral Density

The power spectral density is an auto-correlation function of a given stochastic process in the frequency domain. Under the assumption of stationary process, the power spectral density of a stochastic process $X(t)$ is defined as the Fourier transform of the auto-correlation function of the stochastic process:

$$S_X(\omega) = \mathcal{F}\Big[\mathrm{Cor}\big[X(\tau)\big]\Big] = \frac{1}{2\pi}\int_{-\infty}^{\infty} \mathrm{Cor}\big[X(\tau)\big]e^{-i\omega\tau}d\tau. \tag{B.16}$$

Similarly, the inverse Fourier transform of the power spectral density is the auto-correlation function of the stochastic process:

$$\mathrm{Cor}\big[X(\tau)\big] = \mathcal{F}^{-1}\big[S_X(\omega)\big] = \int_{-\infty}^{\infty} S_X(\omega)e^{i\omega\tau}d\omega. \tag{B.17}$$

It can be easily shown that if there is no time shift, the power spectral density is the expectation of the square of the stochastic process:

$$\mathrm{Cor}\big[X(0)\big] = \mathbb{E}\big[X^2(t)\big] = \int_{-\infty}^{\infty} S_X(\omega)d\omega. \tag{B.18}$$

B.3 Gaussian Processes

A Gaussian process is a stochastic system with random variables indexed by time or space, where any finite subset follows a multivariate normal distribution. White noise $W(t)$ is a Gaussian process with zero mean and a constant power spectral density S_0. Then the following properties hold:

$$S_W(\omega) = S_0, \tag{B.19}$$

$$\mathrm{Cor}\big[W(\tau)\big] = \mathbb{E}\big[W(t)W(t+\tau)\big] = 2\pi S_0\delta(\tau). \tag{B.20}$$

The first result is self-explanatory from the assumption of constant power spectral density. The second result can be obtained by substituting the power spectral density in the equation (B.17):

$$\mathrm{Cor}\big[W(\tau)\big] = \int_{-\infty}^{\infty} S_0e^{i\omega\tau}d\omega = S_0\int_{-\infty}^{\infty} e^{i\omega\tau} = 2\pi S_0\delta(\tau). \tag{B.21}$$

Note that the complex integral with residue theory [91] is being used here:

$$\int_{-\infty}^{\infty} e^{i\omega\tau}d\omega = \int_{-\infty}^{0} e^{i\omega\tau}d\omega + \int_{0}^{\infty} e^{i\omega\tau}d\omega = \pi\delta(\tau) + \frac{1}{i\tau} + \pi\delta(\tau) - \frac{1}{i\tau} = 2\pi\delta(\tau). \tag{B.22}$$

Eq. (B.19) and (B.20) imply that the Gaussian white noise is completely characterized by its constant power spectral density.